Spring 5-15-2016

Understanding the Interactions of Developing Thymocytes and Antigen Presenting Cells in the Thymic Medulla

Justin Shaun Arnold Perry
Washington University in St. Louis

WASHINGTON UNIVERSITY IN ST. LOUIS

Division of Biology and Biomedical Sciences
Immunology

Dissertation Examination Committee:

Chyi-Song Hsieh, Chair
Paul Allen
Brian Edelson
Takeshi Egawa
Kenneth Murphy

Understanding the Interactions of Developing Thymocytes and Antigen Presenting Cells in the Thymic Medulla

By

Justin Shaun Arnold Perry

A dissertation presented to the
Graduate School of Arts and Sciences
of Washington University in
partial fulfillment of the
requirements for the degree
of Doctor of Philosophy

May 2016

Saint Louis, Missouri

TABLE OF CONTENTS

LIST OF FIGURES

Chapter Two **Page**

LIST OF ABBREVIATIONS

Aire	Autoimmune regulator
APC	Antigen presenting cell
Batf3	Basic leucine zipper transcription factor, ATF-like 3
BM	Bone marrow
C2TA	Class II transactivator
CD	Cluster of differentiation
CTV	Cell trace violet
DC	Dendritic cell
DT	Diphtheria toxin
DTA	Diphtheria toxin antigen
DTR	Diphtheria toxin receptor
FACS	Fluorescence activated cell sorting
FLT3L	Fms-Related Tyrosine Kinase 3 Ligand
GPR	G protein-coupled receptor
GVHD	Graft versus host disease
IRES	Internal ribosome entry site
LN	Lymph node
MHC	Major histocompatibility complex
mTEC	Medullary thymic epithelial cell
NOD	Non-obese diabetic (mice)
OVA	Ovalbumin
PS	Phosphatidylserine

PTA	Peripheral tissue antigen
RAG	Recombination-activating gene
TCR	T cell receptor
Tconv	Conventional T cell
Treg	Regulatory T cell

ACKNOWLEDGEMENTS

I would like to thank Chyi for his mentorship. He always held me to a higher standard and afforded me the room to develop my own ideas. His rigorous approach to science has osmosed to me, a trait that will serve me no matter what career lies ahead.

I would also like to thank the Hsieh lab members. The Hsieh lab has been much like a family, remaining together through highs and lows. Their helpful criticism of my work helped to shape the stories in this thesis. I would additionally like to thank our collaborators without whom much of this work would not be possible. In particular, I would like to thank the Murphy, Abumrad, DiPersio, and Colonna labs within WUSTL.

I owe much gratitude to my thesis committee members. They have each provided helpful advice and poignant questions, often suggesting experiments that were important for project progression. They were always there for me if I had questions, and were always quick to provide whatever assistance they could.

Graduate school is hard, and without the many friends and acquaintances I've made this would have been nearly impossible. Often the discussions with friends in other fields led to ideas in my own, or when I needed to talk about anything but science, I could always rely on them.

Finally, I would like to thank my wife and my two amazing children. No words can express what they have meant to me over these last few years. Without my wife, I would certainly not be where I am today. And without my number one motivator (my children), I certainly would not have had the success that I've been fortunate enough to experience.

ABSTRACT OF THE DISSERTATION

Understanding the Interactions of Developing Thymocytes and Antigen Presenting Cells in the Thymic Medulla

By

Justin Shaun Arnold Perry

Doctor of Philosophy in Biology and Biomedical Sciences

Immunology

Washington University in St. Louis, 2016

Professor Chyi-Song Hsieh, Chair

Various thymic APC subsets have been invoked in deletional tolerance and Treg cell induction, but previous studies either assessed total T cell numbers or used TCR transgenic lines, obscuring roles that individual thymic APC subsets might serve for particular antigen-specific T cell populations. Utilizing T cell receptor sequencing, we found that medullary thymic epithelial cells (mTECs) and bone marrow-derived (BM) APCs delete or select unique conventional and Treg cell TCR repertoires, demonstrating distinct roles for these APCs. We show that BM APCs and mTECs each contribute to Aire-dependent T cell tolerance development, albeit through either cooperative or autologous antigen presentation respectively, and that cooperative antigen transfer is likely performed by thymic CD8α^+ DCs. Using our established TCR sequencing approach, In addition, we sought to understand CD8α^+ DC-mediated cooperative antigen presentation further. We quantified the extent of CD8α^+ DC-dependent Treg cell and negative selection and the proportion of this selection that is achieved through Aire-dependent cooperative antigen transfer. We also found that CD36 expression by CD8α^+ DCs facilitates Aire-dependent cooperative antigen transfer

both in vivo and via TCR sequencing. Finally, we found that in the absence of thymic CD8α^+ DCs or CD36 expression; direct allo-tolerance fails to develop leading to catastrophic acute GVHD.

CHAPTER 1

Background and Significance

A defining feature of adaptive immunity is its ability to harness somatic gene rearrangement to generate a diverse antigen receptor repertoire, which allows for the recognition of a variety of pathogens including those not previously encountered by the host species. For most T cells, rearrangement of the TCR α and β chains occurs early during T cell development in a specialized organ–the thymus. Thymocytes expressing functional TCR genes can then undergo positive selection, where weak TCR recognition of self-antigen MHC complexes on cortical thymic epithelial cells allows continued T cell development and CD4 and CD8 lineage commitment (Klein et al., 2014; Stritesky et al., 2012; Vrisekoop et al., 2014). These mechanisms serve to generate the T cell population responsible for immunity to pathogens.

However, the potential cost of this randomly generated TCR repertoire is the presence of TCRs that recognize self-antigens and contribute to the pathogenesis of autoimmune disease. An important component of T cell development is therefore to limit the autoreactivity within the T cell population in the thymus prior to their release into the periphery of the host. This process in the thymus, generally referred to as central tolerance, is achieved through deletion of autoreactive clones (i.e. negative selection), and for $CD4^+$ T cells, diversion of autoreactive clones into the regulatory T (Treg) cell lineage (Hsieh et al., 2012b; Klein and Jovanovic, 2011; Rudensky, 2011), a subset of T cells that inhibit, rather than induce, inflammatory responses (Sakaguchi and Powrie, 2007).

Although central tolerance can occur throughout the thymus (Stritesky et al., 2012), the majority of this process appears to occur in the medulla, which consists of a secondary lymphoid tissue-like structure populated by hematopoiesis-derived dendritic cells, macrophages, and B cells; as well as thymic epithelial cells (mTECs) and fibroblasts (Klein, 2009; Koble and Kyewski, 2009a). Thus, a diverse assortment of cell types appears to be involved in central tolerance.

Role of mTECs and BM APCs in self-tolerance

The importance of TCR specificity in the process of T cell tolerance necessitates an effective means of thymic presentation of the self-antigenic repertoire, including those antigens expressed in an organ specific manner. In both thymic compartments, it appears that hematopoietic and non-hematopoietic cells contribute to T cell tolerance (Atibalentja et al., 2011; Gallegos and Bevan, 2004; Hinterberger et al., 2010; Hubert et al., 2011; Koble and Kyewski, 2009b; Proietto et al., 2008b; Taniguchi et al., 2012). Although T cell tolerance occurs at any stage in their development after rearrangement of a functional TCR (McCaughtry et al., 2008; Stritesky et al., 2013), the majority of T cell tolerance appears to occur in the thymic medulla (reviewed in (Anderson and Su, 2011; Mathis and Benoist, 2009b)). We discuss here our current understanding of how the array of medullary APC subsets contributes to thymic T cell tolerance.

mTEC antigen presentation

it remains technically challenging to delineate the specific contributions of each medullary APC to T cell tolerance development (Klein et al., 2014). For instance,

reduction or deletion of MHCII on either compartment results in only a partial effect on Treg cell numbers or on negative selection (Aschenbrenner et al., 2007; Hinterberger et al., 2010). Additionally, mTECs require crosstalk with thymocytes via MHCII for successful organization of the medulla (Irla et al., 2008), precluding targeted deletion of MHCII on mTECs. An important advance came from Klein and colleagues who developed a mouse with mTEC-targeted reduction of MHCII expression using Aire promoter driven shRNA knockdown of the class II transactivator (C2TAkd) (Hinterberger et al., 2010), which does so without altering medulla organization. They observed a modest increase in the polyclonal CD4SP compartment due to loss of negative selection as well as increased Treg cell selection to a model antigen expressed in mTECs. Thus, these data demonstrate that direct mTEC antigen presentation plays a role in T cell tolerance.

mTECs, however, are known to be inefficient at using conventional antigen presenting pathways (Atibalentja et al., 2009; Klein et al., 2001). Moreover, conventional pathways are not focused on presenting proteins generated endogenously within the cell. Current data suggests that mTECs use macroautophagy for presentation of cell-autonomous antigens (Aichinger et al., 2013a; Nedjic et al., 2008b). Transplantation of $Atg5^{-/-}$ autophagy-deficient thymi under the kidney capsule of select TCR transgenic mice resulted in increased CD4SP numbers, suggesting decrease negative selection. In addition, T cells selected on $Atg5^{-/-}$ thymi were capable of inducing multi-organ autoimmunity (Nedjic et al., 2008b). Recent work suggested that mTECs specifically require autophagy to load peptides onto MHCII from model antigens targeted to the autophagosome or the mitochondria, but not the cell membrane (Aichinger et al.,

2013a). These data on mTECs are consistent with reports from other contexts showing a role for autophagy in loading of intracellular antigen onto MHC class II (Dengjel et al., 2005; English et al., 2009; Lee et al., 2010; Paludan et al., 2005; Schmid et al., 2007).

However, another group reported that mTEC-targeted deletion of Atg7 via the K14-Cre resulted in no alteration of the thymocyte compartment or autoimmune disease despite ablation of autophagy in TECs (Sukseree et al., 2012). One possible explanation for the discrepancy between results from Atg5 versus Atg7 deficient mice is that autophagy associated antigen presentation may utilize different components than the autophagy pathway itself (Lee et al., 2010; Li et al., 2015; Liu et al., 2015; Zhao et al., 2008). Interestingly, a recent report suggested that knockdown of Clec16a, an autophagy/mitophagy-associated protein (Soleimanpour et al., 2015; Soleimanpour et al., 2014), is protective in the NOD model of type 1 diabetes (Schuster et al., 2015). They proposed that this was due to alterations in the generation and presentation of ligands by mTECs responsible for selecting diabetogenic T cells, rather than tolerance to islet associated antigens. Additional studies are required to determine whether an effect on mTEC antigen presentation explains the observation that an CLEC16A SNP results in increased susceptibility to human type 1 diabetes (Polychronakos and Li, 2011).

In summary, these data suggest that direct mTEC presentation of intracellular antigens to T cells is mediated at least in part by autophagy proteins. Future work is required to dissect the specific mechanism by which intracellular antigens are processed via the canonical autophagy versus alternative antigen presentation pathways in mTECs. Moreover, future analysis of TCR repertoires in mice with

autophagy deficient mTECs would be useful to determine the extent that autophagy affects mTEC antigen presentation.

BM APCs

Whereas mTECs arise within the thymus, the other major medullary APC subsets arise from the bone marrow. Several lines of evidence suggest an important role for BM APCs in T cell tolerance. First, deletion of MHCII on BM APCs results in an increase in the CD4SP thymocyte compartment (Aschenbrenner et al., 2007; Hinterberger et al., 2010; Ohnmacht et al., 2009), suggestive of a role in negative selection. The impact of MHCII deletion on BM APCs on Treg cell numbers have been reported to be mild (Aschenbrenner et al., 2007; Hinterberger et al., 2010; Liston et al., 2008; Ohnmacht et al., 2009; van Meerwijk et al., 1997) to moderate (Román et al., 2010). Second, use of neo-self antigen systems such as RIP-membrane OVA (mOVA) suggest that BM APCs, and in particular DCs, can contribute to both negative and Treg cell selection of antigen-specific TCRs (Atibalentja et al., 2011; Baba et al., 2009a; Hubert et al., 2011; Oh et al., 2013).

Cooperation between BM APCs and mTECs

Antigen transfer from mTECs to BM APCs constitutes another pathway through which T cell tolerance occurs (Gallegos and Bevan, 2004; Hinterberger et al., 2010; Hubert, 2011; Koble and Kyewski, 2009a; Perry et al., 2014; Taniguchi et al., 2012). It is apparent that certain neo-self antigen transgenic models, such as nuclear or membrane OVA, require transfer from mTECs to thymic DCs for deletion of OVA-specific $CD4^+$ and

$CD8^+$ thymocytes (Aschenbrenner et al., 2007; Gallegos and Bevan, 2004). Antigen transfer was also reported by a separate group, although they also observed a concurrent role for cell-autonomous antigen presentation (Hubert et al., 2011). In addition to model antigens, Anderson and colleagues examined this issue using MHCII tetramers with interphotoreceptor retinoid-binding protein (IRBP), a naturally occurring Aire-dependent peripheral tissue antigen (PTA) (Taniguchi et al., 2012). Consistent with the notion that IRBP undergoes cooperative antigen presentation, they observed that deletion of MHCII on BM APCs resulted in a significant increase in tetramer-positive cells, despite IRBP expression being restricted to mTECs. .

Role of Aire in T cell tolerance

A key component of tolerance is the presentation of self-antigens in the thymus. It has become clear that the Autoimmune Regulator (Aire) protein plays a critical role in this process by inducing the expression of tissue specific antigens in mTECs as well as mTEC function and development (reviewed in (Abramson et al., 2010; Akirav et al., 2011; Anderson and Su, 2011; Mathis and Benoist, 2009a)).

Control of tissue specific antigen production by Aire

It is clear that generation of PTA is one of the main functions of Aire (Taniguchi and Anderson, 2011). As an mTEC matures into the $CD80^+$ $MHCII^+$ phenotype, Aire expression becomes detectable which coincides with a dramatic increase in PTA expression. Despite the ability of the mTEC population to produce thousands of unique PTAs, previous reports estimate that a single mTEC expresses only ~1-3% of the total

PTA ligandome (Abramson et al., 2010). How a small subset of cells expressing a fraction of the possible PTA ligandome at any given time could facilitate tolerance remains unclear. Two recent studies utilizing single cell RNA-sequencing (scRNA-seq) address this complex process (Brennecke et al., 2015; Meredith et al., 2015). Analysis of ~200 individual mature mTECs confirmed previous estimates showing that each mTEC expressed only a small fraction of the total PTA ligandome. Combined, however, mTECs expressed the majority of known PTAs. Interestingly, both studies found that correlated sets of PTAs were generated in multiple distinct, small fractions of mTECs, providing evidence for a mosaic model of PTA expression (Brennecke et al., 2015; Meredith et al., 2015). Additionally, these “co-expressed genes” tended to cluster in the genome (Meredith et al., 2015), providing a potential explanation for why a set of mTECs express a small, related fraction of PTAs at a particular time. Taken together, it appears that subsets of mature mTECs express clusters of PTAs and together these clusters of mTECs converge to express the breadth of the PTA ligandome.

Recently, Takayanag and colleagues have identified the transcriptional regulator Fezf2 as an Aire-independent mechanism for inducing PTA production in mTECs (Takaba et al.). Unlike Aire, deletion of Fezf2 is lethal in young (~3-4 week old) mice due to a failure of forebrain neuronal development and subsequent malnutrition (Eckler and Chen, 2014). Moreover, Fezf2 is regulated by the lymphotoxin receptor β, whereas Aire is affected by the RANK/CD40 pathway. TEC-specific deletion of Fezf2 via Foxn1-cre results in lymphocytic infiltrates in the lung, liver, kidneys and small intestine but not the retina or pancreas of C57BL/6 mice, consistent with Fezf2 being required for expression of a different array of PTAs than Aire (Takaba et al., 2015). The discovery of

Fezf2 poses interesting new questions in its relationship to Aire and its relevance in human disease. Nonetheless, it appears that PTA expression in mTECs can be generated via multiple mechanisms.

The small numbers of mTECs that express any given PTA raises the question of how thymocytes are efficiently exposed to those antigens. One hypothesis is that the motility of thymocytes could allow them to scan hundreds to thousands of APCs over the period of time it resides in the medulla (Klein et al., 2014). Given the findings above, encountering ~200-500 mTECs would be sufficient for a single thymocyte to see the majority of the PTA ligandome. Another non-mutually exclusive possibility, as discussed in the preceding section, is that antigen transfer to BM APCs can increase the overall presentation of a given antigen.

Early studies supported the notion that Aire-induced PTA facilitates negative selection (Anderson et al., 2005; Liston et al., 2003; Taniguchi et al., 2012). However, its role in Treg cell selection has been controversial. Initial reports suggested that Aire is not required for Treg cell selection as Aire deletion does not alter polyclonal Treg cell numbers (Anderson et al., 2005). Additionally, Ignatowicz and colleagues reported that the absence of Aire has no effect on the Treg cell TCR repertoire (Daniely et al., 2010). On the other hand, Treg cell selection of TCR transgenic cells can be induced by the genetic expression of cognate antigen on $Aire^{+}$ mTECs (Aschenbrenner et al., 2007). Furthermore, a recent report by Savage and colleagues showed that two independent prostate specific TCR transgenic cells underwent Aire-dependent Treg cell selection (Malchow et al., 2013). Together, these data suggest that Aire play a role in negative selection and can affect Treg cell selection at least in a limited capacity.

As discussed above, the rationale for antigen transfer from mTECs might be to expand the number of APCs presenting any given antigen considering the stochastic nature of Aire-dependent PTA expression. This would increase the likelihood that a single thymocyte can encounter all PTAs expressed in the thymus, and functionally increase the “antigenic niche size” for Treg and negative selection. Another intriguing possibility is that transfer to BM APCs insures that the processing and presentation of antigens are consistent between the thymus and periphery. For example, cathepsins are differentially expressed between TECs and BM APCs (Bania et al., 2003; Beers et al., 2005; Nakagawa et al., 1998; Stoeckle et al., 2012), potentially resulting in the loading of different peptide fragments onto the MHC II of these APC subsets. Although this hypothesis has not been tested, a dichotomy between thymic and peripheral antigen presentation has been hypothesized as a determining factor for the loss of tolerance to insulin in NOD mice (Calderon et al., 2014). Thus, cooperative antigen presentation may limit discordant antigen peptide presentation by thymic versus peripheral APCs.

BM-derived APC subsets

There are a variety of different BM-derived APC subsets in the thymic medulla, including B cells, macrophages, and DCs, consisting of conventional DCs and pDCs (Wu and Shortman, 2005), each with potentially unique roles in thymic T cell tolerance.

Conventional DCs

The conventional DC subset is comprised of the CD8α^+ and SIRPα^+ DC subsets (Li et al., 2009). It remains to be seen whether these thymic DC subsets can be further subdivided, such as that seen in the peripheral tissue SIRPα^+ DC equivalent, the CD11b$^+$ DCs (Satpathy et al., 2012). While these two cDC subsets are both efficient at presenting exogenous antigen, there are notable difference. For instance, thymic SIRPα^+ DCs originate from outside of the thymus, presumably entering the thymus via the vascular plexus connected to the outer portion of the medulla (Li et al., 2009; Wu and Shortman, 2005). By contrast, CD8α^+ DCs arise primarily within the thymus. SIRPα^+ DCs also show a different localization, and generally remain close to vascular regions within the medulla whereas CD8α^+ DCs are distributed throughout the thymus parenchyma (Klein et al., 2014).

These differences suggest non-overlapping functions in antigen presentation (Oh and Shin, 2015). For instance, SIRPα^+ DCs have been shown to efficiently present blood-borne antigen for negative and Treg cell selection, potentially related to their predilection for vascular regions (Atibalentja et al., 2009; Atibalentja et al., 2011; Baba et al., 2009a; Proietto et al., 2008b).

The extra-thymic origin of SIRPα^+ DCs may also be a vehicle for antigen transport into the thymus. One study using fluorescent beads too large to permeate into the thymus showed that SIRPα^+ DCs and pDCs, but not CD8α^+ DCs, have the capacity to acquire and transport antigen into the thymus (Wendland et al., 2007). Similar findings were reported using skin-painting of FITC (Bonasio et al., 2006). Finally, mOVA expressed specifically in cardiomyocytes led to deletion of OT-II thymocytes mediated

by circulating DCs (Bonasio et al., 2006). Taken together, SIRPα^+ DCs may present extra-thymic antigen both via DC migration as well as capture of blood-borne antigens.

Factors that determine if a SIRPα^+ DC enters the thymus with extra-thymic antigen remain unclear. In addition, the relative importance of this extra-thymic versus intra-thymic antigen presentation is unknown. Another question is whether the extra-thymic antigen presentation pathway can induce tolerance to pathogens or commensal bacteria. New tools are therefore required to understand the importance of SIRPα^+ DCs and the extent that they present extra- versus intra-thymic antigens.

Unlike SIRPα^+ DCs, CD8α^+ DCs are more likely to present antigen generated within the thymus because of their localization (Joffre et al., 2012). CD8α^+ DCs constitutively express the chemokine receptor XCR1 (Bachem et al., 2012) which directs migration in response to XCL1 from mTECs (Lei et al., 2011). This crosstalk between CD8α^+ DCs and mTECs is supported by the observation that XCL1-deficient mice show a decrease in Treg cell numbers and transfer of thymocytes from XCL1 deficient mice into nude mice develop dacryoadenitis (Lei et al., 2011). Moreover, the enhanced ability of CD8α^+ DCs to cross-present exogenous antigen on MHCI allows concomitant CD8$^+$ T cell tolerance, as observed in both in vitro (Proietto et al., 2008a) and in vivo studies (Gallegos and Bevan, 2004).

My thesis will cover three main areas: 1) the contributions of aire and antigen presenting cell subsets to the generation of self-tolerance in the thymus, 2) evaluate the necessity of antigen transfer from Aire-dependent mTECs to CD8α^+ DCs for T cell tolerance, and 3) determine the molecular mechanism for Aire-dependent mTEC to CD8α^+ DC antigen transfer. Taken together, my work has broadened our understanding

of T cell development and the unique roles each antigen presenting cell plays in this process.

CHAPTER 2

Contributions of Aire and antigen presenting cell subsets to the generation of self-tolerance in the thymus

The results presented in this chapter have been adapted from a manuscript published in Immunity, 2014.

Abstract

The contribution of thymic APC subsets in selecting a self-tolerant T cell population remains unclear. We show that BM APCs and mTECs played non-overlapping roles in shaping the TCR repertoire by deletion and Treg cell selection of distinct TCRs. Aire, which induces tissue-specific-antigen expression in mTECs, affected the TCR repertoire in a manner distinct from mTEC presentation. Approximately half of Aire-dependent deletion or Treg cell selection utilized a pathway dependent on antigen presentation by BM APCs. Batf3-dependent CD8α$^+$ DCs were the crucial BM APC for Treg cell selection via this pathway, showing enhanced ability to present antigens from stromal cells. These results demonstrate the division of function between thymic APCs in shaping the self-tolerant TCR repertoire, and reveal an unappreciated cooperation between mTECs and CD8α$^+$ DCs for presentation of Aire-induced self-antigens to developing thymocytes.

Introduction

The enormous diversity of adaptive immune receptors allows for the recognition of a wide variety of pathogens, but comes at the potential cost of self-recognition and autoimmunity. For $CD4^+$ T cells, self-tolerance starts during T cell maturation in the thymus where they are instructed by APCs found primarily in the thymic medulla (Derbinski and Kyewski, 2010; Klein et al., 2014; Stritesky et al., 2012; Weissler, 2014). $CD4^+$ T cells bearing TCRs that recognize self-antigens at this stage can be eliminated by negative selection, which prevents the release of autoreactive Tconv cells into the periphery (Palmer, 2003; Stritesky et al., 2012)**.** Alternatively, self-reactive T cells can undergo differentiation into Treg cells, which are required for the prevention of spontaneous autoimmunity (Hsieh et al., 2012a; Josefowicz et al., 2012; Wing and Sakaguchi, 2010). Because both of these thymic tolerance mechanisms are driven via TCR signaling, the display of self-antigen on medullary APCs is crucial for the education of a self-tolerant T cell population (Klein et al., 2014).

The process of generating and presenting a diverse array of self-antigens is remarkable for its complexity. In contrast to the involvement of a single APC type for positive selection in the thymic cortex, multiple APC types contribute to T cell tolerance in the medulla (Anderson and Su, 2011; Derbinski and Kyewski, 2010; Klein et al., 2014). Broadly, medullary APCs are classified as being of epithelial origin (e.g. mTECs), or of BM origin. Their role in tolerance is supported by two key observations. First, genetic deletion or knockdown of MHCII expression in either BM cells or mTECs increases the total number of CD4SP thymocytes, suggesting that both APC types are involved in deletion (Bonasio et al., 2006; Hinterberger et al., 2010; Ohnmacht et al., 2009). However, changes in cell numbers may also reflect differences in cell survival,

cytokine niches, and/or the rate of thymic egress (Hinterberger et al., 2011; Lio et al., 2010). Second, TCR transgenic studies reveal that both mTECs and BM APCs are capable of inducing Treg cells and negative selection upon presentation of cognate antigens expressed via a second transgene (Atibalentja et al., 2011; Cowan et al., 2013; Hinterberger et al., 2010; Proietto et al., 2008b; Román et al., 2010). However, restricting TCR:peptide/MHC interactions to single specificities may not be representative of the naturally occurring T cell population or developmental niche. While these results highlight potential roles for these APC types, they do not quantify the impact of BM APCs and mTECs on the processes of clonal deletion and Treg cell selection (Klein et al., 2014).

Medullary tolerance is further complicated by the requirement of mTEC production of PTAs to maintain self-tolerance. Aire has been shown to induce the ectopic expression of PTAs in mTECs (Mathis and Benoist, 2009a; Metzger and Anderson, 2011). Despite the importance of Aire in facilitating negative selection (Liston et al., 2003), its role in Treg cell development is controversial. One TCR repertoire analysis suggests that Aire has little effect on Treg cell selection (Daniely et al., 2010), which is consistent with the observation that Aire-deficient mice have normal Treg cell numbers (Anderson et al., 2005). However, these findings are contrary to a recent study showing that Aire is required for thymic Treg cell selection of two TCR transgenic lines specific to endogenous prostate-specific antigen (Malchow et al., 2013), as well as studies of TCR:cognate antigen transgenic models. As the differences in methodologies and conclusions cannot be easily resolved, the role of Aire in thymic Treg cell selection remains unclear.

Interestingly, T cell tolerance may also require the interaction of mTECs and BM APCs for presentation of PTAs. Although Aire-dependent antigens can be autologously presented on mTECs via autophagy (Aschenbrenner et al., 2007; Hinterberger et al., 2010; Liston et al., 2003), mTECs can also transfer antigens to BM APC for presentation (Aschenbrenner et al., 2007; Gallegos and Bevan, 2004; Hubert et al., 2011; Taniguchi et al., 2012). Antigen transfer may therefore blur the distinction between antigens that are displayed on BM APCs and mTECs. Because this has only been addressed using TCR transgenic or MHC tetramer studies (Gallegos and Bevan, 2004; Hubert et al., 2011; Koble and Kyewski, 2009a; Taniguchi et al., 2012), the importance of the antigen transfer pathway versus autologous mTEC antigen presentation in mediating Aire-dependent tolerance remains unknown.

To systematically characterize the role of Aire and antigen presentation by BM APCs and mTECs at a TCR clonal level, we used a fixed TCRβ model to analyze the thymic TCR repertoires that arise upon blockade of antigen presentation on BM APCs or mTECs, and compared them to TCR repertoires that arise in the context of Aire-deficiency. Our results demonstrate that BM APCs and mTECs play non-redundant roles in deletion and Treg cell selection, and unexpectedly reveal that a major pathway of Aire-dependent tolerance is mediated by antigen transfer from mTECs to Batf3-dependent CD8α^+ DCs.

Materials and Methods

Mice

All experiments involving mice were performed using protocols approved by the Washington University Animal Studies Committee. Mice were on a C57BL/6 genetic background. Animals were housed and bred in a specific pathogen-free animal facility. TCliβ mice (Wong, et al., 2000) and *Batf3*$^{-/-}$ (Hildner et al., 2008) mice, have been previously described. *CLEC4C*-HBEGF (BDCA2-DTR) mice were a gift from M. Colonna (WUSTL); CD11c-cre x ROSA-DTA; C2TAkd mice from L. Klein (LMU Munich); β-actin-GFP from M. Miller (WUSTL); and *Foxp3*^{gfp} mice from A. Rudensky (MSKCC). MHCII-deficient (Stock# 003239), *Aire*$^{-/-}$ (Stock# 004743), *Rag1*$^{-/-}$ (Stock# 002216), and *Foxp3*$^{IRES\text{-}GFP}$ (Stock# 006772) mice were purchased from The Jackson Laboratory. Animals were typically 6-8 weeks old at the time experiments were performed.

Reagents, antibodies and flow cytometry

Fluorescently conjugated antibodies were purchased from Biolegend, eBioscience, and Becton Dickenson. Y-Ae anti-I-A^{b}:Eα peptide was obtained from Affymetrix. Samples were analyzed using a FACSAria (Becton Dickinson) and data were processed with FlowJo (Treestar).

Thymic dendritic cell isolation

Based on (Hildner et al., 2008), whole thymus was mechanically separated with scissors and digested with Liberase (125 μg/ml, Roche) and DNase I (50 μg/ml, New England Biolabs) in DMEM for 30 min at 37°C.

TCR sequencing

Synthesis of TCRα cDNAs from purified T cells was performed as described (Hsieh, et al., 2006). PCR was performed using a forward primer containing the GS FLX Titanium Amplicon Primer A sequence followed by sequence directed against TRAV14 (italics) 5'- CGTATCGCCTCCCTCGCGCCATCAG *ATGGACAAGATCCTGACAGC* - 3'. The reverse primer contained the GS FLX Titanium Primer B, followed by the 12 bp error correcting ("Golay") barcode (Ns) (Fierer et al., 2008) and a sequence complementary to C alpha (italics), 5'- CTATGCGCCTTGCCAGCCCGCTCAG **NNNNNNNNNNNN** *ACACAGCAGGTTCTGGGTTC*. The ~500 bp amplicons were quantified using Qubit (Invitrogen) and pooled in equimolar ratios for emulsion PCR and 454 pyrosequencing (Titanium chemistry). Pyrosequencer reads were demultiplexed by sample and analyzed to determine the CDR3 sequence. Briefly, we used a custom BLAST database of V- and J- sequences (acquired from IMGT) (Giudicelli et al., 2006) to determine the boundaries of the V and J regions to identify the CDR3 amino acid sequence. Raw sequence data can be found in the European Nucleotide Archive (accession # PRJEB6458).

Assessment of thymic Treg cell selection in vivo

As described previously (Lathrop, et al., 2011), TCRα chains of interest were cloned into the TCRα-P2A-TCliβ retroviral vector. *Foxp3*$^{\text{IRES-GFP}}$ *Rag1*$^{-/-}$ thymocytes were transduced with TCRs *in vitro*, injected intrathymically into sublethally (600 rad) irradiated mice, and analyzed approximately 2.5 weeks later. In many experiments, thymocytes were transduced with TCR vector containing an IRES-Thy1.1 marker, and mixed with thymocytes transduced with a TCR vector lacking Thy1.1 prior to injection.

Bone marrow chimeras

BM was obtained by flushing donor humerus, tibia, and femur. After RBC lysis, $5x10^6$ cells were injected into 1000 rad lethally irradiated host mice.

Statistical analysis

Graphpad Prism v6, SPSS v21, and R v3.0.2 were used for used for statistical and graphical analysis. The Mann-Whitney U (MWU) test was used for between-subjects analyses. PCA and k means clustering were performed to analyze individual-group relationships. Morisita-Horn indices estimate species similarity between data sets.

Results

Both BM APCs and mTECs mediate negative selection

Because the great diversity in polyclonal T cells precludes experimental analysis at the individual TCR level, we and others have utilized mice in which TCR diversity is limited by a transgenic fixed TCRβ chain (Hsieh et al., 2004; Pacholczyk et al., 2007; Wong et al., 2007). This allows high throughput analysis of the TCR repertoire at the individual TCR level via sequencing of the variable TCRα chains. To assess the role of MHC II presentation by BM APCs, TCliβ TCR transgenic *Foxp3*^{gfp} *Tcra*$^{+/-}$ MHC II deficient mice were used as BM donors into irradiated wild-type (WT) mice. To assess the role of mTECs, TCliβ *Foxp3*^{gfp} *Tcra*$^{+/-}$ BM was transplanted into irradiated C2TAkd mice, in which MHC II expression is markedly reduced in mTECs owing to expression of an shRNA to CIITA driven by the Aire promoter (Hinterberger et al., 2010).

Within the CD4SP subset, we sorted Foxp3^{+} Treg cells and Foxp3^{-} CD24^{lo} CD62L^{hi} mature Tconv and sequenced their TRAV14 (Vα2) chains (Figure 2.1A). To allow for statistical comparisons of TCR frequencies between conditions, the pyrosequencing data were filtered to include those reads present in more than one third of mice in at least one condition, and those present >0.01% in at least one mouse (Figure 2.1B). We then plotted the average percentage of each TCR in the MHC manipulated versus WT conditions. In the Tconv repertoire, many TCRs were significantly enriched in MHC II-deficient BM APCs compared with MHC II-sufficient BM APCs (Figure 2.2A, data points found below reference line of MHC II deficient BM plot). By contrast, fewer TCRs were enriched when MHC II was reduced on mTECs (Figure 2.2A, C2TAkd).

We classified TCRs as negatively selected based on an arbitrary >5 fold increase in frequency and statistical significance versus the WT condition. Using these criteria, BM APCs negatively selected approximately 25% of the TCR clones (Figure 2.2B, top), representing ~30% of the Tconv cell population (Figure 2.2B, bottom). While a quantitative comparison of negative selection between BM APCs and mTECs was limited due to differences in the degree of MHC II reduction achieved experimentally, the TCR repertoire analysis suggested that both BM APCs and mTECs are capable of mediating negative selection.

Principal component analyses (PCA) were performed to further explore the clonal relationship between Tconv TCRs from various backgrounds (Figure 2.2C). Analysis of MHC II deficient BM APCs versus WT data sets revealed two distinct clusters representing TCRs negatively selected on BM APCs (red arrow) and unaffected TCRs (black arrow). Analysis of C2TAkd versus WT data sets showed a three factor structure representing TCRs negatively selected on mTECs (red arrow), unaffected TCRs (black arrow), and TCRs de-enriched by C2TAkd (blue arrow) that corresponded to the group of TCRs in Figure 2.2A (data points found above reference line, left panel). It is unclear why Aire-driven C2TAkd leads to a loss of Tconv TCR specificities. One possibility is that these TCRs are simply the result of stochastic mouse-to-mouse variability. However, these TCRs show statistical significance by nonparametric tests and clustering by PCA, suggesting that this is unlikely. Another untested possibility is that C2TAkd inhibits the positive selection of these particular Tconv TCRs. Because our primary goal was to study the role of APC subsets in tolerance, we focused our analysis on TCRs affected by deletion and Treg cell selection.

We observed negative selection of the Treg repertoire by both mTECs and BM APCs (Figure 2.3A). Several TCRs were significantly enriched when MHC II was deleted from BM APCs (red dots found below the reference line), a phenomenon that was less pronounced with mTECs. Treg TCRs classified as negatively selected by BM APCs represent approximately 35% of TCR clones, which accounted for ~30% of the Treg cell population (Figure 2.3B). PCA analysis revealed a cluster of TCRs associated with negative selection (red arrows) by BM APCs, but not mTECs (Figure 2.3C). Together with the Tconv analysis, these data demonstrate that ablation of MHC II on BM APCs has a marked effect on the negative selection of a diverse array of both Treg and Tconv cell TCRs, estimated to comprise ~30% of the analyzed TCR repertoire.

The results of this TCR repertoire analysis implied that certain TCRs instruct developing Tconv and Treg cells to undergo negative selection. For example, TCR clone NS1 is rare in the normal Treg TCR repertoire, but common when MHC II is deficient in BM APCs (Figure 2.4 & 2.5A). To demonstrate the functional role of TCRs in instructing cell-fate decisions *in vivo*, we used a retroviral vector to express NS1 in *Rag1*$^{-/-}$ thymocytes, and injected them into the thymi of chimeras with selective MHC II deficiency in either mTECs or BM APCs (Figure 2.4). CD4SP cells were readily observed when MHC II was absent from BM APCs (~20%, Figure 2D), a portion of which were Foxp3^{+} (data not shown). Similar results were obtained with another TCR, NS3 (Figure 2.5B). Thus, these *in vivo* results provide independent validation for the TCR repertoire analysis showing negative selection by BM APCs.

BM APCs and mTECs select non-redundant thymic Treg cell pools

In conjunction with the enrichment of certain Treg cell TCRs with MHC II ablation on BM APCs, there was also a loss of distinct TCRs from the Treg cell repertoire (Figure 2.3A, red dots above reference line). As Treg cell differentiation is driven by self-recognition, the decrease in frequency of certain TCRs would be consistent with the loss of Treg cell selection mediated by BM APC antigen presentation (Figure 2.3B). While the diminished MHC II expression on mTECs affected the negative selection of a small number of Tconv and Treg cell TCRs, it led to a decrease in the frequency of many more Treg cell TCRs (Figure 2.3A, data points above reference line in the left panel). The effect of MHC II-deficiency in BM APCs on the Treg cell population as a whole was much greater than the effect of C2TAkd on mTECs suggesting that BM APCs facilitate Treg cell selection of more frequent Treg cell TCRs (~60% compared to ~20%, Figure 2.3B). PCA analysis confirmed that a cluster of TCRs associated with Treg cell selection (blue arrow) was present in both MHC II deficient BM and C2TAkd mTEC conditions (Figure 2.3C). These results suggest that both APC types are directly involved in Treg cell selection.

BM APCs and mTECs presumably present distinct arrays of antigens related to different mechanisms of antigen processing and presentation, as well as different transcriptional landscapes partially attributable to the expression of Aire in mTECs. However, antigen transfer from mTECs to BM APCs may blur the distinction between antigens that are specific to mTECs or BM APCs. We therefore asked whether the TCR repertoires selected by BM APCs versus mTECs were similar. Consistent with the estimated effect on the Treg cell TCR repertoire (Figure 2.3B), the Morisita-Horn index showed dissimilarity between the Treg cell TCR repertoires of MHC II deficient versus

WT BM conditions (Figure 2.6A). The Treg cell TCR repertoire selected by BM APCs was also quite different than that selected by mTECs (~0.1, Morisita-Horn index, Figure 2.6B). Thus, these findings suggest that ablation of MHC II on BM cells has more profound effects on the Treg cell population than does silencing of MHC II on mTECs.

The difference in the Treg cell TCR repertoire suggested by global analysis could also be visualized upon inspection of the 15 most frequent Treg cell TCRs in WT mice (Figure 2.6C). There was a marked reduction of 10 TCRs in MHCII deficient BM APCs, including the top 3 most frequent TCRs, often with concomitant increase in the Tconv cell subset (Figure 2.7). By contrast, only 6 of the 15 most frequent TCRs were decreased with silenced MHCII in mTECs.

Despite the involvement of mTECs in selecting Treg cells with certain TCR specificities (Figure 2.3A-C), Morisita-Horn analysis of the Treg cell TCR repertoires between C2TAkd and WT showed high similarity (Figure 2.6A). A follow-up assessment of the top 15 C2TAkd Treg TCRs revealed that the top 3 most frequent TCRs are also the top 3 most frequent Treg cell TCRs in the WT (Figure 2.8A), which was not the case with BM APCs (Figure 2.6C). Because the Morisita-Horn similarity index is abundance weighted, we asked whether successive removal of these TCRs from the analysis would alter this similarity. Indeed, removal of the top 3 TCRs suggested that, similar to BM APCs, mTECs do select a substantial portion of the Treg cell TCR repertoire, albeit less frequent Treg cell TCRs (Figure 2.8B). As independent validation, retroviral expression of mTEC-dependent Treg cell TCRs confirmed that MHC II presentation by mTECs was important for Treg cell selection (Figure 2.8C, 2.9). These results suggest

that a substantial portion of the Treg cell repertoire is selected via antigen presentation by mTECs.

DCs are the primary BM APC subset involved in Treg cell selection

Because BM APCs consist of multiple populations capable of antigen presentation, we next sought to identify the population mediating Treg cell selection. To do so, we used mice in which conventional DCs are constitutively deleted via a CD11c-cre transgene that activates diphtheria toxin conditionally expressed under the control of the ROSA locus (Ohnmacht et al., 2009). Thymocytes with retroviral expression of the top four WT Treg cell TCRs (G25, G69, G41, R19) showed poor Treg cell development in CD11c-cre ROSA-DTA mice in comparison with WT or C2TAkd mice (Figure 2.9). By contrast, the mTEC-dependent TCR G126 showed normal Treg cell selection in WT and CD11c-cre ROSA-DTA mice, but not in C2TAkd mice (Figure 2.9). These findings suggest that conventional DCs are the primary BM-derived APC subset that mediates thymic Treg cell selection.

Aire is required for selection of a subpopulation of thymic Treg cells

An important feature of mTECs is their expression of Aire, a gene responsible for promiscuous expression of tissue specific antigens (Anderson and Su, 2011; Mathis and Benoist, 2009a). The role of Aire in Treg cell selection has been controversial (Anderson et al., 2005; Daniely et al., 2010; Malchow et al., 2013). Therefore, we assessed the TCR repertoire of *Aire*$^{-/-}$ mice with a TCliβ transgene. We found that a number of Tconv and Treg cell TCRs were enriched in *Aire*$^{-/-}$ compared to isogenic

Aire$^{+/+}$ mice (Figure 2.10A, B), suggesting that Aire plays a role in negative selection of both Tconv and Treg cells.

We also observed that a number of Treg cell TCRs were significantly diminished in frequency in *Aire*$^{-/-}$ mice, consistent with Aire-dependent Treg cell selection (Figure 2.10A, C). This contrasted with the high degree of similarity between Aire-deficient and --sufficient Treg TCR repertoires based on the Morisita-Horn similarity index. However, we found that this was based primarily on the top three TCRs, as their removal markedly lowered the Morisita-Horn similarity values (Figure 2.11A), consistent with an effect of Aire on lower frequency TCRs. Thus, depending on whether the analytic approach favors more abundant TCRs or assesses them at an individual TCR level, Aire may be viewed as having no effect to having a significant effect on Treg cell selection, potentially explaining previously conflicting studies on the role of Aire in Treg cell selection (Daniely et al., 2010; Malchow et al., 2013).

Because Aire is exclusively expressed in TECs in the thymus, we asked whether Aire-dependent TCRs were selected via antigen presentation by mTECs. Consistent with this hypothesis, Morisita-Horn analysis indicated that the Aire-deficient Treg cell TCR repertoire was quite similar to the C2TAkd repertoire (~ 0.8) but not to the MHC II deficient BM Treg TCR repertoire (~0.35). However, upon removal of the top 3 TCRs from the analysis, the Aire-deficient Treg cell TCR repertoire was much less similar to the C2TAkd repertoire (~0.5) and equivalently similar to the MHC II deficient BM repertoire (~0.5, Figure 2.11B), consistent with a role for Aire in selecting lower frequency Treg cell TCRs. Cross-referencing the list of Treg cell TCRs that were Aire-dependent with those that were BM APC- or mTEC-dependent confirmed the

substantial role of both BM APCs and mTECs in mediating Aire-dependent central tolerance (Figure 2.10B,C). This can also be visualized in the analysis of the top 15 Treg cell TCRs found in WT condition (Figure 2.11B). Of the 7 TCRs that were Aire-dependent (G25, G41, G126, R25, R35, JP13, R117), 4 were also dependent on BM APCs (G25, G41, R35, R117) and 2 on mTECs (G126, R25). These findings suggest that the presentation of Aire-dependent antigens by BM APCs plays a major role in central tolerance.

To independently confirm these sequencing analyses, we used retrovirus to express Aire-dependent Treg TCRs in *Rag1*$^{-/-}$ thymocytes and then assessed Foxp3^{+} Treg cell development in Aire-deficient or -sufficient hosts. The *in vivo* behavior of six Aire-dependent and five Aire-independent Treg cell TCRs recapitulated the patterns observed via TCR sequencing (2.11C, D). This sample set of Treg cell TCRs also included those dependent on MHC II presentation by CD11c^{+} DCs or mTECs as assessed previously (Figure 2.8, 2.9), confirming the non-redundant roles of these APC subsets in mediating the effects of Aire seen by TCR sequencing. Thus, while many Aire-dependent Treg cell TCRs are selected in response to autologous antigen presentation by mTECs, others are selected via antigen presentation by CD11c^{+} DCs that do not express Aire.

Aire has been suggested to facilitate the recruitment of DCs via production of chemokines by mTECs (Lei et al., 2011). However, Aire-deficiency did not abrogate all Treg cell selection by BM APCs, as six of 10 common BM-dependent Treg cell TCRs were Aire-independent by TCR sequencing (Figure 2.11B). Moreover, four of eight BM APC-dependent TCRs expressed on *Rag1*$^{-/-}$ thymocytes *in vivo* also facilitated Treg

cell selection independent of Aire as predicted based on TCR sequencing (Figure 2.11C, D). Thus, Aire does not appear to affect Treg cell selection via a global effect on the total thymic DC population.

Batf3-dependent CD8α^+ DCs preferentially acquire and present Aire-dependent antigens to mediate Treg cell selection

BM APCs play a major role in Aire-dependent and -independent Treg cell selection (Figure 2.10C). As there are a number of distinct cell types within the BM APC population, we sought to identify the subset(s) relevant to Treg cell selection. Our data using retroviral TCR expression in thymocytes suggested that the major BM APC subset responsible for Treg cell selection were CD11c$^+$ DCs (Figure 2.9). Thymic CD11c$^+$ DCs can be subdivided into two primary subsets, the SIRPα^+ DCs and CD8α^+ DCs, which may be functionally redundant because they both acquire and present blood-derived antigens (Atibalentja et al., 2011). To test whether CD8α^+ DCs were necessary for Treg cell selection, we used a retroviral vector to express BM APC-dependent Treg cell TCRs in *Rag1*$^{-/-}$ thymocytes and intrathymically transferred these cells into CD8α^+ DC-deficient *Batf3*$^{-/-}$ hosts (Figure 2.12) (Hildner et al., 2008). We observed that CD8α^+ DCs were required for four out of eight BM APC dependent TCRs tested (Figure 2.13A). By contrast, depletion of plasmacytoid DCs in the thymus had no effect on Treg cell selection of 4 BM APC-dependent TCRs (Figure 2.13B). We conclude that in a polyclonal repertoire, CD8α^+ DCs and SIRPα^+ DCs play non-redundant roles in Treg cell selection.

CD8α^+ DCs were required for Treg cell selection of TCRs co-dependent on Aire and BM APCs, as all four CD8α^+ DC-dependent Treg cell TCRs were Aire-dependent, whereas all 4 CD8α^+ DC-independent Treg cell TCRs were Aire-independent (Figure 2.11B-D; 2.13A). To assess whether our observations reflect antigen transfer from mTECs to CD8α^+ DCs, we generated BM chimeras in which host cells (i.e. mTECs) expressed GFP under the chicken beta actin promoter, and analyzed the acquisition of GFP by congenically marked donor DCs. We found that CD8α^+ DCs acquired significantly more GFP than SIRPα^+ DCs, consistent with antigen transfer from mTECs to CD8α^+ DCs (Figure 2.13C). However, it is possible that the increased amount of GFP in CD8α^+ DCs might reflect a differential ability to degrade GFP. Therefore, we tested whether host cell-generated antigens could be presented on MHCII of donor cells by generating BM chimeras with H-2^b donors into H-2^d hosts and assessing the presentation of host derived Eα on donor I-Ab using the monoclonal antibody Y-Ae (Humblet et al., 1994; Rudensky et al., 1991). Indeed, CD8α^+ DCs presented more Eα on I-A^b than SIRPα^+ DCs, corroborating our hypothesis that CD8α^+ DCs are more efficient at acquiring and presenting mTEC-derived antigens (Figure 2.13D). Taken together, these findings suggest that CD8α^+ DCs show an enhanced ability compared with SIRPα^+ DCs to acquire and present antigens from thymic epithelial cells. Thus, our results indicate that CD8α^+ DCs play an important role in acquiring and presenting Aire-dependent antigens for thymic Treg cell development.

Figure Legends

Figure 2.1. TCR sequencing output for MHC II-deficient, C2TAkd, and control mice.

(A) 454 pyrosequencing of TCRs from MHC II deficient (def.) BM and C2TAkd chimeras and the corresponding controls which are wild-type (WT) for MHC expression. Chimeras were generated using TCliβ *Tcra*$^{+/-}$ (MHC II def. or WT) TCR transgenic donors. After 6 weeks, Foxp3^{+} (CD4^{+}CD8^{-}Foxp3^{gfp+}) and Foxp3^{-} (CD4^{+}CD8^{-} CD62L^{hi}CD24^{lo}Foxp3^{gfp-}) cells were sorted and the TCRs sequenced by 454 pyrosequencing. (B) Effect of filtering TCRs that are found > 0.1% in at least one mouse in a given condition. Shown are plots of the total frequency captured by the filtered TCRs (left) and the average frequency in a given experimental condition of the TCRs lost by this filtering criteria in the WT → WT Treg and Tconv repertoires (right).

Figure 2.2. Both BM and mTEC APCs mediate negative selection.

(A) Changes in Tconv TCR frequency with manipulation of MHC II expression on BM APCs or mTECs. Data shown are the frequency of Foxp3^{-} CD4SP TCRs in MHC II deficient (def) BM or C2TAkd chimeras cross-referenced with their frequency in control chimeras, which are wild-type (WT) for MHC expression. Red dots indicate TCRs that were significantly different ($p < .05$) by Mann-Whitney U test. (B) Summary of effects on the Tconv cell TCR repertoire with modulating MHC II expression on mTECs or BM APCs. Data shown are the percentage of unique TCRs (top) or total sequences (bottom) in the filtered data set that are negatively selected based on the following criteria (statistically significant effect; ≥ 80% decrease in WT frequency). (C) Principal

component analysis of the TCR frequencies. Red dots/arrow form a cluster of TCRs (variances: MHC II def. BM = 27.5%, C2TAkd = 11.1%) that correlate with, but are not necessarily identical to, the negatively selected TCRs in (A). Similarly, black dots/arrow represents TCRs unaffected by deficiency of MHC II in a given APC, and blue dots/arrow represent TCRs enriched in WT mice relative to C2TAkd mice (variance = 12.6%). Centroids represent the middle of a given cluster. A shorter line represents greater similarity to the centroid. Data represent three independent experiments with 2-3 replicates per experiment.

Figure 2.3. Treg cell TCR sequencing of MHC II-deficient and C2TAkd mice.

(A) Changes in Treg cell TCR frequency with manipulation of MHC II expression on BM APCs or mTECs. Similar to Figure 1A, data shown are the frequency of Foxp3$^+$ CD4SP TCRs in MHC II def. BM or C2TAkd chimeras cross-referenced with their frequency in WT chimeras. Red dots indicate TCRs that were significant ($p < .05$) by Mann-Whitney U test. (B) Summary of effects on the Treg cell TCR repertoire, with modulating MHC II on mTECs or BM APCs. Data shown are the percentage of unique TCRs (top) or total sequences (bottom) in the filtered data set that are interpreted to undergo APC-dependent negative selection (left), or Treg cell selection (right), based on the following criteria: statistical significance (as judged by Mann-Whitney U test) and ≥ an 80% percent change in frequency versus WT. (C) Principal component analysis of the TCR frequencies. Like Figure 1C, red dots/arrow correlate with negatively selected TCRs (variances: MHC II def. BM = 17.5%, C2TAkd = 11.6%), black dots/arrow

unaffected TCRs, and blue dots/arrow Treg TCRs (variances: MHC II$^{-/-}$ BM = 41.6%, C2TAkd = 28.0%).

Figure 2.4. Negative selection of an abundant BM APC-dependent Treg cell TCR.

Data represent three independent experiments with 2-3 replicates per experiment. BM APCs negatively select TCR NS1 in vivo. Data shown are representative flow cytometry plots (top) and summary (bottom) of intrathymic injection of *Rag1*$^{-/-}$ thymocytes retrovirally-transduced with NS1 and transferred into WT versus C2TAkd (left) or WT versus MHCII def. BM (right) chimeric mice (data were pooled from at least two independent experiments with 2 replicates per experiment). Mann-Whitney U test for significance, ***$p < .001$.

Figure 2.5. Negative selection of a low frequency BM APC-dependent Treg cell TCR.

(A) Distribution of NS1 and NS3 in the TCR repertoires of WT, MHC II def. BM and C2TAkd conditions. (B) NS3 is negatively selected by BM APCs. Representative FACS plots of *Rag1*$^{-/-}$ thymocytes retrovirally-transduced with TCR NS3 and transferred into the thymi of WT, MHC II def. BM and C2TAkd chimeric mice. Plots are representative of 2 independent experiments with 1-2 replicates.

Figure 2.6. Role of BM APCs and mTECs in thymic Treg cell selection.

(A, B) Morisita-Horn similarity analysis of Treg and Tconv cell TCR repertoires. In (A), the TCR repertoire from each MHC manipulation is compared with the WT

repertoire, whereas in (B) the comparison is between the MHC II def. BM APC and C2TAkd repertoires. An index value of 1 indicates that the two samples are completely similar whereas an index value of 0 means they are completely dissimilar. (C) Analysis of individual Treg cell TCRs from the WT condition. The top 15 individual Foxp3$^+$ CD4SP TCRs from aggregated WT data sets are shown sorted by frequency, along with the corresponding frequency in the C2TAkd or MHC II def. BM Treg TCR repertoires.

Figure 2.7. Behavior of the WT Treg cell TCRs across conditions.

Amino acid sequence of the top 15 WT TCRs and their frequencies in the WT, MHC II def. BM, and C2TAkd Treg and Tconv cell data sets.

Figure 2.8. mTEC antigen presentation is required for in vivo Treg cell selection of certain TCRs.

(A) Analysis of individual Treg cell TCRs from C2TAkd chimeras. The top 15 Foxp3$^+$ TCRs in the C2TAkd dataset are shown sorted by frequency, along with the corresponding frequency in the WT and MHC II def. BM datasets. (B) Change in Morisita-Horn index with removal of most common TCRs. Similarity between Foxp3$^+$ TCR repertoires of C2TAkd versus WT (left) and MHC II def. BM APC versus WT (right) were assessed after removing the top 1, 2, or 3 highest frequency WT TCRs from the analysis. (C) In vivo validation of Treg cell TCRs dependent on mTEC antigen presentation. Three high frequency mTEC-dependent Treg TCRs were identified by sequencing, including G126, a common C2TAkd Treg TCR that is reduced in frequency in comparison with WT (Figure 3A). These TCRs were assessed for their ability to

facilitate Treg cell selection after transduction into *Rag1*$^{-/-}$ thymocytes, which were then injected into the thymi of WT or C2TAkd hosts. After 2.5 weeks, donor T cells were analyzed for Foxp3 expression by flow cytometry gating on CD45.1^{+} CD45.2^{-} Vα2^{+} CD4SP cells. Data were pooled from at least two independent experiments with 2 replicates per experiment.

Figure 2.9. DCs are the primary BM APC subset involved in Treg cell selection.

The top 5 WT Treg cell TCRs, of which the top 4 are BM APC-dependent, were retrovirally transduced into *Rag1*$^{-/-}$ thymocytes and then intrathymically injected into WT, CD11c-Cre ROSA-DTA, or C2TAkd hosts. Data shown are representative flow cytometry plots (left) and summary graphs (right) with each dot representing the data from one host. Each TCR was analyzed in at least 2 independent experiments with 2-3 replicates. Mann-Whitney U test for significance, **p < .01, ***p < .001, ns = not significant.

Figure 2.10. Role of Aire in Tconv and Treg cell selection and deletion.

(A) Changes in TCR frequency with Aire. The frequencies of Foxp3^{-} (top panel) and Foxp3^{+} (bottom panel) TCRs in WT and *Aire*$^{-/-}$ mice are plotted as per Figure 1A and 2A. Red dots indicate TCRs that are significantly different by Mann-Whitney U (p < .05). (B, C) Summary of the effects of Aire on the TCR repertoire. Data shown are the percentage of unique TCRs (top) or total sequences (bottom) interpreted to undergo Aire-dependent negative selection (B) or Treg cell selection (C), as described in Figures 1B and 2C.

Figure 2.11. Aire-dependent Treg cell selection is mediated through both mTEC- and BM APC-dependent pathways.

(A) Morisita-Horn similarity analysis of Treg cell TCR repertoires from *Aire*$^{-/-}$ versus WT mice (top), or MHC II def. BM (bottom) or C2TAkd (middle), with leave-one-out analysis as per Figure 3B removing the top 1, 2, or 3 highest frequency *Aire*$^{-/-}$ TCRs. (B) Analysis of the top 15 WT Treg cell TCRs for their dependence on BM APCs, mTECs, and Aire. The heatmap shows the effect of an indicated experimental condition on an individual TCR (% of TCR in condition / [% in WT + % in condition]). Values < 0.5 indicate a loss of the TCR in the condition (green color), implying that the Treg cell TCR is dependent on the condition. Red represents values > 0.5 indicating enrichment of TCR in condition relative to WT, suggestive of negative selection. (C) *In vivo* analysis of BM APC and mTEC dependent Treg cell TCRs. Treg cell differentiation in response to Aire was assessed using *Rag1*$^{-/-}$ thymocytes transduced with retrovirus expressed Treg cell TCRs showing varying dependence on Aire, BM APCs, and mTECs by TCR repertoire analysis. Each dot represents data from a single host. Mann-Whitney U test, ***$p < .001$. (D) Representative FACS plots of (C). Data are representative of at least 2 independent experiments with 1-3 replicates per experiment.

Figure 2.12. Deletion of CD8α^+ DCs in Batf3$^{-/-}$ mice.

FACS plots of CD8α^+ and SIRPα^+ DCs from the thymi of *Batf3*$^{+/-}$ or *Batf3*$^{-/-}$ mice. Plots are representative of 4 replicates.

Figure 2. 13. CD8α^+ DCs preferentially acquire and present Aire-dependent antigens to developing Treg cells.

(A) *In vivo* analysis of the role of CD8α^+ DCs in Treg selection of TCRs that are dependent on both BM APC and Aire. *Rag1*$^{-/-}$ thymocytes expressing TCRs were injected into the thymi of *Batf3*$^{-/-}$ or WT hosts. (B) Plasmacytoid DCs are not required for Treg cell differentiation of Aire and BM APC co-dependent Treg TCRs. As per (A), except the Treg TCRs were tested in BDCA2^{DTR} mice treated with diphtheria toxin (120 ng/mouse) or PBS. (C) Protein transfer from radioresistent host thymic cells to CD8α^+ and SIRPα^+ DCs. BM chimeras of Ly5.1 (donor) into Actin-GFP (host) mice were harvested after 4 weeks. Thymi were digested and the presence of host-derived GFP in donor DCs was assessed. Representative flow cytometry histogram overlays and pooled data are shown. (D) Antigen transfer from radio-resistant thymic epithelial cells to CD8α^+ DCs. BM chimeras of Ly5.1 H-2^b (donor) into H-2^d (host) mice were harvested after 4 weeks. The presence of host-derived Eα 52-68 peptide bound to I-A^b on donor DCs was assessed using the Y-Ae antibody. Mann-Whitney U test for significance, *p < .05, **p < .01, ***p < .001, ns = not significant. Plots shown are pooled data from at least two experiments with 1-3 replicates per experiment. Each dot represents data from an individual host.

Figures

A

	Foxp3$^-$				Foxp3$^+$			
Chimera	n mice (n expts)	Sorted # x10^3 Mean (SE)	# of reads	Unique # of TCRs	n mice (n expts)	Sorted # x10^3 Mean (SE)	# of reads	Unique # of TCRs
WT → WT	7 (3)	420 (35)	19762	4558	7 (3)	35 (4)	21545	1451
MHC II def. → WT	7 (3)	613 (55)	18276	5021	7 (3)	41 (4)	17480	1488
WT → WT	6 (3)	540 (40)	10960	1978	6 (3)	36 (1)	6694	768
WT → C2TAkd	7 (3)	345 (22)	13029	2173	7 (3)	22 (3)	9941	734

B

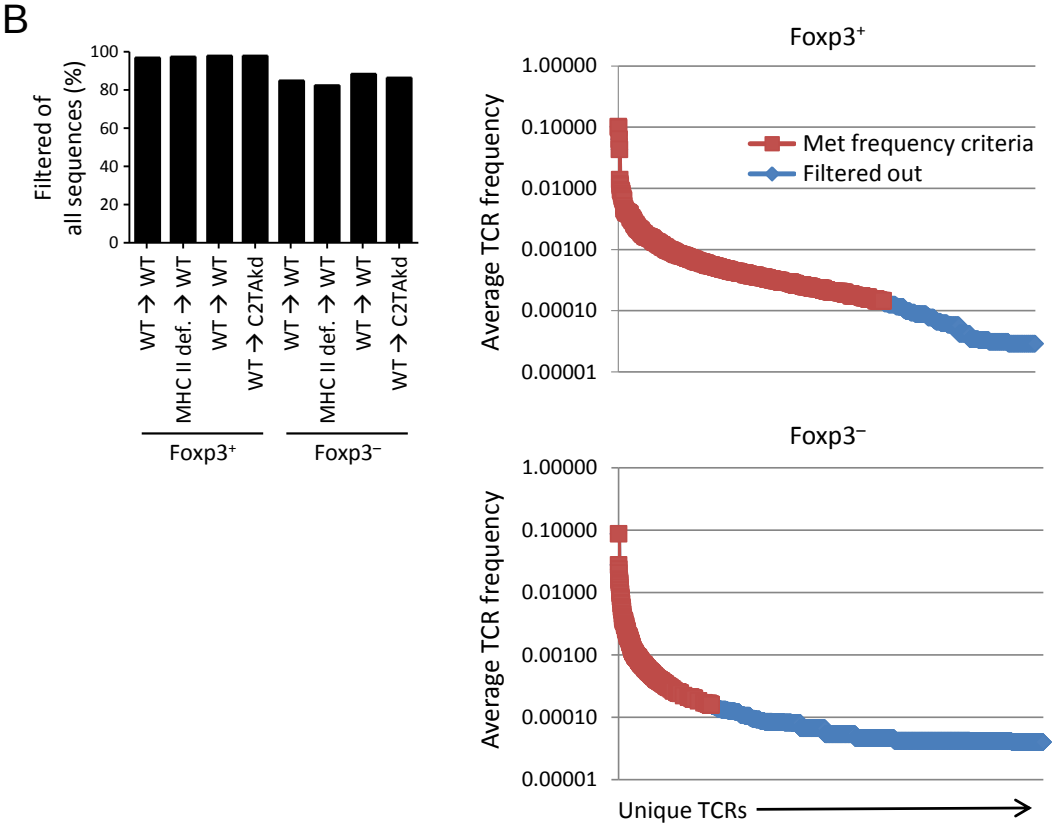

Figure 2 1. TCR sequencing output for MHC II-deficient, C2TAkd, and control mice.

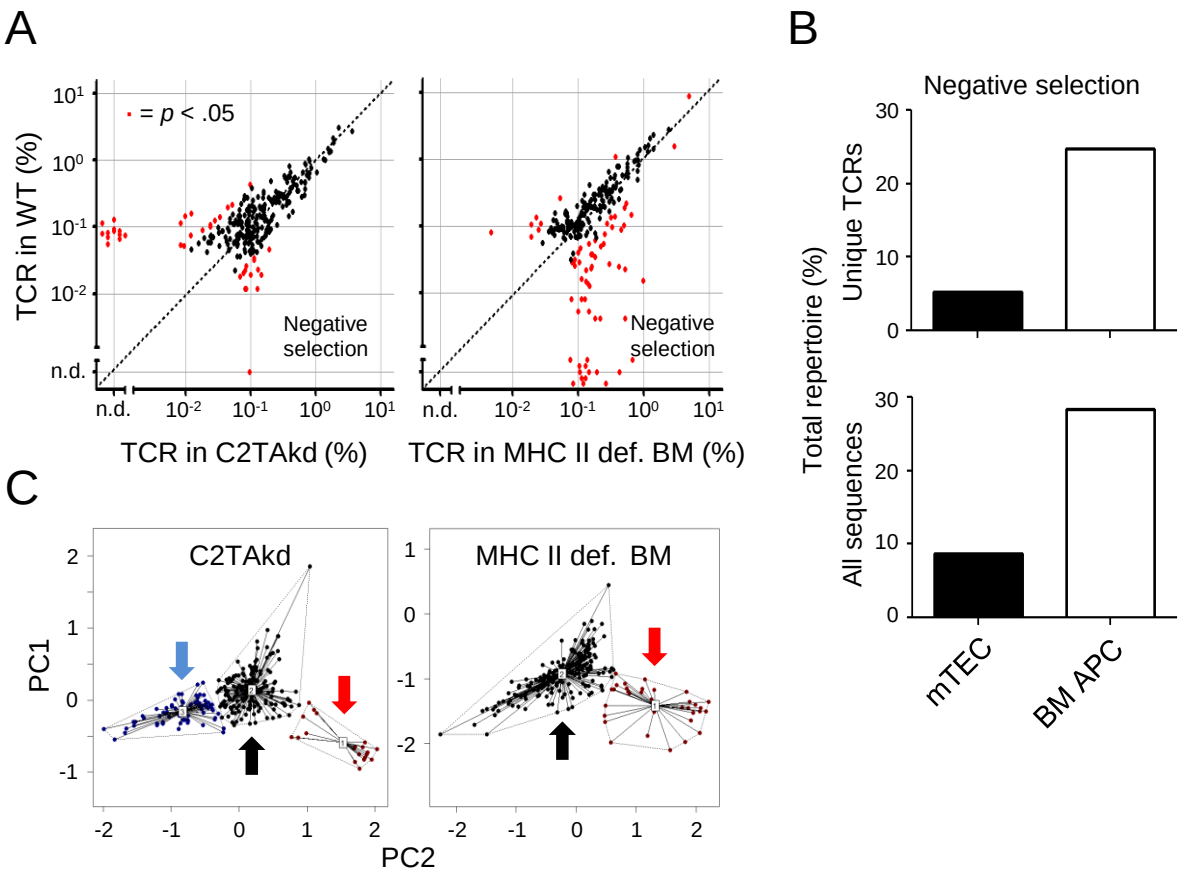

Figure 2 2. Both BM and mTEC APCs mediate negative selection.

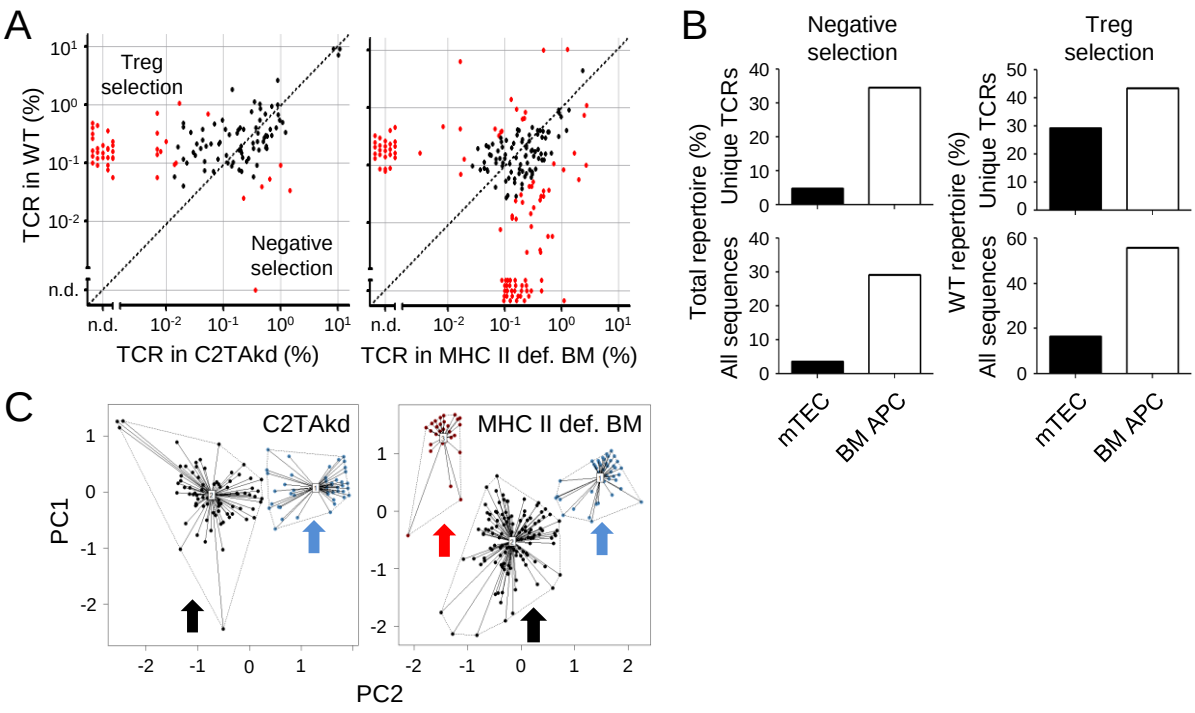

Figure 2 3. Treg cell TCR sequencing of MHC II-deficient and C2TAkd mice

.

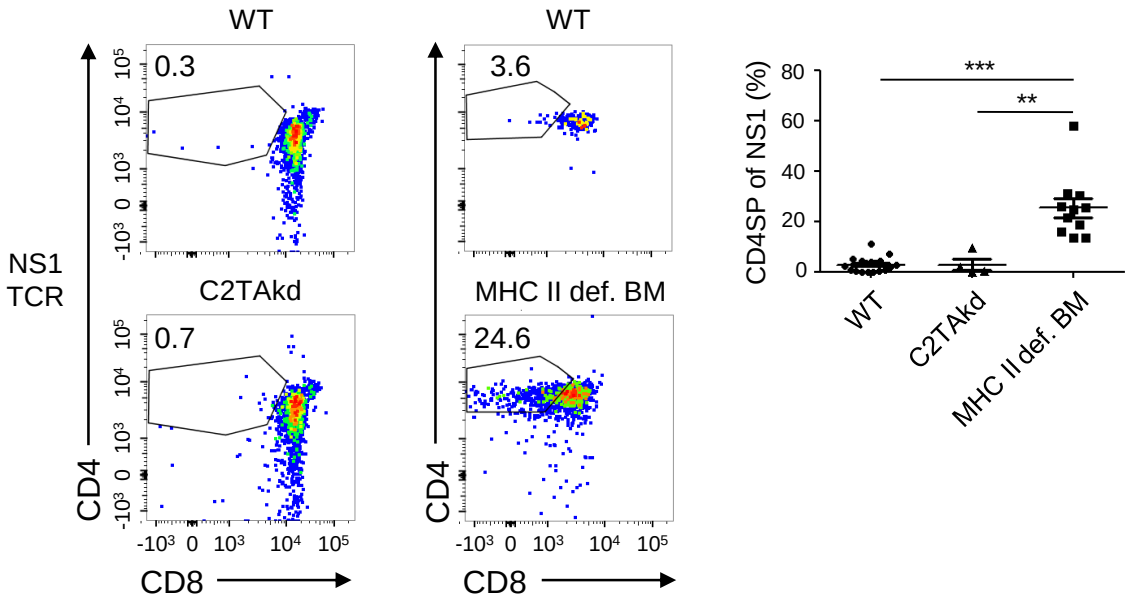

Figure 2 4. Negative selection of an abundant BM APC-dependent Treg cell TCR.

A

	Expt.	CDR3 a.a. sequence	Frequency of TCR: Wild Type % (SD)	MHC II def. BM % (SD)	C2TAkd % (SD)
Foxp3+	NS1	AASGSNNRIF	0.10 (0.2)	2.70 (0.8)	0.04 (0.0)
	NS3	AARGTGGYKVV	0.08 (0.1)	1.67 (1.0)	0.00 (0.0)
Foxp3−	NS1	AASGSNNRIF	0.00 (0.0)	0.01 (0.0)	0.00 (0.0)
	NS3	AARGTGGYKVV	0.00 (0.0)	0.02 (0.0)	0.00 (0.0)

B

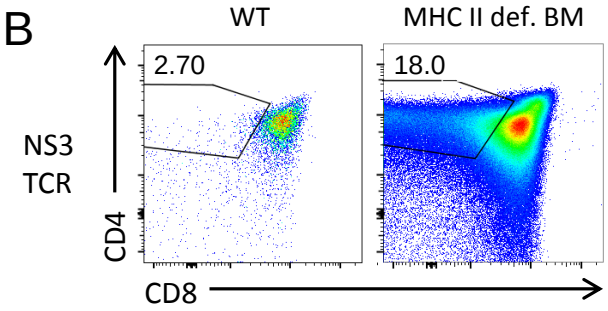

Figure 2 5. Negative selection of a low frequency BM APC-dependent Treg cell TCR.

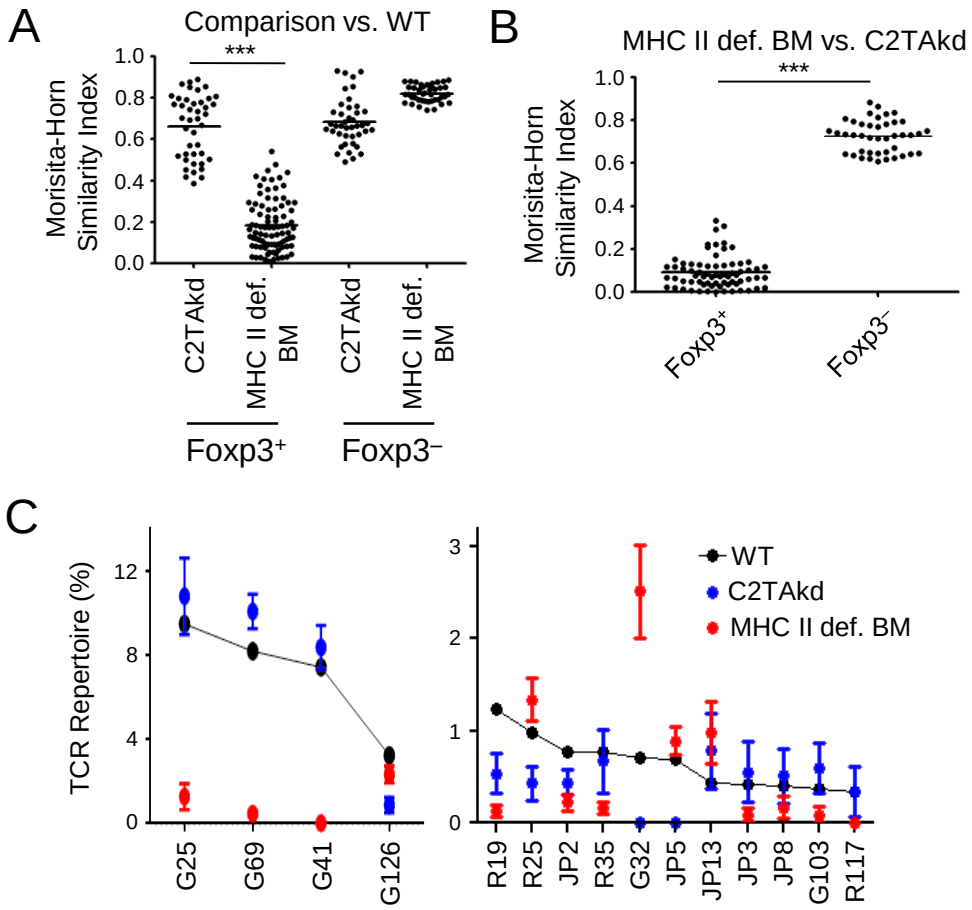

Figure 2 6. Role of BM APCs and mTECs in thymic Treg cell selection.

Frequency of Top 15 WT Foxp3$^+$ CD4$^+$ TCR in indicated subsets

		Wild Type		MHC II def. BM		C2TAkd	
TCR Name	CDR3 a.a. sequence	Foxp3$^+$ Mean (SD)	Foxp3$^-$ Mean (SD)	Foxp3$^+$ Mean (SD)	Foxp3$^-$ Mean (SD)	Foxp3$^+$ Mean (SD)	Foxp3$^-$ Mean (SD)
G25	AASADYSNNRLT	9.49 (2.4)	0.00 (0.0)	1.28 (1.6)	0.52 (0.2)	10.81 (4.8)	0.01 (0.0)
G69	AARNYNQGKLI	8.19 (3.0)	0.01 (0.0)	0.48 (0.3)	0.02 (0.0)	10.08 (2.2)	0.01 (0.0)
G41	AASAGYSNNRLT	7.44 (2.5)	0.00 (0.0)	0.02 (0.0)	0.98 (0.3)	8.38 (2.7)	0.01 (0.0)
G126	AANSGTYQR	3.24 (2.4)	0.00 (0.0)	2.33 (1.1)	0.00 (0.0)	0.88 (1.0)	0.00 (0.0)
R19	AASSGTYQR	1.24 (0.8)	0.10 (0.0)	0.13 (0.2)	0.50 (0.1)	0.54 (0.6)	0.07 (0.1)
R25	AASFYNQGKLI	0.99 (0.8)	0.00 (0.0)	1.34 (0.6)	0.03 (0.0)	0.43 (0.5)	0.00 (0.0)
JP2	AAKGNNNAPR	0.77 (0.6)	0.00 (0.0)	0.22 (0.2)	0.13 (0.0)	0.44 (0.4)	0.00 (0.0)
R35	AASSDYSNNRLT	0.76 (0.5)	0.02 (0.0)	0.16 (0.2)	0.02 (0.0)	0.96 (1.6)	0.00 (0.0)
G32	AASAGNYAQGLT	0.70 (0.7)	0.31 (0.2)	2.51 (1.3)	0.05 (0.0)	0.01 (0.0)	0.47 (0.3)
JP5	AAKSGSFNKLT	0.70 (0.7)	0.00 (0.0)	0.89 (0.4)	0.00 (0.0)	0.89 (1.7)	0.00 (0.0)
JP13	AASVSGSFNKLT	0.44 (0.5)	0.04 (0.0)	0.98 (0.9)	0.30 (0.1)	1.21 (2.1)	0.05 (0.0)
JP3	AAKDNNNAPR	0.43 (0.2)	0.01 (0.0)	0.09 (0.2)	0.08 (0.0)	0.84 (1.6)	0.00 (0.0)
JP8	AARGTNAYKVI	0.40 (0.4)	0.00 (0.0)	0.17 (0.3)	0.14 (0.0)	1.08 (2.2)	0.01 (0.0)
G103	AASAQTGGYKVV	0.38 (0.4)	0.02 (0.0)	0.09 (0.2)	0.02 (0.0)	0.59 (0.7)	0.05 (0.0)
R117	AASLDYSNNRLT	0.33 (0.3)	0.00 (0.0)	0.00 (0.0)	0.15 (0.0)	0.34 (0.7)	0.00 (0.0)

Figure 2 7. Behavior of the WT Treg cell TCRs across conditions.

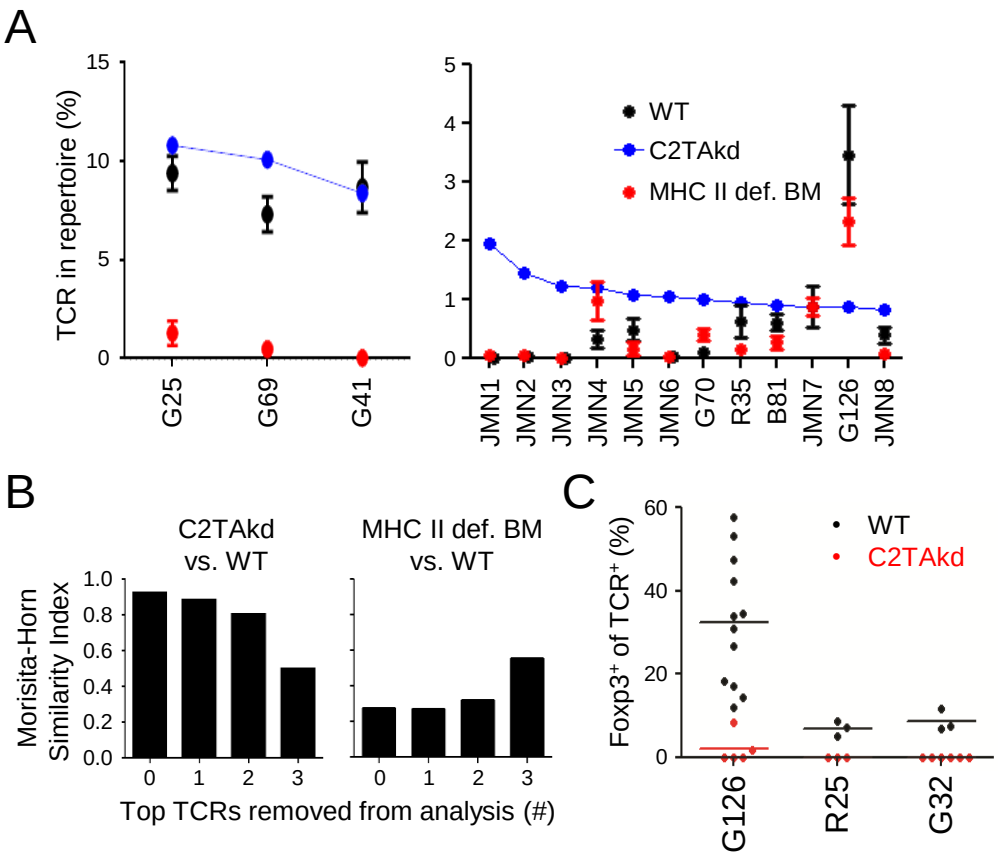

Figure 2 8. mTEC antigen presentation is required for in vivo Treg cell selection of certain TCRs.

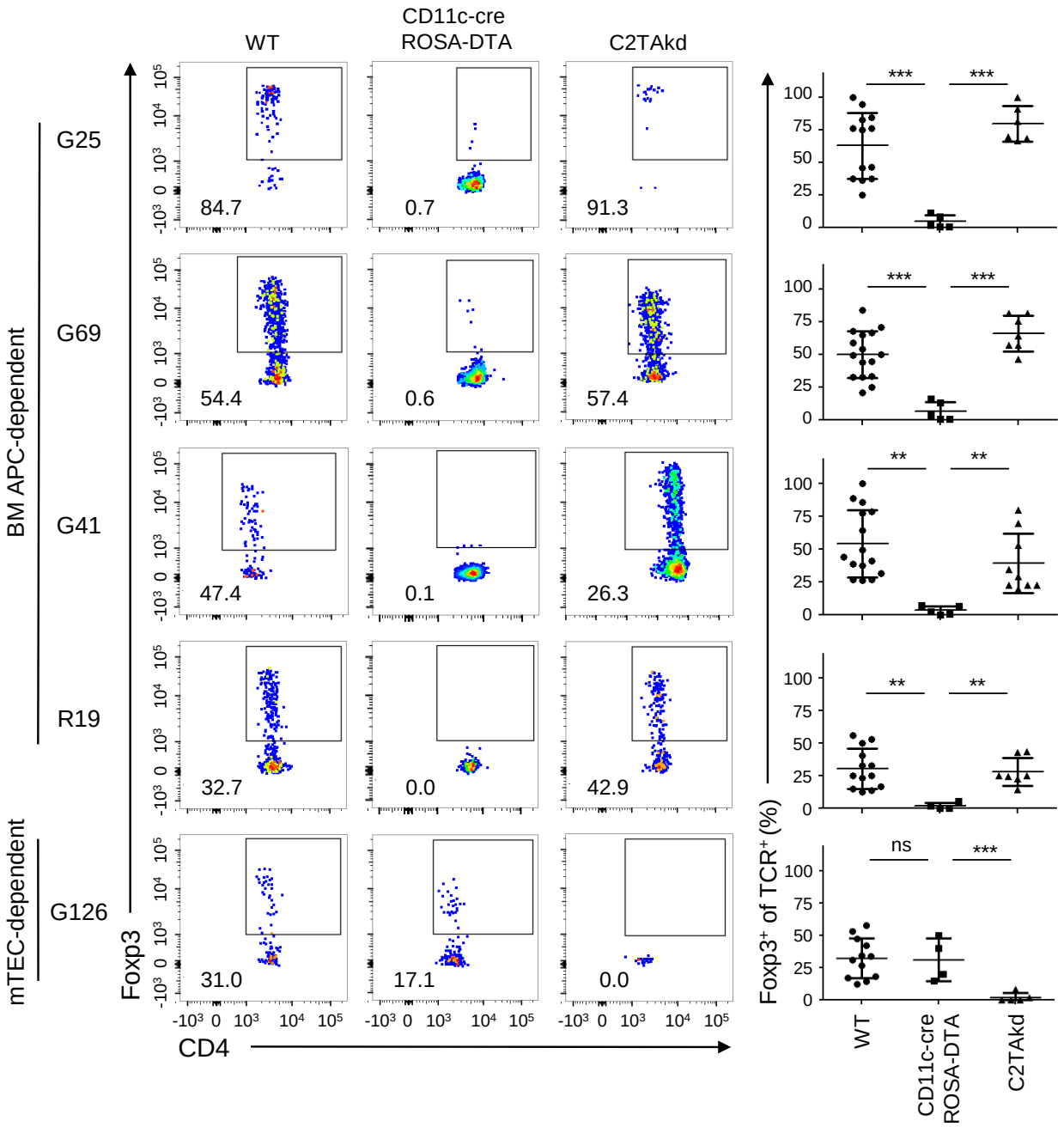

Figure 2 9. DCs are the primary BM APC subset involved in Treg cell selection.

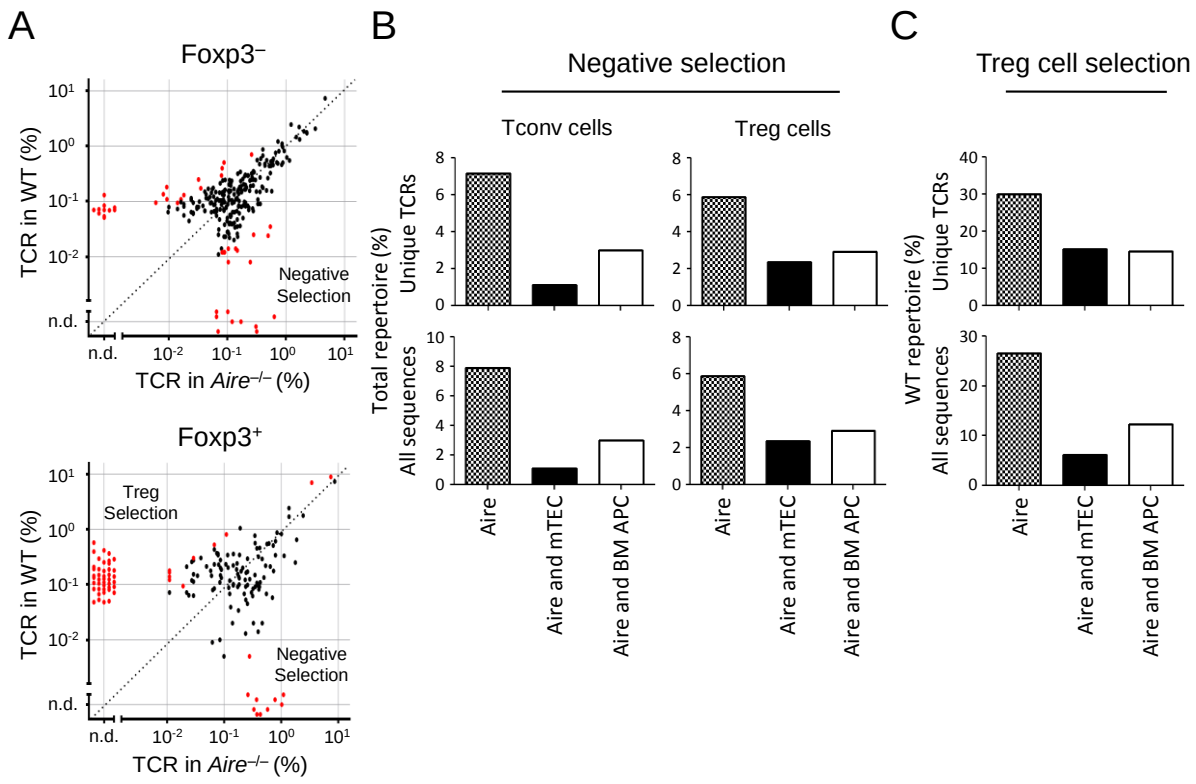

Figure 2 10. Role of Aire in Tconv and Treg cell selection and deletion.

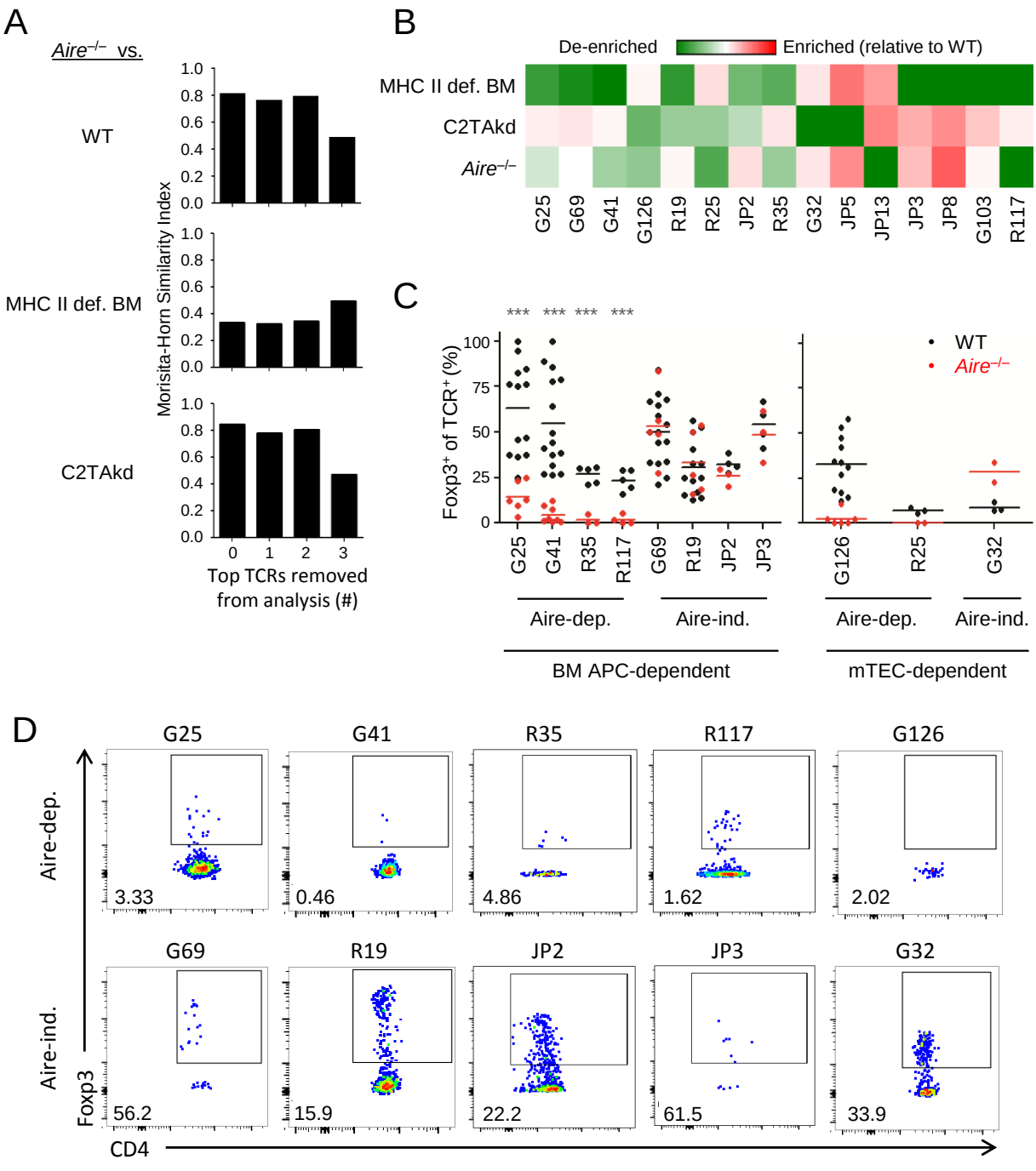

Figure 2 11. Aire-dependent Treg cell selection is mediated through both mTEC- and BM APC-dependent pathways.

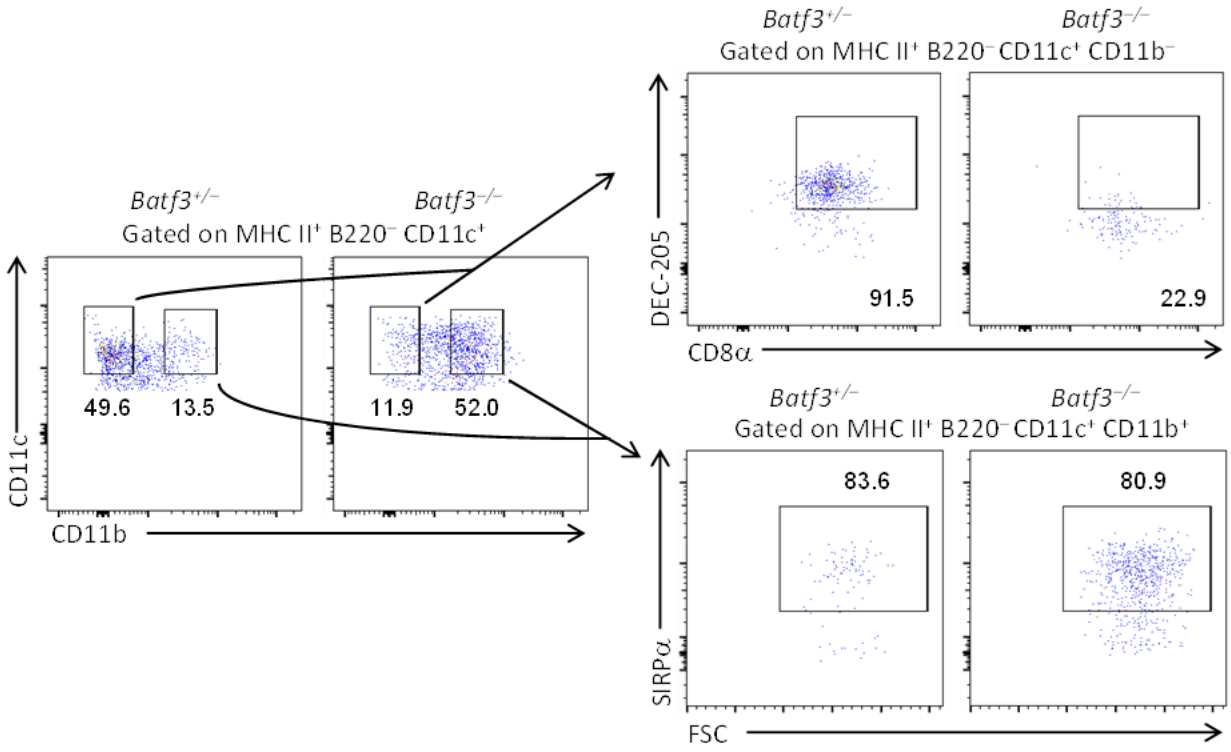

Figure 2 12. Deletion of CD8α^+ DCs in *Batf3*$^{-/-}$ mice.

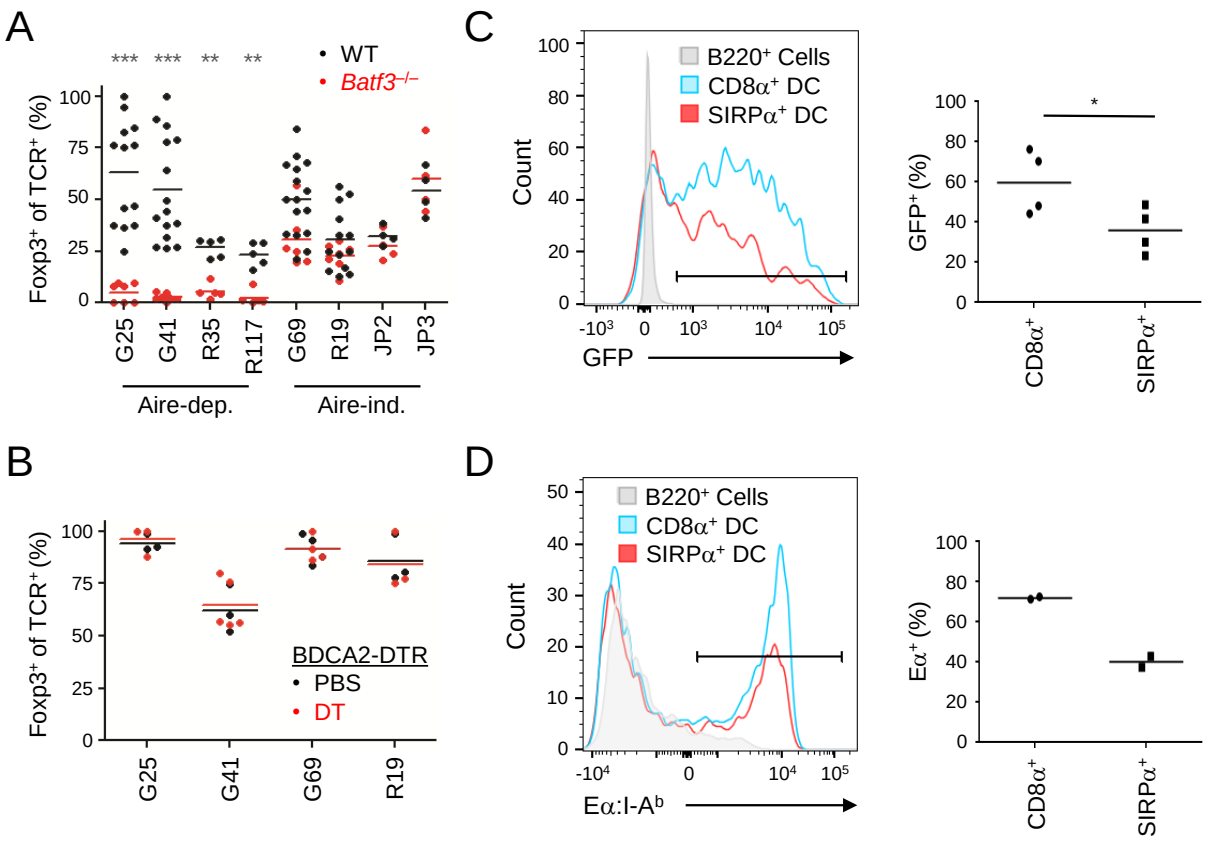

Figure 2 13. CD8α$^+$ DCs preferentially acquire and present Aire-dependent antigens to developing Treg cells.

Discussion

Thymocyte encounter with self-antigen in the thymic medulla is crucial for the generation of self-tolerance – a process notable for its involvement of a myriad of APCs and transcription factors. Although previous work has suggested contributions of each APC subset and Aire to T cell tolerance at a population level, it remained unclear if these components functioned uniquely or redundantly. Here, we made several observations regarding $CD4^+$ T cell tolerance by analyzing TCR repertoires in a fixed TCRβ model. First, mTECs and BM APCs make non-redundant contributions to deletion and Treg cell selection, suggesting that each APC subset differs in the self-antigens that they functionally display. Within the BM APC population, $CD11c^+$ DCs were the primary subset involved in Treg cell selection. Second, Aire expression in mTECs affected both deletion and Treg cell selection. However, Aire had a greater impact on lower frequency TCRs, which may explain previous conflicting reports depending on whether the analysis favored more global versus individual T cell clonal assessments. Third, the presentation of antigens induced by Aire occurred by both BM APCs and mTECs. Because Aire is not expressed in BM cells, this implies that antigen transfer is a major mechanism involved in Aire-dependent tolerance. Finally, of the thymic DC subsets, Batf3-dependent $CD8\alpha^+$ DCs were primarily responsible for taking up Aire-dependent antigens from mTECs for inducing Treg cell selection. Thus, these data reveal a remarkable complexity and interdependence between Aire and the medullary APC subsets.

The extent of negative selection by BM APCs and mTECs estimated by our TCR repertoire analysis is within range of previous estimates. For example, it has been

suggested that BM APCs may delete up to half of the positively selected $CD4^+$ T cell population based on the observation that chimeras with MHC II deficient BM donors had anywhere from 50% (Hinterberger et al., 2010) to 70% (van Meerwijk et al., 1997) greater CD4SP cell numbers. Similar results were reported for genetic depletion of DCs (Ohnmacht et al., 2009) and deletion of MHC II on DCs (Liston et al., 2008). However, a recent report by Hogquist et al incorporating mathematical modeling suggests that only ~10% of CD4SP cells undergo negative selection in total (Sawicka, 2014). For mTEC-mediated negative selection, it was reported that C2TAkd mice have an increase of ~20% in CD4SP cells, and ~46% in Treg cells (Hinterberger et al., 2010).

Our TCR repertoire analysis suggested that around ~30% and ~10% of the CD4SP population were negatively selected by BM APCs and mTECs, respectively. This is based primarily on our estimates of negative selection in Tconv cells, as negatively selected Treg cells are $1/10^{th}$ in number. Potential differences between these various estimates could arise from the different analytic approaches. For example, extrapolating negative selection from changes in CD4SP cell numbers may not account for differences in cell survival, proliferation, or emigration. Additionally, our use of a fixed TCRβ chain may not entirely reflect the WT TCR repertoire. However, data from previous groups using limited repertoire models have generally been consistent (Hsieh et al., 2004; Pacholczyk et al., 2007; Wong et al., 2007), albeit sometimes with different interpretations (Hsieh et al., 2012a; Klein et al., 2014). The use of MHC II deficient BM APCs does not exclude the possibility that they may be able to acquire intact MHC II from mTECs. Finally, the use of C2TAkd may underestimate the contribution of mTECs as the blockade of MHC II synthesis is incomplete (Hinterberger et al., 2010). While

further studies are required to resolve these quantitative differences, our data support the pre-existing notion that BM APCs, and to a lesser extent mTECs, both play important and non-redundant roles in the negative selection of a substantial number of TCR clones.

By contrast, our TCR repertoire analysis revealed a major alteration in Treg cell selection imparted by BM APCs, which was unexpected based on current studies. Previously, it was suggested that BM APCs were not required for Treg cell selection as normal Treg cell frequencies or numbers occurred with expression of MHC II only on thymic cortical epithelial cells (Bensinger et al., 2001) or with ablation of MHC II on DCs (Hinterberger et al., 2010; Liston et al., 2008). Our TCR repertoire analysis suggests that BM APCs alter the composition of the thymic Treg cell repertoire without changing overall Treg cell numbers by facilitating both the addition and removal of TCR clones from the Treg cell population.

Our data may help resolve an ongoing controversy regarding the role of Aire in Treg cell selection. Some have argued against a role for Aire in Treg cell selection based on normal polyclonal Treg cell numbers (Anderson et al., 2005) and minimal change in the global TCR repertoire in a limited TCR repertoire model (Pacholczyk et al., 2007). Others have reported that there are differences in Treg cell numbers in Aire-deficient mice (Lei et al., 2011), and that two TCR transgenic lines were dependent on Aire for thymic Treg cell selection (Malchow et al., 2013). Our TCR repertoire analysis suggests that Aire affects both Treg cell selection and deletion. However, because Aire more commonly affects lower frequency TCRs, its effect is likely masked when

analyzing bulk Treg cell numbers or TCR repertoire similarity using abundance weighted assessments.

In addition to addressing the role of Aire on Treg cell selection, we quantified the antigen presentation requirements for Aire by cross-referencing sequences from Aire and APC data sets. Our observation of mTEC and Aire co-dependent Treg cell TCRs is consistent with recent studies showing that antigens expressed in mTECs can be autologously presented via an autophagy-dependent pathway (Aichinger et al., 2013b; Nedjic et al., 2008a). Unexpectedly, we also found that many Aire-dependent Treg cell TCRs were dependent on BM APCs. Because Aire is not expressed in BM APCs, our findings suggest that mTEC antigens are transferred to BM APCs, a phenomenon that has been observed at the level of individual antigens using TCR transgenic models or MHC II tetramers (Gallegos and Bevan, 2004; Hubert et al., 2011; Koble and Kyewski, 2009a; Taniguchi et al., 2012). Our data suggests that the process of antigen-transfer is quite common, being involved in approximately 50% of Aire-dependent deletion and Treg cell selection.

Because the TCR repertoire studies were performed at the level of individual TCRs, we were able to utilize sequencing results to isolate representative TCRs to further interrogate the BM APC population involved in the transfer and presentation of Aire-dependent antigens. Our *in vivo* analysis of TCRs that were co-dependent on BM APC and Aire revealed that CD8α^+ DCs were required for antigen transfer-mediated Treg cell selection. Consistent with this, we found that CD8α^+ DCs were more efficient at acquiring I-Eα and the neo-self antigen GFP from thymic stromal cells than SIRPα^+ DCs. Although previous work demonstrates that CD8α^+ and SIRPα^+ DCs equivalently

present blood-derived antigens (Atibalentja et al., 2011), our results suggest that CD8α^+ DCs may have additional properties that facilitate antigen transfer from mTECs. One such property may be the expression of the chemokine receptor XCR1 by thymic CD8α^+ DCs, which recognizes XCL1 produced by mTECs in an Aire-dependent manner (Lei et al., 2011) and could facilitate DC:mTEC interactions. Taken together, these data suggest that Batf3-dependent CD8α^+ DCs are the primary BM APC subset responsible for antigen transfer-mediated Treg cell selection of Aire-dependent antigens.

Batf3-deficiency was previously reported to result in the loss of the CD8α^+ DC subset by phenotypic markers and functional assays in the periphery (Hildner et al., 2008). Similarly, we observed functional deficiencies in the selection of certain Treg TCR clones associated with loss of phenotypic CD8α^+ DCs. However, our data cannot definitively exclude the possibility that DCs in the CD8α^+ lineage remain with altered function and cell-surface phenotype in Batf3 deficient mice. It is worth noting that the difference in CD8α^+ and SIRPα^+ DCs in presenting mTEC derived antigens may be quantitative, as we did see antigen transfer occur with both DC subsets. Further studies will be required to address the role of SIRPα^+ DCs in T cell selection at the clonal level.

Another distinct property of CD8α^+ DCs is that they are much more efficient at cross-presenting exogenous antigens onto MHC I than other DC subsets (Hildner et al., 2008; Joffre et al., 2012; Proietto et al., 2008a). It is notable that thymic deletion of MHC I restricted T cells has also been shown to occur via antigen transfer to BM APCs (Gallegos and Bevan, 2004; Hubert et al., 2011). Thus, we speculate that the ability to cross-present would allow CD8α^+ DCs to efficiently educate both CD4$^+$ and CD8$^+$ T cells to self-antigens acquired from Aire-expressing mTECs.

If CD8α^+ DCs play an important role in Treg cell selection, why has spontaneous autoimmunity not been reported for *Batf3*$^{-/-}$ mice? In this regard, it is interesting to note that immunopathology is reportedly mild in *Aire*$^{-/-}$ mice on the same C57BL/6 background as the mice in our study (Hubert et al., 2009). For *Batf3*$^{-/-}$ mice, an additional possibility is that CD8α^+ DCs are required both for selection in the thymus and activation of the same TCR specificities in the periphery (Klein et al., 2014). Future studies are required to address these possibilities.

In summary, our analysis of a fixed TCRβ repertoire provides insights into how medullary APCs and Aire educate the developing T cell population. We have shown that both mTECs and BM APCs make non-overlapping contributions to thymic deletion and Treg cell selection to shape the mature CD4$^+$ T cell population, and that Aire-mediates its effects via both BM and mTEC antigen presentation. Furthermore, we have demonstrated that of the BM APCs, CD8α^+ DCs primarily acquire and present Aire-dependent antigens to developing Treg cells. However, it remains unclear why certain Aire-dependent TCRs undergo Treg cell selection on mTECs and others on BM APCs. Is it because some antigens are more readily loaded onto MHC II via macroautophagy for autologous presentation on mTECs, whereas other antigens are not? Are there specific features of Aire-dependent antigens such as cell surface association that favor transfer to CD8α^+ DCs? Thus, future experiments are required to understand the mechanistic and functional rationale for the transfer of Aire-dependent antigens from mTECs to CD8α^+ DCs in mediating central tolerance.

CHAPTER 3

Necessity of antigen transfer from Aire-dependent mTECs to CD8α+ DCs for T cell tolerance

The results in this chapter describing the role of CD8α^+ DCs for thymic T cell tolerance are adopted from a manuscript submitted for publication.

Abstract

Generation of T cell tolerance is mediated in part through cooperative antigen presentation between bone marrow and mTECs in the thymus. However, the mechanisms by which this occurs remain unknown. Here, we show that Batf3-dependent CD8α^+ DCs facilitate thymic tolerance via negative selection and Treg cell generation to antigens dependent on Aire expressed in mTECs. This tolerance is mediated in part by CD36, a scavenger receptor preferentially expressed by CD8α^+ DCs. Notably, CD36 is important for acquisition of cell-surface, but not cytoplasmic, antigens from mTECs. These transferred antigens are likely displayed on the cell surface, as thymocytes from Batf3- or CD36-deficient donors are not tolerant to host MHC after allogenic bone marrow transplantation. Thus, these data suggest that CD36 mediates the “cross-dressing” of mTEC-derived cell-surface antigens to facilitate tolerance to self-antigens as well as allo-antigens during bone marrow transplantation.

Introduction

During T cell ontogeny, TCR gene segments are rearranged to generate a diverse TCR repertoire necessary for immunity to invading pathogens (Klein et al., 2014; Vrisekoop et al., 2014; Weissler and Caton, 2014). A consequence of this diversity is the recognition of self-antigen and the potential for autoimmunity. For T cells, two primary processes generate tolerance to self in the thymus (a.k.a. central tolerance) prior to their release into the periphery: negative selection of autoreactive TCR clones, and the generation of Treg cells (Bluestone et al., 2015; Klein et al., 2014; Li and Zheng, 2015; Richards et al., 2016). Both processes are driven by TCR recognition of self-antigens presented by APCs. Although this can occur throughout the thymus, it commonly occurs in the thymic medulla and involves both mTECs and BM-derived DCs, B cells, and macrophages (Chan and Anderson, 2015; Klein et al., 2014; Oh and Shin, 2015). Thus, a diverse array of medullary APCs is involved in thymic T cell tolerance.

The mTEC population is notable for its expression of the Autoimmune Regulator (Aire), which plays an important role in mTEC development, thymic architecture, and the ectopic expression of PTAs in the thymus (Chan and Anderson, 2015). mTECs can tolerize T cells to these PTAs via non-conventional cell-autonomous antigen presentation (Aichinger et al., 2013b; Aschenbrenner et al., 2007; Cowan et al., 2013; Hinterberger et al., 2010; Oukka et al., 1996; Perry et al., 2014). It has become increasingly clear, however, that an equally important mechanism of thymic tolerance to Aire-dependent antigens involves transfer of mTEC antigens to BM APCs (Gallegos and Bevan, 2004; Hubert et al., 2011; Koble and Kyewski, 2009a; Lin et al., 2016; Millet et al., 2008; Perry et al., 2014).

Recently, we proposed that CD8α^+ DCs may be the primary BM APC recipient of antigen transferred from mTECs (Perry et al., 2014). This is consistent with previous observations showing that XCR1-expressing CD8α^+ DCs home to mTEC-rich regions of the medulla due to mTEC-derived chemokine XCL1 (Atibalentja et al., 2011; Baba et al., 2009b; Klein et al., 2014; Lei et al., 2011). Our conclusion was based on an in vivo developmental assessment of 8 Treg cell TCRs dependent on MHC II expression on BM APCs, of which 4 TCRs were co-dependent on Aire. All 4 of the BM and Aire-co-dependent TCRs required CD8α^+ DCs for Treg cell development, suggesting that this DC subset is an important component of cooperative antigen presentation of mTEC antigens. While these data with individual TCRs serve as proof-of-principle, the effect of CD8α^+ DCs and their relationship to Aire at the level of the TCR repertoire remains unknown.

The phenomenon of antigen transfer from mTECs to BM APCs has been recognized for over two decades (Klein et al., 2014). It has been proposed that thymic epithelial cells deliver antigen through exosomes, apoptotic bodies, or direct membrane transfer (Gray et al., 2007; Humblet et al., 1994; Koble and Kyewski, 2009a; Millet et al., 2008; Skogberg et al., 2015). The specific mechanism(s) by which this occurs in the thymus remains unknown. CD8α^+ DCs, on the other hand, have been studied for their ability to cross-present and prime CD8$^+$ T cells in the periphery (Joffre et al., 2012). Several non-mutually exclusive mechanisms have been reported, including uptake of apoptotic or necrotic cells, exosome transfer, and by transfer of intact peptide/MHC complexes (a.k.a. “cross-dressing) (Wakim and Bevan, 2011). For example, the scavenger receptor CD36, which recognizes the apoptosis-induced expression of

phosphatidylserine (PS), was reported to facilitate cross-presentation to MHCI-restricted CD8 T cells by recognizing and phagocytosing apoptotic cells in one report (Albert et al., 1998) but not others (Belz et al., 2002; Schulz et al., 2002). Whether CD36 affects antigen transfer from mTECs for presentation to MHC II-restricted CD4 T cells is unknown. Thus, the mechanisms by which mTEC-derived antigens are transferred to CD8α^+ DCs remain unclear.

Although we proposed that CD8α^+ DCs are an important APC subset in thymic tolerance, Batf3-deficient mice, which are unable to generate CD8α^+ DCs, have not been reported to develop spontaneous autoimmunity. In fact, Batf3-deficient mice are protected in the NOD model of type 1 diabetes (Ferris et al., 2014). Furthermore, Batf3-deficient mice are susceptible to West Nile infection and immunogenic syngeneic tumors (Hildner et al., 2008), suggesting an immunodeficient phenotype. An explanation for these two opposing roles of Batf3-dependent DCs has not yet been reported. In fact, there does not appear to be a clear indication regarding the biological importance of mTEC to CD8α^+ DC antigen transfer for T cell tolerance.

By analyzing TCR repertoires in a fixed TCRβ model, we confirmed that Batf3-dependent CD8α^+ DCs are required for negative and Treg cell selection, and that approximately one-third of Aire-dependent TCRs were co-dependent on Batf3. We found that CD36, a class B scavenger receptor preferentially expressed on CD8α^+, but not SIRPα^+, DCs was required for the acquisition of mTEC membrane-bound I-Eα but not cytoplasmic GFP, potentially via the recognition of apoptotic bodies. Finally, we show that CD36-dependent transfer and display of cell-surface MHC on CD8α^+ DCs was required for the development of direct allo-tolerance during bone marrow

transplantation. Thus, these data suggest that CD8α^+ DCs utilize CD36 to acquire cell-surface antigens from mTECs to mediate thymic T cell tolerance.

Materials and Methods

Mice

Animal breeding and experiments were performed in a specific pathogen-free animal facility using protocols approved by the Washington University Animal Studies Committee. All mice were on a C57BL/6 genetic background unless otherwise indicated. TCliβ mice (Wong et al., 2007), *Batf3*$^{-/-}$ (Hildner et al., 2008), *Cd36*$^{-/-}$ (Febbraio et al., 1999), Aire-G6pc2/GFP (Adig, Gardner, et al., 2008), and *Gpr105*$^{-/-}$ (P2Y14R, Lee, et al., 2003) have all been described previously. *Aire*$^{-/-}$ (Stock# 004743), *Rag1*$^{-/-}$ (Stock# 002216), *Tcra*$^{-/-}$ (Stock# 002116), *Tcrb*$^{-/-}$*Tcrd*$^{-/-}$ (Stock# 002121) and *Foxp3*$^{\text{IRES-GFP}}$ (Stock# 006772) mice were purchased from The Jackson Laboratory. Male Balb/c mice (Stock# 028) were ordered from Charles River and allowed one week acclimation prior to use. G25 TCR transgenic mice were generated by cloning the cDNA for G25 TCRα chain into the VA-hCD2 expression vector, which was then co-injected with the TCli TCRβ chain in the pTβ vector (Bautista et al., 2009). G25 transgenic mice did not show any overt signs of autoimmunity, even on a *Rag1*$^{-/-}$ background. Expression of TCRβ was comparable between transgenic and WT cells from the thymus or spleen (data not shown). G25 TCR transgenic mice were bred to *Foxp3*$^{\text{IRES-GFP}}$ *Rag1*$^{-/-}$ mice. Animals were typically 6-10 weeks old of either sex at the time experiments were performed.

Reagents, antibodies and flow cytometry

Fluorescently conjugated monoclonal antibodies were purchased from Biolegend, eBioscience, and Becton Dickenson. Y-Ae anti-I-A^b:Eα (52-68) peptide was obtained from Affymetrix. Samples were analyzed using a FACSAria or FACSCanto (Becton Dickinson) and data were processed with FlowJo (Treestar).

Thymic dendritic cell isolation and staining

Thymus was mechanically separated with scissors and digested with Liberase (125 μg/ml, Roche) and DNase I (50 μg/ml, New England Biolabs) in DMEM for 30 min at 37°C. Cells were stained with 2.4G2, B220, MHCII, CD11c, CD11b, CD8α, SIRPα, CD24 and experiment-specific antibodies as indicated. DC subsets were identified as follows: CD8α^+ DCs (CD11c^{hi} MHCII^{hi} B220$^-$ CD11b$^-$ SIRPα^- CD24$^+$ CD8α^+), SIRPα^+ DCs (CD11c^{hi} MHCII^{hi} B220$^-$ CD11b$^+$ SIRPα^+ CD24$^-$ CD8α^-), and pDCs (CD11c$^+$ B220$^+$).

Assessment of thymic Treg cell selection in vivo

As described previously (Bautista et al., 2009), TCRα chains of interest were cloned into the TCRα-P2A-TCliβ retroviral vector. *Foxp3*$^{IRES\text{-}GFP}$ *Rag1*$^{-/-}$ thymocytes were transduced with TCRs *in vitro*, injected intrathymically into sublethally (600 rad) irradiated mice, and analyzed approximately 2.5 weeks later. Thymocytes were transduced with TCR vector containing no reporter, an IRES-Thy1.1 or an IRES-huCD2 prior to injection.

Bone marrow chimeras

BM was obtained by flushing donor humerus, tibia, and femur. BM was then RBC lysed and T cell-depleted by labeling cells with biotinylated anti-CD4 and anti-CD8 and anti-biotin microbeads, followed by magnetic cell separation using an AutoMACS (Miltenyi Biotech). $5x10^6$ cells were injected into either 950 rad lethally irradiated C57BL/6 host mice or 750 rad lethally irradiated Balb/c host mice. Mice were maintained on antibiotic water one day prior and one week after transplantation. Over 99% chimerism was confirmed using CD45.1 WT donors.

In vitro phagocytosis assay

BM from *Cd36*$^{+/-}$ and *Cd36*$^{-/-}$ mice was cultured in 100ng/ml of Flt3L for 11 days. $CD24^+$ DCs were sorted, CTV labeled, and cultured with apoptotic $H2^d$-expressing TA3 cells for 6h. Induction of apoptosis was induced with 150mJ UV-C using a Stratalinker UV Crosslinker. CTV^+ cells were then analyzed by FACS for Y-Ae and $I\text{-}A^d$ expression. In some experiments, TA3 cells were pre-treated with 50uM z-VAD-FMK for 1h prior to induction of apoptosis; or TA3 cells were cultured on the top layer of 0.4μm Corning HTS 96 well transwell plates separated from the DCs on the bottom layer. All experiments were carried out at 37°C, as well as on ice (0°C), which allows binding but inhibits phagocytosis.

Imaging studies

Mice were withheld food 12-24 h prior to imaging. On the day of imaging, mice were anesthetized with 1.5-2% isoflurane in oxygen inside of a Plexiglas chamber and subsequently injected with fludeoxyglucose (FDG, 100μl/20g mouse). Mice were

imaged using microCT to obtain anatomical scans, and then undergo a 10 min transmission scan followed by a 10 min emission scan. All imaging was performed via a Siemens Inveon-MM microCT/PET imager. Co-registration and analysis was performed using Siemens Inveon Research Workplace software.

Naïve T cell transfer studies

Foxp3^{-} CD44^{lo} CD62L^{hi} G25 TCR transgenic *Rag1*$^{-/-}$ cells were sorted and retro-orbital injected into indicated mice. In some experiments, cells were first labeled with CellTrace violet (Thermo Fisher). For histological studies, 6-8 week old littermate male TCR$\beta\delta^{-/-}$ mice were used. In peripheral activation studies, 6-8 week old littermate *Batf3*$^{+/-}$ and *Batf3*$^{-/-}$ mice were used. 10^5 naïve T cells were injected per mouse. For peripheral activation studies, pooled lymph nodes and spleens were harvested 4 days after transfer.

Allogeneic bone marrow chimeras, mixed lymphocyte reaction, and acute GVHD

Initial BM chimeras were performed as described above. Eight weeks post-transplant, thymic CD62L^{hi} CD24^{lo}CD4SP Tconv cells were sorted. For *in vitro* experiments, sorted cells were CTV labeled and co-cultured with irradiated (2000 rad) splenocytes from Balb/c mice. Samples were analyzed for CD25 expression and CTV dilution 5 days post co-culture. Donor Tconv cells were distinguished from Balb/c splenocytes by H-2K^{b} (AF6-88.5) and H-2K^{d} (SF1-1.1) expression. For *in vivo* experiments, 10^6 sorted Tconv cells were injected into lethally-irradiated Balb/c mice concurrently receiving allogenic 5x10^6 T cell-depleted B6 BM. In some experiments, Tconv cells came from adult mice

instead of from BM chimeras. Mice were assessed for weight loss beginning 4 days post injection. Mice were sacrificed after ≥20% loss of initial body weight. Additionally, mice were scored for disease severity using a standard 10 point scale that assesses weight loss, posture, mobility, fur texture, and skin integrity (Cooke et al., 1996).

Data processing and statistical analysis

For TCR analysis, only TRAVs with summed reads greater than 1% in the WT multiplex TCR data were analyzed. This accounted for more than 95% of the total TRAV repertoire. TRAV_CDR3 species frequencies were then multiplied by a correction factor determined by the ratio of template switch TRAV frequency to multiplex TRAV frequency using data obtained from 2 biological replicates each with 2 technical replicates sequenced both ways. These frequencies were used to determine the number of a particular TRAV_CDR3 clonotype.

Graphpad Prism v6, IBM SPSS v21, and R v3.2.3 were used for used for graphical and statistical analysis. Student's t-tests and one-way ANOVAs with Tukey's post hoc test were used for between-subjects analyses unless otherwise noted. The R package Deseq2 was used for differential TCR expression analysis; and vegan for dimensional analysis, rarefaction, and visualization.

Results

TCR repertoire analysis of Batf3-dependent BM derived APCs

Our previous study suggested that Batf3-dependent CD8α^+ DCs are the primary subset involved in the transfer of Aire-dependent antigens from mTECs to BM APCs (Perry et al., 2014). As this was based only on the analysis of 8 TCRs, we assessed the impact of Batf3-deficiency globally on the TCR repertoire. Because of the great diversity of the normal TCR repertoire, we utilized a fixed TCRβ model as previously described (Perry et al., 2014), generating *Batf3*$^{-/-}$ TCRβ transgenic *Tcra*$^{+/-}$ *Foxp3*$^{Thy1.1}$ mice for use as BM donors into congenic Ly5.1 hosts. We sorted CD4SP (CD4$^+$CD8$^-$) Foxp3$^+$ (Treg) and mature CD62L^{hi} CD24^{lo} CD4SP Foxp3$^-$ (Tconv) cells, whose frequencies was not affected by Batf3-deficiency (Figure 3.1A, B). For the amplification of TRAV gene products, we used multiplex PCR as it was more efficient than template-switch PCR in initial experiments, permitting the analysis of smaller cell numbers (data not shown). Barcoded amplicons were then sequenced via the Illumina MiSeq platform. To limit the analysis to TCRs that are reproducibly detected, we excluded TRAV families that were present at <1% of the sequences, which accounted for ~5% of the data. We also used our previous filtering criteria (Perry et al., 2014), keeping only TCRs present at a frequency of ≥0.01% in ≥30% of individual mice within one experimental condition (e.g. WT Treg), leaving approximately 1600 Tconv cell TCRs in both conditions and 857 and 314 Treg cell TCRs in Batf3-sufficient and -deficient mice, respectively (Figure 3.2A). Finally, a correction factor using template-switch PCR data as a reference standard was

applied to limit effects of differential priming and sequencing efficiencies associated with multiplex PCR (Figure 3.2B).

Using this processed data set, we plotted the average frequency of each TCR in the Batf3-sufficient and -deficient conditions for both Tconv and Treg cell subsets (Figure 3.3A). Dots in red represent individual TCRs that are markedly affected by Batf3, based on our previous criteria (Perry et al., 2014) of $p<0.05$ by Mann Whitney U (MWU) and an effect size of ≥5-fold difference in frequency (Figure 3.3A). We observed a number of Tconv and Treg cell TCRs enriched in Batf3-deficient mice, consistent with CD8α^+ DC mediated negative selection (Figure 3.3A, data points found below reference line; 3.3B). The effect of Batf3-deficiency could also be visualized within the Tconv cell TCR repertoire using unsupervised clustering (Figure 3.3C). In total, Batf3-dependent DCs negatively selected ~3% and 1% of the Tconv and Treg cell TCR repertoire, which represents ~1% and 2% of the total Tconv and Treg cell population, respectively (Figure 3.4A, B). These estimates of negative selection are likely to be conservative, as we observed a number of TCRs that were ≥5-fold enriched but did not meet our significance criteria (not shown) or vice versa (Figure 3.3B), suggesting that analysis of more mice or altering the fold-change criteria could improve these estimates. As an alternative approach, analysis of the TCR data using the DESeq2 package (Love et al., 2014), commonly used for count data in RNA-Seq, generated comparable conclusions (Figure 3.4B). As expected, the estimates of negative selection by Batf3-dependent DCs are lower than historical assessments of negative selection by BM APCs using TCR repertoire analysis (Perry et al., 2014). Thus, these data suggest that CD8α^+ DCs play only a partial role in BM APC-dependent negative selection.

By contrast to Batf3-dependent negative selection, we observed a greater requirement for CD8α^+ DCs in Treg cell selection (Figure 3.3A, red dots above reference line; 3.3B). The effect of Batf3-deficiency could also be visualized by unsupervised clustering of Treg cell TCRs (Figure 3.3C). Notably, TCRs that we previously identified as Batf3-dependent using retroviral expression of individual TCRs on Rag1-deficient thymocytes (Perry et al., 2014), were also decreased in this Treg TCR data set with Batf3-deficiency (Figure 3.5A). Although all 4 TCRs tested *in vivo* showed statistical difference in the TCR repertoire data, G25 and G41 would not meet our 5-fold effect size criteria. In addition, Batf3-deficiency results in a lower diversity in the Treg TCR repertoire compared with the WT repertoire (Figure 3.5B), suggesting that the selection of low frequency Treg TCRs may be compromised by deletion of CD8α^+ DC s. In summary, we observed that CD8α^+ DCs were required for selection of approximately 20% of the unique Treg cell TCR repertoire accounting for approximately 13% of the total Treg cell TCR repertoire (Figure 3.6A, B).

Role of CD8α^+ DCs in Aire-dependent thymic tolerance

Aire plays an important role in T cell tolerance, in part via the induction of tissue-specific antigen production in mTECs. Aire-dependent antigens can be presented autologously on mTECs, and may also be transferred to CD8α^+ DCs (Hubert et al., 2011; Koble and Kyewski, 2009; Perry et al., 2014). Although we had previously assessed the Aire-dependent repertoire using analysis of TRAV14 TCRs, we generated new data using multiplex PCR to permit direct comparison with the Batf3-dataset. Within

the range of previous results, we found that Aire was involved in the deletion of both Tconv (~3%) and Treg (~5%) cells as well as Treg cell selection (~20%) (Figure 3.7).

We then compared the repertoires of Batf3- and Aire-dependent TCRs. Relatively few Tconv or Treg cell TCRs were co-dependent on Batf3 and Aire for negative selection (Figure 3.8A). By contrast, ~31% of Batf3-dependent Treg cell TCRs were Aire-dependent and ~34% of Aire-dependent Treg cell TCRs were Batf3-dependent (Figure 3.8B). These estimates are in line with our previous data suggesting that approximately 50% of Aire-dependent TCRs are also BM APC dependent (Perry et al., 2014). Other BM APC subsets such as SIRPα^+ DCs, plasmacytoid DCs, macrophages, and B cells (Klein et al., 2014), likely contribute to negative selection, although changes in the sequencing methodology could also affect the estimates. In summary, the cross-comparison of Batf3 and Aire-dependent TCRs (Figure 3.9A, B) support our previous proposal that Aire-dependent antigens are transferred to CD8α^+ DCs.

T cell selection by CD8α^+ DCs prevents tissue-specific autoimmunity

The TCR repertoire data demonstrated that Baft3-dependent CD8α^+ DCs are involved in deletion and Treg cell selection. To address whether these TCRs that escape thymic tolerance are capable of inducing autoimmunity, we transferred mature thymic Tconv and Treg cells from Batf3- or Aire-deficient mice into T cell-deficient *Tcrb*$^{-/-}$*Tcrd*$^{-/-}$ (TCR$\beta\delta^{-/-}$) mice and assessed tissue inflammation using Positron Emission Tomography (PET). We observed a number of tissues with increased fludeoxyglucose (FDG) uptake in mice receiving cells from either Aire- or Batf3-deficient mice (Figure

S3A). FDG uptake was particularly apparent in the lungs, and corresponded to obvious inflammation on histology (Figure 3.10A, B). In addition to analysis of polyclonal T cells, we asked whether pathology could be induced by naïve T cells expressing the Treg TCR G25, which we had previously observed to be Batf3/Aire-codependent for Treg cell selection *in vivo* via retroviral TCR expression in thymocytes (Perry et al., 2014). Transfer of Tconv cells from G25 transgenic *Foxp3*$^{\text{IRES-GFP}}$ *Rag1*$^{-/-}$ mice into TCR$\beta\delta^{-/-}$ mice resulted in significant weight loss and lung inflammation (Figure 3.11A) reminiscent of polyclonal T cell transfers from Batf3- or Aire-deficient mice. Thus, these data support the notion that Batf3, like Aire, limits autoimmunity via induction of thymic T cell tolerance.

However, Batf3-deficient mice have not been reported to develop overt autoimmunity (Hildner et al., 2008). We hypothesized that this might result from a defect in peripheral antigen presentation. Consistent with this hypothesis, it was reported that Batf3-deficiency abrogates the development of Type 1 Diabetes in the NOD model (Ferris et al., 2014). To further test this possibility, we asked whether peripheral CD8α^{+} DCs were required to activate cells expressing the thymic Batf3-dependent Treg TCR G25 *in vivo*. Naïve G25 TCR transgenic cells were labelled with cell trace violet (CTV) and injected into Batf3-sufficient or -deficient hosts. We observed that the proliferation of G25 TCR transgenic cells was diminished in Batf3-deficient mice (Figure 3.11B). We also tested peripheral activation of 7 additional TCRs that were Batf3-dependent or -independent for thymic Treg cell induction (Perry et al., 2014), via retroviral transduction of these TCRs into TCli$\alpha\beta$ TCR transgenic *Rag1*$^{-/-}$ CD4^{+} cells (Hsieh et al., 2006). Notably, TCRs that exhibited Batf3-dependence in the thymus also showed decreased

expression of TCR activation markers after transfer into Batf3-deficient compared with Batf3-sufficient hosts (Figure 3.11C). Thus, analysis of these 8 TCRs support the hypothesis that CD8α^+ DCs are involved in presenting a distinct array of antigens in both the thymus as well as the periphery.

CD36 is involved in transfer of cell-surface antigens from mTECs

We next sought to determine the mechanism(s) by which CD8α^+ DCs acquire antigens from mTECs. One possibility was that CD8α^+ DCs, via their expression of the chemokine receptor XCR1 (Bachem et al., 2012; Lei et al., 2011), are in closer physical proximity to mTECs than other BM APC subsets. Another non-mutually exclusive hypothesis is that CD8α^+ DCs uniquely express receptors that facilitate antigen transfer from mTECs. Query of the Immunological Genome Project (ImmGen) (Heng et al., 2008) database revealed one potential candidate, CD36, which was expressed at a much higher level on thymic and splenic CD8α^+ DCs compared with other DC subsets. Notably, CD36 has previously been reported to recognize PS (Rigotti et al., 1995) and facilitate the acquisition and presentation of antigens derived from apoptotic cells (Albert et al., 1998). In addition, apoptosis has been reported as part of the normal mTEC life cycle (Gray et al., 2007). Thus, the published expression and function of CD36 suggested it might play a role in mTEC antigen transfer to CD8α^+ DCs.

To address this possibility, we first confirmed that CD36 is uniquely expressed on the CD8α^+ subset of thymic DCs (Figure 3.12). We then tested whether CD36 was involved in the transfer of cell-surface antigens using BM chimeras into Balb/c hosts that express the MHC II molecule Eα. As B6 mice do not express Eα, the generation of Eα:I-

A^b complexes, as detected using the peptide-in-groove antibody Y-Ae, occurs via antigen transfer from mTECs (Humblet et al., 1994). Consistent with our previous report (Perry et al., 2014), we observed preferential presentation of Eα:I-A^b by donor-derived CD8α$^+$ versus SIRPα$^+$ DCs (Figure 3.13). Notably, this was markedly diminished in CD8α$^+$ DCs from *Cd36*$^{-/-}$ bone marrow (Figure 3.13), which was not a result of lower MHCII levels (data not shown). Thus, CD36 plays an important role in mediating the transfer of cell-surface antigens from mTECs to CD8α$^+$ DCs.

We also asked whether CD36 was involved in mediating antigen transfer of cytoplasmic antigen from mTECs. Previously, we had utilized BM chimeras to assess whether GFP expressed in host cells via an Actin-GFP transgene could be transferred to transgene-negative donor BM APCs (Perry et al., 2014). Because Actin-GFP is expressed on all radioresistant host cells, and not just mTECs, we instead used the Adig BAC transgene, where GFP is expressed only in mTECs via the Aire promoter (Gardner et al., 2008). Analysis of *Cd36*$^{+/+}$ bone marrow donor APC subsets into Adig$^+$ hosts confirmed our previous conclusion that CD8α$^+$ DCs preferentially acquired GFP from host mTECs, with little uptake in SIRPα$^+$ DCs (Figure 3.14). In contrast to its effect on Eα transfer, CD36 expression did not affect cytoplasmic GFP acquired by CD8α$^+$ DCs. Thus, the requirement of CD36 for cell-surface, but not cytoplasmic, model antigens, demonstrates the existence of multiple pathways of antigen transfer from mTECs to CD8α$^+$ DCs.

Effect of CD36 on the Tconv and Treg cell TCR repertoire

Though the effect of CD36-deficiency on the transfer of Eα was substantial, it remained possible that this was a unique interaction between CD36 and Eα and not a general effect of CD36-deficiency on CD8α$^+$ DC antigen presentation. We therefore asked whether CD36-deficiency affected the thymic TCR repertoire. We bred *Cd36*$^{-/-}$ TCliβ transgenic mice and used them as BM donors into congenic hosts, and sequenced the Treg and mature Tconv cell subsets (Figure 3.15). As with Baft3-deficiency (Figure 3.1A, B), we did not observe effects of CD36 deficiency on the CD4SP, Tconv, or Treg cell frequencies (data not shown). Similarly, we found that most TCRs were unaffected by CD36 deficiency (Figure 3.16A, points on the diagonal). However, the TCR repertoire analysis revealed a requirement for CD36 for negative selection of a subset (~2%) of the Tconv cell TCR repertoire and the selection of ~7% of the Treg cell TCR repertoire (Figure 3.16B, C). The effects of CD36 on the TCR repertoire could also be delineated by PCA analysis (Figure 3.16D). In addition, we corroborated our sequencing data with *in vivo* development studies of CD36-dependent (R35, R117) and -independent (G25, G41) Treg cell TCRs (Figure 3.17A-C). Of note, all of these TCRs were previously reported to be Batf3- and Aire-codependent for selection of Treg cells *in vivo* (Perry et al., 2014). We also tested 4 Batf3/Aire-independent Treg cell TCRs *in vivo* and found that they were not affected by CD36 deficiency as expected (Figure 3.18). Taken together, these data demonstrate that CD36 has a clear effect on the Treg and Tconv cell TCR repertoire.

By cross-referencing our data sets from CD36 and Batf3-deficient conditions, we observed that the majority of Batf3-dependent TCRs were not affected by CD36,

suggesting that CD36 does not globally affect CD8α^+ DC antigen presentation. Since CD36 is expressed on macrophages in addition to CD8α^+ DCs, we also asked if there were TCRs affected by CD36 that were not dependent on Batf3. However, all of our CD36-dependent TCRs were Batf3-dependent (Figure 3.19), suggesting that the effect of CD36 on the TCR repertoire is due to its expression on CD8α^+ DCs.

We then asked whether CD36 was important for antigen transfer, which we infer based on TCRs that are codependent on Aire and Batf3. Of the few Tconv cell TCRs codependent on Batf3 and Aire for negative selection, 50% were also dependent on CD36 (Figure 3.19). Similarly, approximately half of the Treg cell TCRs codependent on Batf3 and Aire also required CD36 for Treg cell selection (Figure 3.19). Thus, these data suggest that CD36 contributes substantially to cooperative antigen presentation of Aire-dependent antigens by Batf3-dependent CD8α^+ DCs for the development of T cell tolerance.

CD36 acquires cell-surface antigen via scavenging of apoptotic bodies

We next sought to determine the process by which CD36 facilitated antigen acquisition from mTECs in vitro. As we are not aware of an Aire$^+$ H-2^d-expressing mTEC line, we used the TA3 hybridoma line as an imperfect surrogate (Glimcher et al., 1983). CD36-sufficient and -deficient BM-derived CD24$^+$ DCs, which are of a similar developmental lineage as thymic CD8α^+ DCs (Naik et al., 2005), were co-cultured with apoptotic TA3 cells for 6 hours and then stained for Y-Ae binding. Consistent with our *in vivo* data (Figure 3.13), we observed that the transfer and presentation of TA3-derived Eα on I-A^b in DCs was CD36-dependent (Figure 3.20A).

MHC molecules can be acquired through endocytosis, in which transferred Eα would be degraded and presented via the typical MHC II peptide-loading pathway. A non-mutually exclusive possibility is that intact MHC molecules are transferred via trogocytosis, such that the initial site of uptake would be the DC cell-surface membrane, followed by MHC internalization and degradation. Consistent with the latter, we observed diminished I-A^d expression on CD36-deficient $CD24^+$ DCs after co-culture with apoptotic TA3 cells (Figure 3.20B). We also asked whether I-A^d could be picked up in this manner by $CD8\alpha^+$ DCs *in vivo*. However, it appeared that the process of enzymatic digestion at 37°C for DC isolation in itself might result in cell-surface MHC transfer, rendering the *in vivo* analysis uninterpretable (Figure 3.21). The 30 minute digestion appears to be insufficient to result in Eα:I-A^b complexes detectable by Y-Ae (Figure 3.21). While accurate *in vivo* data is unavailable, our in vitro data suggests that CD36 may be involved in the "cross-dressing" of intact cell surface MHC molecules to be displayed on $CD8\alpha^+$ DCs.

CD36 has several known ligands, including PS and thrombospondin on apoptotic bodies or exosomes that could be involved in antigen transfer from mTECs. To assess the role of apoptotic bodies in Eα acquisition and presentation in vitro, we pre-treated TA3 cells with the pan-caspase inhibitor z-VAD-FMK prior to co-culture with $CD24^+$ DCs. Inhibition of apoptosis resulted in significantly diminished acquisition and presentation of Eα, which was further decreased in conjunction with CD36-deficiency (Figure 3.22). To assess the role of exosomes, we cultured cells separated by a 0.4μm membrane sufficient to allow their passage. This reduced the acquisition and presentation of Eα, arguing against a role for exosomes (Figure 3.22). However, it

remains possible that the concentration of exosomes generated was insufficient to overcome the different physical characteristics of the culture system. While these data cannot exclude a role for exosomes, our in vitro data support the published notion that CD36 is involved in the recognition of apoptotic bodies.

Along with “eat me” signals, the phagocytosis of apoptotic cells also requires a signal to home to a dying cell (a.k.a. “find me”), including purine nucleosides and nucleotides, such as ATP (Poon et al., 2014). We asked whether there were purinergic receptors that were differentially expressed by thymic CD8α^+ DCs. Analysis of ImmGen revealed that Gpr105 (a.k.a. P2Y14R), an UDP-glucose-responsive metabotropic receptor (Abbracchio et al., 2003; Lee et al., 2003), is highly expressed by both thymic and splenic CD8α^+ DCs but not SIRPα^+ DCs. Transfer of Gpr105-deficient BM into Balb/c mice resulted in a significant decrease in Eα presentation by CD8α^+, but not SIRPα^+, DCs (Figure 3.23). Taken together, our in vitro and *in vivo* data support the notion that CD8α^+ DCs use CD36 to acquire cell-surface antigens from apoptotic mTECs.

CD36-dependent antigen transfer is necessary for direct allo-tolerance development

Based on previous reports (Dolan et al., 2006; Li et al., 2012; Qu et al., 2009; Wakim and Bevan, 2011), as well as our in vitro observation that MHC II can be transferred directly to the cell surface of CD8α^+ DCs, we asked whether this might be involved in the development of thymic tolerance *in vivo* during allo-mismatched bone marrow transplantation. In a fully mismatched allogeneic BM chimera, donor thymocytes are positively selected by host MHC on cTECs, and negatively selected by donor MHC

on BM APCs as well as host MHC on cTECs and mTECs. Antigen transfer of MHC molecules from mTECs to DCs would therefore be predicted to facilitate thymic tolerance to host MHC.

To test this, we generated fully-MHC mismatched allogeneic BM chimeras using C57BL/6 (B6) donors and Balb/c hosts. Mature Tconv thymocytes from these mice were then assessed for their ability to induce acute graft-versus-host disease (GVHD) in the context of BM transplantation (Figure 3.24). As expected, thymic Tconv cells from *Batf3*$^{+/-}$ B6 → Balb/c BM chimeras showed minimal evidence of acute GVHD compared with Tconv cells from B6 → B6 autologous BM chimeras that were not exposed to H-2^{d} in the thymus (Figure 3.25A). The process of BM chimera generation did not appear to affect acute GVHD, as Tconv cells from normal B6 mice were equivalent to syngeneic B6 BM chimeras in their ability to induce acute GVHD (Figure 3.25B). Thus, these data confirm that thymic T cell tolerance to host MHC occurs during allogeneic BM transplantation.

By contrast, loss of thymic tolerance occurred with deficiency in either Batf3 or CD36 in the donor B6 background BM. Tconv cells from the respective BM chimeras induced acute GVHD as assessed by weight loss, clinical score, and time to euthanasia (Figure 3.25A). Tconv cells from *Cd36*$^{-/-}$ → Balb/c chimeras were marginally less potent than *Batf3*$^{-/-}$ → Balb/c chimeras, consistent with the incomplete block of MHC transfer with CD36 deficiency (Figure 3.13). We did not find evidence for a cell-intrinsic T cell hyper-reactivity imparted by Batf3-deficiency, as T cells from non-chimeric Batf3-deficient and -sufficient mice showed similar induction of GVHD (Figure 3.25C). Thus,

these data suggest that CD36-dependent MHC transfer to CD8α^+ DCs is required for thymic allo-tolerance.

Allo-recognition can occur via direct recognition of allogeneic MHC by the TCR, or indirectly via recognition of allogeneic peptides presented on self-MHC (e.g.. Eα peptide on I-A^b). To test direct allo-recognition, we sorted Tconv cells and cultured them in the presence of irradiated Balb/c splenocytes (Figure 3.24). Tconv cells from *Batf3*$^{+/-}$ → Balb/c chimeras showed minimal proliferation, consistent with the *in vivo* results suggesting that these cells are allo-tolerant (Figure 3.26). However, we observed a clear population of proliferated Tconv cells from *Batf3*$^{-/-}$ → Balb/c or *Cd36*$^{-/-}$ → Balb/c chimeras (Figure 3.26), consistent with direct allo-recognition. However, the frequency of proliferated cells was lower than Tconv cells from non-tolerant conditions using autologous B6 hosts (Figure 3.26), suggesting that a partial degree of allo-tolerance does occur to host MHC presented on cTECs and mTECs. A deficiency in tolerance to direct allo-recognition is also consistent with the early time course of GVHD *in vivo* (Figure 3.25A), as donor APCs would not have seeded the periphery in large numbers. In summary, these data suggest that complete tolerance to direct host MHC recognition during allogeneic BM transplantation requires CD36-dependent “cross-dressing” of CD8α^+ DCs.

Figure Legends

Figure 3.1. Thymocyte subset frequencies in TCliβ^{+} *Batf3*$^{-/-}$ mice.

(A,B) No change in thymic T cell population due to Batf3-deficiency. Summary of Foxp3^{+} CD4^{+} (Treg), Foxp3^{-} CD4^{+} CD8^{-} (CD4SP) and CD8^{+} CD4^{-} (CD8SP) thymocyte frequencies (A) or HSA^{lo} CD62^{hi} and HSA^{hi} CD62^{lo} CD4^{+} frequencies (B) from TCliβ transgenic *Batf3*$^{+/+}$ or *Batf3*$^{-/-}$ → Ly5.1 BM chimeras. Data are presented as mean + SEM.

Figure 3.2. TCR sequencing output for *Batf3*$^{+/+}$ and *Batf3*$^{-/-}$ mice.

(A) Illumina sequencing of Tconv and Treg cell TCRs from *Batf3*$^{+/+}$ and *Batf3*$^{-/-}$ BM chimeras. Chimeras were generated using TCliβ TCR transgenic *Tcra*$^{+/-}$ (*Batf3*$^{+/+}$ or *Batf3*$^{-/-}$) donors. After 8 weeks, Foxp3^{+} Treg (CD4^{+}CD8^{-}Foxp3^{gfp+}) and Foxp3^{-} Tconv (CD4^{+}CD8^{-}CD62L^{hi}CD24^{lo}Foxp3^{gfp-}) cells were sorted. Synthesis of TCRα cDNAs from purified T cells was performed using the Cα-specific primer 5'-GTGAATCAGGGCCAAC-3'. A two-step PCR was used in order to amplify multiple TRAV genes (multiplex PCR, see Table S1). Amplicons were purified after each PCR reaction using the Agencourt AMPure XP magnetic purification system. The ~200-600 bp amplicons were quantified using Qubit dsDNA BR assay kit (Invitrogen) and pooled in equimolar ratios for 250 bp paired end sequencing via the MiSeq platform (Illumina). Sequences were demultiplexed and analyzed using blastn to identify the TRAV and TRAJ gene segments using the IMGT database (Giudicelli et al., 2006). This information was then used to determine the CDR3 sequence. A unique TCR is identified by its TRAV and CDR3 amino acid sequence. Data shown is the summary of sorting, sequencing, and filtering. Frequency filtering ("# of TCRs > .01%") keeps TCRs > 0.01% of raw data in any individual sample. Consistency filtering ("# TCRs > 30% of condition") keeps TCRs

that are found in 30% of samples at > 0.01% frequency within an experimental condition defined by T cell subset and genotype. Raw sequence data can be found in the European Nucleotide Archive (accession #). (B) Primer efficiency of multiplex PCR. Template switch (Mamedov et al., 2013) or conventional cDNA synthesis was performed on thymic Tconv cells and sequenced (2 biologic and 2 technical replicates). The frequency of each TRAV is shown. TRAVs with a frequency below 1% of the total population in multiplex PCR were excluded to limit variability from low read numbers due to low primer efficiency. The TRAV frequency in template switch divided by the frequency in multiplex PCR was used as a correction factor.

Figure 3.3. Treg and Tconv cell TCR sequencing of *Batf3*$^{+/+}$ and *Batf3*$^{-/-}$ mice.

(A) Batf3-dependent CD8α^+ DCs are required for T cell tolerance. The average TCR frequency in the Tconv (Foxp3$^-$ HSA^{lo} CD62^{hi}) and Treg (Foxp3$^+$) cell subset in *Batf3*$^{+/+}$ or *Batf3*$^{-/-}$ → Ly5.1 BM chimeras are shown. Red dots indicate TCRs that show $p < .05$ MWU and 5-fold change between *Batf3*$^{-/-}$ and *Batf3*$^{+/+}$. (B) Plots of raw TCR frequencies for the top 10 Treg TCRs in *Batf3*$^{+/+}$ and *Batf3*$^{-/-}$ BM chimeras (left) and the top 10 negative or Treg selected TCRs sorted by MWU *p* value (right). Dots indicate data from individual mice and bars indicate the mean. *$p < .05$, **$p < .01$, ***$p < .001$, MWU. (C) Unsupervised clustering analysis of Tconv and Treg cell TCR repertoires from *Batf3* BM chimeras.

Figure 3.4. CD8α^+ DCs mediate negative selection of Tconv and Treg cells.

(A) Summary of the effect of Batf3 on negative selection and Treg cell selection. Data shown are the percentage of unique TCRs or total sequences affected based on criteria described in (Figure 3.2). All data are representative of at least two independent experiments

with at least 4 mice per condition. (B) Analysis of negative selection using the R package DESeq2. Presented is the unique number of TCRs determined by the false-discovery rate adjusted *p* value (padj), the unadjusted *p* value (pval), with or without a 5-fold change criteria (5xΔ).

Figure 3.5. Cross-validation of *Batf3*$^{-/-}$ sequencing data set.

(A) Frequency in *Batf3*$^{+/+}$ and *Batf3*$^{-/-}$ TCR data sets of Treg cell TCRs previously identified to be Batf3- and Aire-codependent (G25, G41, R117, R35) or -independent (G69, R19, JP2, JP3) in *in vivo* developmental studies (Perry et al., 2014). (B) Rarefaction of Treg cell TCR repertoires from *Batf3*$^{+/+}$ (WT) and *Batf3*$^{-/-}$ (KO) BM chimeras using the R package "vegan" (Oksanen et al., 2016). **p* < .05, ***p* < .01, ****p* < .001, Student's t-test.

Figure 3.6. CD8α^+ DCs mediate Treg cell development.

(A) Summary of the effect of Batf3 on Treg cell selection. Data shown are the percentage of unique TCRs or total sequences affected based on criteria described in (Figure 3.2). All data are representative of at least two independent experiments with at least 4 mice per condition. (B) Analysis of Treg cell selection using the R package DESeq2. Presented is the unique number of TCRs determined by the false-discovery rate adjusted *p* value (padj), the unadjusted *p* value (pval), with or without a 5-fold change criteria (5xΔ).

Figure 3.7. Multiplex TCR sequencing of *Aire*$^{-/-}$ mice.

(A) Summary of TCR sequencing to assess role of Aire. Foxp3$^-$ Tconv or Foxp3$^+$ Treg CD4SP cells from TCliβ^+ transgenic → *Aire*$^{+/+}$ or *Aire*$^{-/-}$ BM chimeras were

sequenced as per Figure 3.2. (B) Average TCR frequencies in the Foxp3^{-} and Foxp3^{+} Aire data sets. Red dots indicate TCRs that are considered Aire-dependent based on $p < .05$ (MWU) and 5-fold change as per Figure 3.3. (C) PCA of Tconv and Treg cell TCR repertoires from *Aire*$^{+/+}$ (blue dots) and *Aire*$^{-/-}$ (red dots) BM chimeras. (D,E) Summary of the effect of *Aire* on negative selection of the Foxp3^{-} and Foxp3^{+} TCR repertoire (D), and on Treg cell selection (E). Data shown are the percentage of unique TCRs or total sequences affected. (F) Rarefaction of Treg cell TCR repertoires from *Aire*$^{+/+}$ (WT) and *Aire*$^{-/-}$ (KO) BM chimeras as per Figure 3.5

Figure 3.8. Analysis of Batf3/Aire-codependence for deletion and Treg cell selection.

(A,B) Intersection between Aire and Batf3-dependent TCRs. Venn diagram of absolute number of TCRs involved in negative selection (A) or Treg cell selection (B).

Figure 3.9. Quantification of cell-autonomous and cooperative antigen presentation by CD8α^{+} DCs for deletion and Treg cell selection.

(A,B) Summary of the effect of Batf3 and Aire on negative selection (A) and Treg cell selection (B). TCRs are identified as Batf3/Aire dependent based on Figure 3.3.

Figure 3.10. T cell selection by CD8α^{+} DCs prevents tissue-specific autoimmunity.

(A) Representative images from FDG PET imaging (top row) and hematoxylin and eosin (H&E) stained lung histology (bottom row) of TCR$\beta\delta^{-/-}$ mice injected with sorted thymic Tconv (10^6) and Treg ($5x10^4$) cells from wild-type (WT), *Aire*$^{-/-}$, or *Batf3*$^{-/-}$ mice. Mice were imaged 2.5 weeks post transfer. Yellow arrows indicate regions of increased radiolabeled glucose uptake.

Images are representative of two independent experiments with 2-3 mice per condition. (B) Quantification of radiolabeled glucose uptake in lung, spleen, and muscle from (A). Data is represented as change from WT (counts KO ÷ WT). Each dot represents data from an individual mouse; bar indicates mean value. *$p < .05$, **$p < .01$, ***$p < .001$; Student's t-test.

Figure 3.11. Peripheral Batf3-dependent DCs are required for activation of thymic CD8α^+ DC-dependent TCRs.

(A) Pathogenic potential of G25 TCR. TCR$\beta\delta^{-/-}$ mice were injected with 10^6 G25 TCR transgenic or polyclonal thymic Tconv cells. Weights (mean ± SEM) were measured weekly, and analyzed using repeated measures ANOVA with Sidak's multiple comparisons correction. Lungs were harvested for H&E staining. (B) Decreased peripheral activation of G25 TCR. 10^5 Naïve G25 TCR transgenic CD4$^+$ T cells were sorted, cell trace violet (CTV) labeled, and injected into *Batf3*$^{+/-}$ or *Batf3*$^{-/-}$ mice. Proliferation of and CD44 expression by G25 cells was assessed by flow cytometry of the spleens and pooled lymph nodes (LN) 4 days after transfer. Each dot represents data from an individual recipient from two independent experiments. (C) Peripheral T cell activation of Batf3-dependent TCRs. CD4$^+$ T cells from TCli$\alpha\beta$ TCR transgenic mice were enriched and CD25-depleted using Automacs, then stimulated for 24h with plate bound CD3/CD28 antibody. T cells were retrovirally transduced (Hsieh et al., 2006) with the indicated TCRα chains and injected into 6-8 week old littermate-controlled *Batf3*$^{+/-}$ and *Batf3*$^{-/-}$ mice. Spleens and pooled lymph nodes were harvested 11 days post injection and stained for CD44 as a surrogate for T cell activation. Data is presented for each replicate, and was obtained in at least two independent experiments. *$p < .05$, **$p < .01$, ***$p < .001$; Student's t-test.

Figure 3.12. CD36 expression is restricted to CD8α^+ DCs in the thymus.

WT thymi were harvested and stained for DC markers and CD36 as described in Methods. Plots are representative of two separate experiments with at least 2 mice per condition.

Figure 3.13. CD36 is involved in transfer of cell-surface antigens from mTECs.

BM from *Cd36*$^{+/-}$ and *Cd36*$^{-/-}$ mice was transferred into irradiated H-2^d hosts. CD8α^+ and SIRPα^+ DC subsets were analyzed for Y-Ae expression 4 weeks after transplantation. Gates were drawn according to H-2^b syngeneic BM chimera controls. Plots summarize data from two experiments with 2 mice per condition (mean + SEM). ***$p < .001$; Student's t-test.

Figure 3.14. CD8α^+ DCs mediate transfer of cytoplasmic antigen independent of CD36.

BM from *Cd36*$^{+/+}$ Ly5.1$^+$ and *Cd36*$^{-/-}$ mice was transplanted at a 1:1 ratio into mice expressing a BAC transgene in which Aire drives GFP expression (Adig). CD8α^+ and SIRPα^+ DC subsets were analyzed for GFP expression 4 weeks after transplantation, using gates from BM chimeras using Adig-negative hosts. Plots summarize data from one experiment with four Adig$^+$ mice (mean + SEM). ***$p < .001$; Student's t-test.

Figure 3.15. TCR sequencing output for *Cd36*$^{+/-}$ and *Cd36*$^{-/-}$ mice.

Summary of TCR sequencing for CD36 BM chimeras as described in Figure 3.2.

Figure 3.16. Treg and Tconv cell TCR sequencing of *Cd36*$^{+/-}$ and *Cd36*$^{-/-}$ mice.

(A) Effect of CD36 on the TCR repertoire. Plotted are the average frequency of Tconv and Treg TCRs in *Cd36*$^{+/-}$ or *CD36*$^{-/-}$ → Ly5.1 BM chimeras. Red dots indicate TCRs that show $p < .05$ MWU and 5-fold change. (B, C) Summary of CD36 on negative selection (B) and Treg cell selection (C). Data shown are the percentage of unique TCRs or total sequences in the filtered data set that are negatively selected based on MWU and fold-change criteria in (A). (D) Unsupervised clustering analysis of Tconv and Treg cell TCR repertoires from *Cd36*$^{+/-}$ and *Cd36*$^{-/-}$ BM chimeras.

Figure 3.17. *In vivo* validation of the behavior of Batf3/Aire-codependent Treg cell TCRs observed in *Cd36*$^{+/-}$ and *Cd36*$^{-/-}$ TCR sequencing.

(A) Frequency of Treg cell TCRs in *Cd36*$^{+/-}$ and *Cd36*$^{-/-}$ BM chimeras previously identified to be Batf3/Aire-codependent (G25, G41, R117, R35) in *in vivo* developmental studies (Perry et al., 2014). (B) In *vivo* developmental studies of Batf3/Aire-dependent Treg cell TCRs: two CD36-independent (G25 and G41) and two CD36-independent (R35 and R117). Representative flow cytometry plots (gated on retrovirally transduced CD4SP cells) of data summarized in (C). Plots are representative of at least two independent experiments with 1-3 replicates per condition. ***$p < .001$, Student's t-test.

Figure 3.18. *In vivo* validation of the behavior of Batf3/Aire-independent Treg cell TCRs observed in *Cd36*$^{+/-}$ and *Cd36*$^{-/-}$ TCR sequencing.

In vivo developmental studies of previously identified $CD11c^+$ DC-dependent Batf3/Aire-independent Treg TCRs (Perry et al., 2014). Each TCR was tested in at least two independent experiments with at least 1 replicate per condition. Summary data and representative FACS plots are shown.

Figure 3.19. Analysis of CD36/Batf3/Aire-codependence for deletion and Treg cell selection.

Cross-referencing of CD36/Batf3/Aire-dependent TCRs. Venn diagram representations of Tconv and Treg cell TCRs dependent on Batf3, Aire, and CD36. Values represent absolute number of TCRs, and Venn diagram sections are sized proportional to number. All sequencing data are representative of two independent experiments with 5 mice per condition.

Figure 3.20. CD36 mediates acquisition and presentation of intact peptide/MHC *in vitro.*

(A) *In vitro* assessment of CD36 function in antigen presentation. $Cd36^{+/-}$ and $Cd36^{-/-}$ BM-derived $CD24^+$ DCs were co-cultured with apoptotic $H\text{-}2^d$-bearing TA3 cells for 6h at 0”C and 37”C. Acquisition and presentation of $E\alpha$ by $CD24^+$ DCs was quantified using the Y-Ae antibody. FACS plots are representative of three independent experiments with at least two independent replicates per condition. Transfer of cell-surface $I\text{-}A^d$ in vitro to BM DCs. As per (A), $Cd36^{+/-}$ and $Cd36^{-/-}$ BM-derived $CD24^+$ DCs were co-cultured with apoptotic $H\text{-}2^d$-bearing TA3 cells for 6h at 0°C and 37°C. Acquisition of intact peptide/MHC from TA3 cells was determined by flow cytometry of I-

A^d expression on $CD24^+$ DCs. FACS plots are representative of two independent experiments with at least two independent replicates per condition. All data are summarized as mean + SEM. $^{**}p < .01$, $^{***}p < .001$, one-way ANOVA with Tukey's post hoc test.

Figure 3.21. Measurement of *in vivo* transferred intact peptide/MHC is obscured by thymic digestion.

Thymic digestion can transfer cell surface MHC. Shown is experiment schematic and representative FACS plots. Thymi from congenic $Ly5.1^+$ B6 (C57BL/6) and Balb/c mice were harvested, split in half, and either digested by itself or with an allogeneic thymus. Thymus preps were stained for DC markers, Y-Ae, and I-A^d, and analyzed by flow cytometry. FACS plots are representative of two independent experiments with two replicates per condition. DC subsets were identified as per Methods.

Figure 3.22. CD36 acquires cell-surface antigen via scavenging of apoptotic bodies.

Blockade of apoptosis and apoptotic bodies decreases Eα presentation. TA3 cells were pre-treated with 50μM z-VAD-FMK (zVAD) 1h prior to co-culture as in (Figure 3.20). For transwell experiments, $CD24^+$ DCs were cultured in the bottom chamber and apoptotic TA3 cells in the top chamber of a 0.4μm transwell plate. FACS plots are representative of two independent experiments with at least two independent replicates per condition. All data are summarized as mean + SEM. $^{***}p < .001$, one-way ANOVA with Tukey's post hoc test.

Figure 3.23. The purinergic receptor GPR105 (P2Y14R) mediates transfer of cell-surface antigen from mTECs.

Gpr105 is required for antigen-transfer of Eα. *Gpr105*$^{+/+}$ Ly5.1^{+} and *Gpr105*$^{-/-}$ BM was injected into lethally irradiated Balb/c mice at a 1:1 ratio. Thymi were harvested 4 weeks post injection, as per Figure 4, and CD8α^{+} and SIRPα^{+} DC subsets were analyzed for Y-Ae expression. Data are representative of two experiments with 3-4 mice per condition. All data are summarized as mean + SEM. ***p < .001, one-way ANOVA with Tukey's post hoc test.

Figure 3.24. Experimental design to assess tolerance during allogeneic bone marrow transplantation.

Schematic for the assessment of tolerance during allogeneic bone marrow transplantation performed in Figures 3.25 and 3.26. T cell-depleted BM was harvested from indicated mice and transplanted into either allogeneic Balb/c or syngeneic C57BL/6 (B6). After 8 weeks, CD4^{+} thymic Tconv cells were sorted and used for either induction of acute GVHD (Figure 3.25) or to detect alloreactivity in a mixed lymphocyte reaction (Figure 3.26).

Figure 3.25. Batf3/CD36-dependent antigen transfer facilitates allo-tolerance development and prevents catastrophic acute GVHD.

. (A) Acute GVHD model: BM from H-2^{b} *Batf3*$^{+/-}$, *Batf3*$^{-/-}$, or Cd36$^{-/-}$ mice was transplanted into Balb/c H-2^{d} hosts. As a positive control, *Batf3*$^{+/-}$ H-2^{b} BM was

transplanted into Ly5.1^{+} H-2^{b} hosts. After 8 weeks, thymic CD4^{+} Tconv cells were sorted and 10^{6} cells were co-injected with T cell-depleted H-2^{b} BM into H-2^{d} hosts. (B) Similar to experiment described in (A), except that thymic CD4^{+} Tconv cells were sorted directly from B6 mice versus syngeneic B6 → B6 BM chimeras. (C) Similar to (B), except Tconv cells from *Batf3*$^{+/-}$ and *Batf3*$^{-/-}$ mice were used to induce acute GVHD. The course of acute GVHD was determined by weight change, clinical score, and the fraction of mice reaching 20% weight loss requiring euthanasia. Summary plots are of 2-4 independent experiments with 2-4 mice per condition (mean ± SEM).

Figure 3.26. CD36-dependent antigen transfer is necessary for direct allo-tolerance in the thymus.

In vitro direct MLR: 2.5x10^{4} Tconv cells obtained as per (Figure 3.25) were CTV labeled and cultured with irradiated H-2^{d} splenocytes (2.5x10^{4} cells) for 5 days. Proliferation of Tconv cells was assessed by CTV dilution using flow cytometry. Plots are representative of 2-3 independent experiments. Each dot in the summary plot represents the average of 2 technical replicates from an individual mouse; bar indicates group mean. ***p < .001, one-way ANOVA with Tukey's post hoc test.

Figures

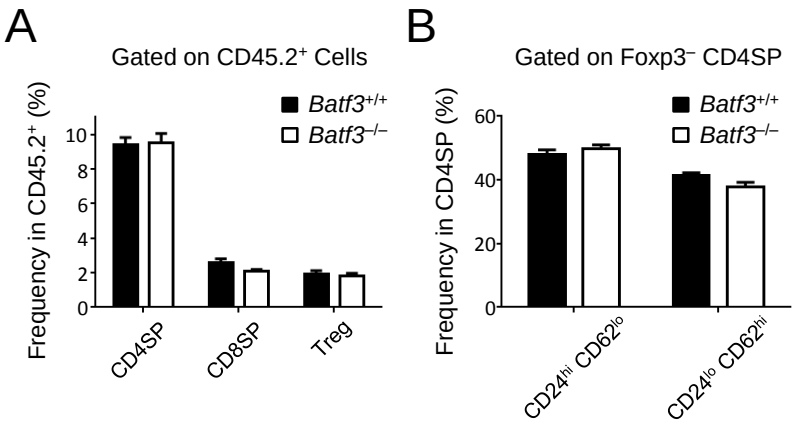

Figure 3. 1. Thymocyte subset frequencies in TCliβ^{+} *Batf3*$^{-/-}$ mice.

A

	Batf3$^{+/+}$					*Batf3*$^{-/-}$				
				# of TCRs					# of TCRs	
Population	n mice (n expts)	Cells x10^3 Mean (SE)	# of reads	>.01% in 1 sample	>30% mice in 1 condition	n mice (n expts)	Cells x10^3 Mean (SE)	# of reads	>.01% in 1 sample	>30% mice in 1 condition
Foxp3$^-$	11 (3)	1468 (107)	250040	9010	1593	12 (3)	1354 (331)	201475	10597	1643
Foxp3$^+$	9 (3)	62.4 (14)	398636	7696	857	9 (3)	67.9 (18)	469148	8112	314

B

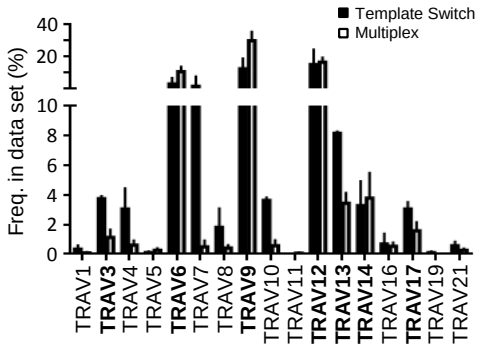

Figure 3. 2. TCR sequencing output for *Batf3*$^{+/+}$ and *Batf3*$^{-/-}$ mice.

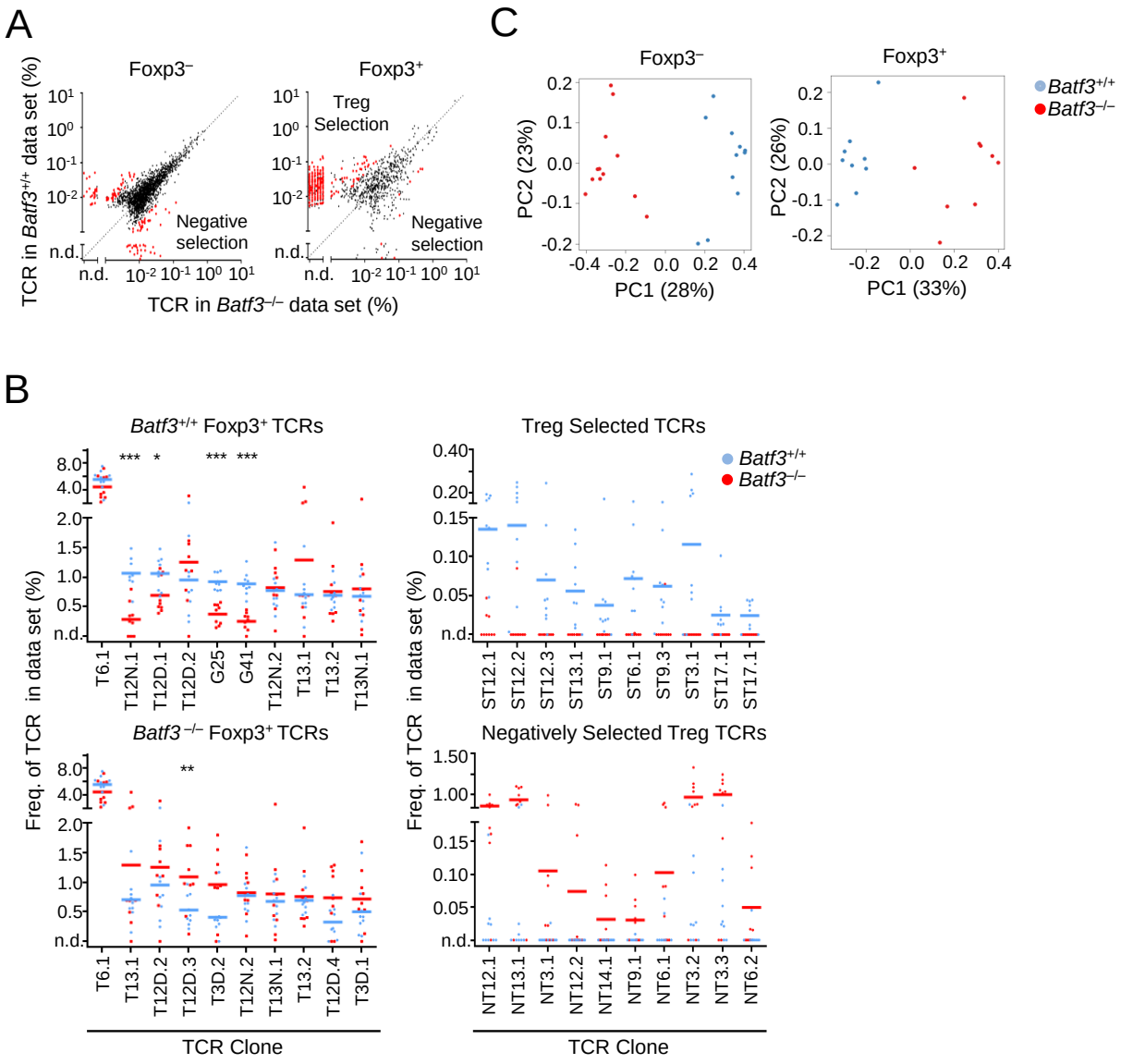

Figure 3. 3. Treg and Tconv cell TCR sequencing of *Batf3*$^{+/+}$ and *Batf3*$^{-/-}$ mice.

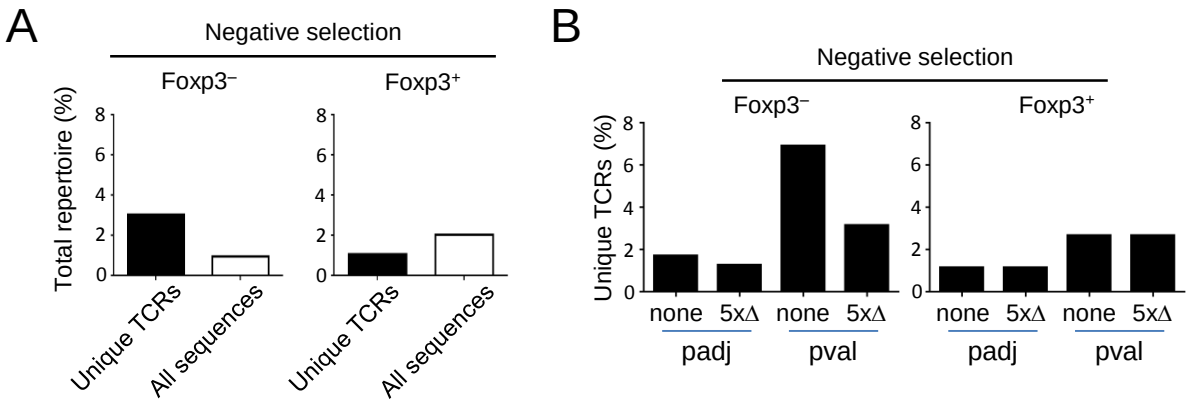

Figure 3. 4. CD8α^+ DCs mediate negative selection of Tconv and Treg cells.

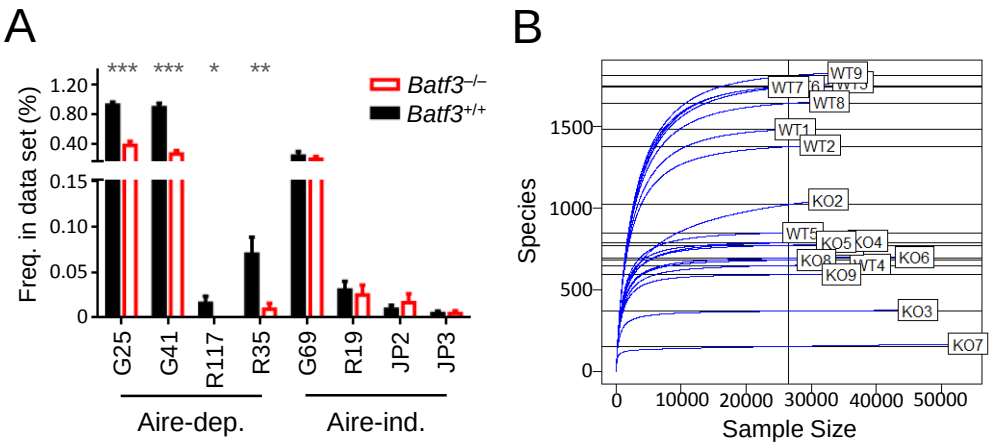

Figure 3. 5. Cross-validation of *Batf3*$^{-/-}$ sequencing data set.

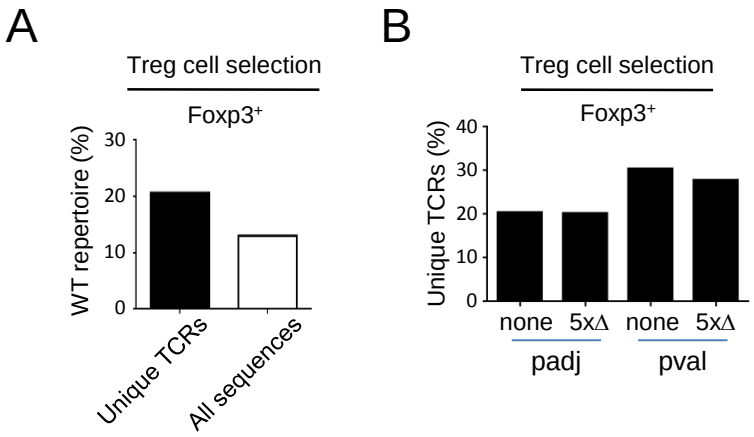

Figure 3. 6. CD8α^+ DCs mediate Treg cell development.

A

	Aire$^{+/+}$					*Aire*$^{-/-}$				
				# of TCRs					# of TCRs	
Population	n mice (n expts)	Cells x10^3 Mean (SE)	# of reads	>.01% in 1 sample	>30% mice in 1 condition	n mice (n expts)	Cells x10^3 Mean (SE)	# of reads	>.01% in 1 sample	>30% mice in 1 condition
Foxp3$^-$	9 (3)	734 (24)	130264	12587	1462	9 (3)	646 (20)	109055	14884	2158
Foxp3$^+$	7 (3)	31 (8)	396854	6789	494	7 (3)	21 (6)	142069	6441	511

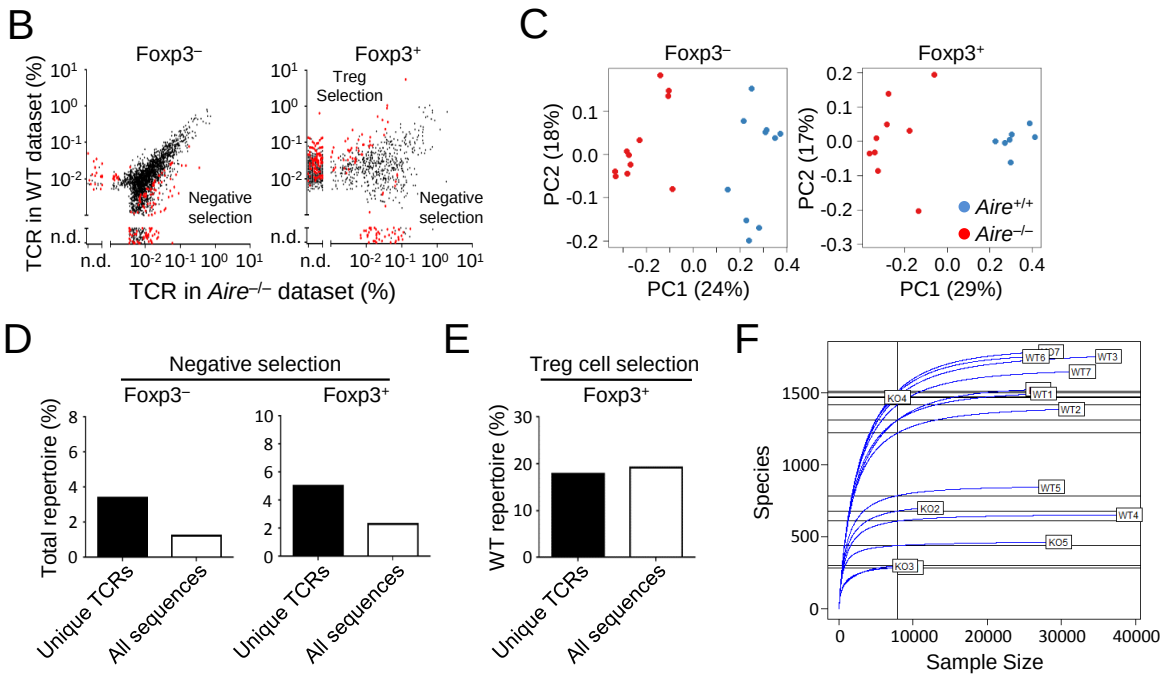

Figure 3. 7. Multiplex TCR sequencing of *Aire*$^{-/-}$ mice.

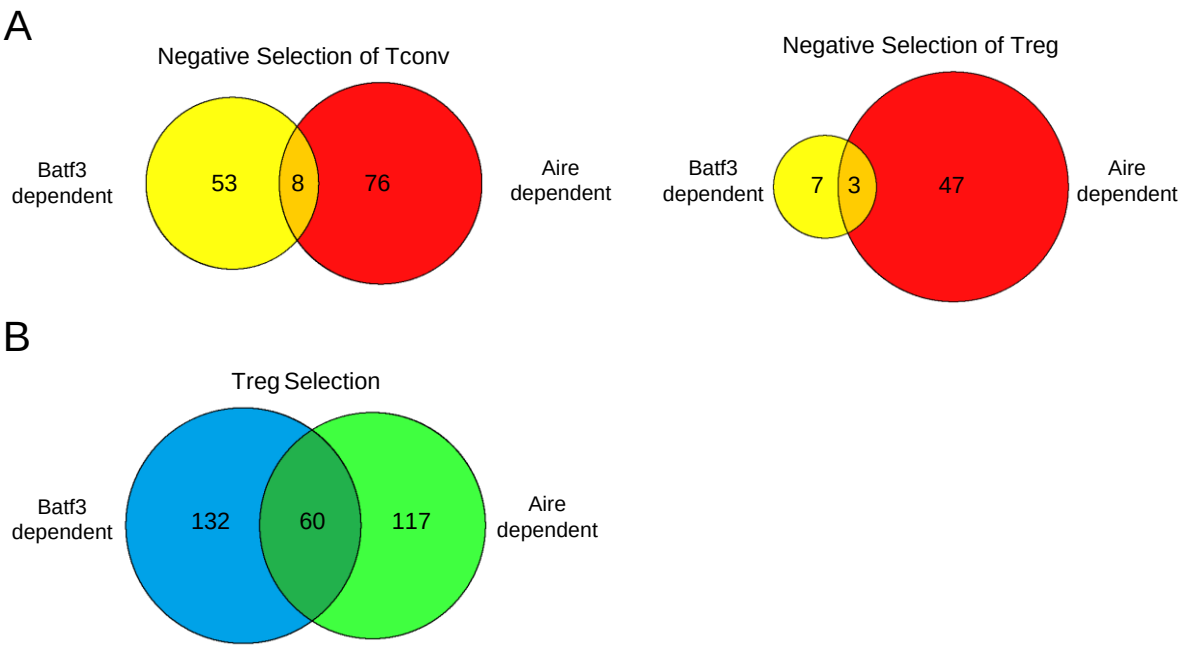

Figure 3. 8. Analysis of Batf3/Aire-codependence for deletion and Treg cell selection.

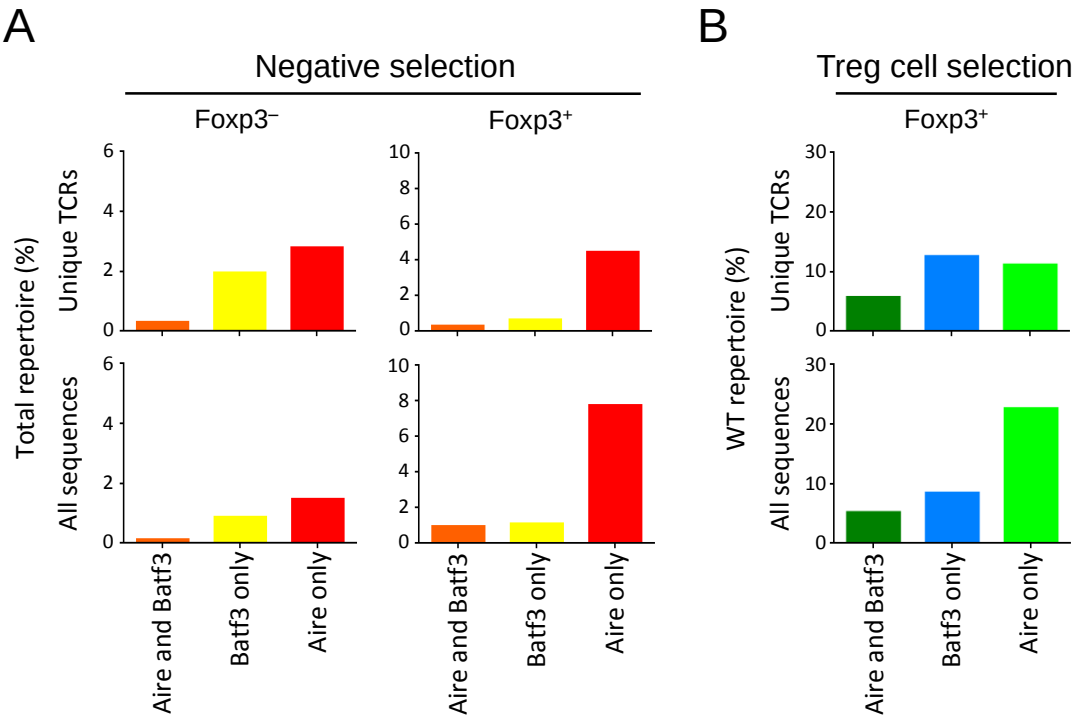

Figure 3. 9. Quantification of cell-autonomous and cooperative antigen presentation by CD8α^+ DCs for deletion and Treg cell selection.

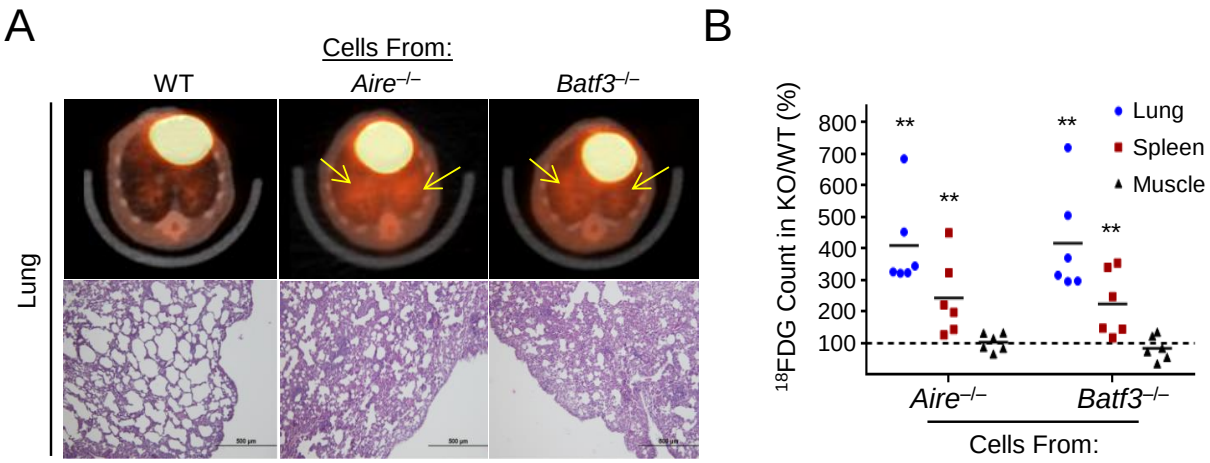

Figure 3. 10. T cell selection by CD8α^+ DCs prevents tissue-specific autoimmunity.

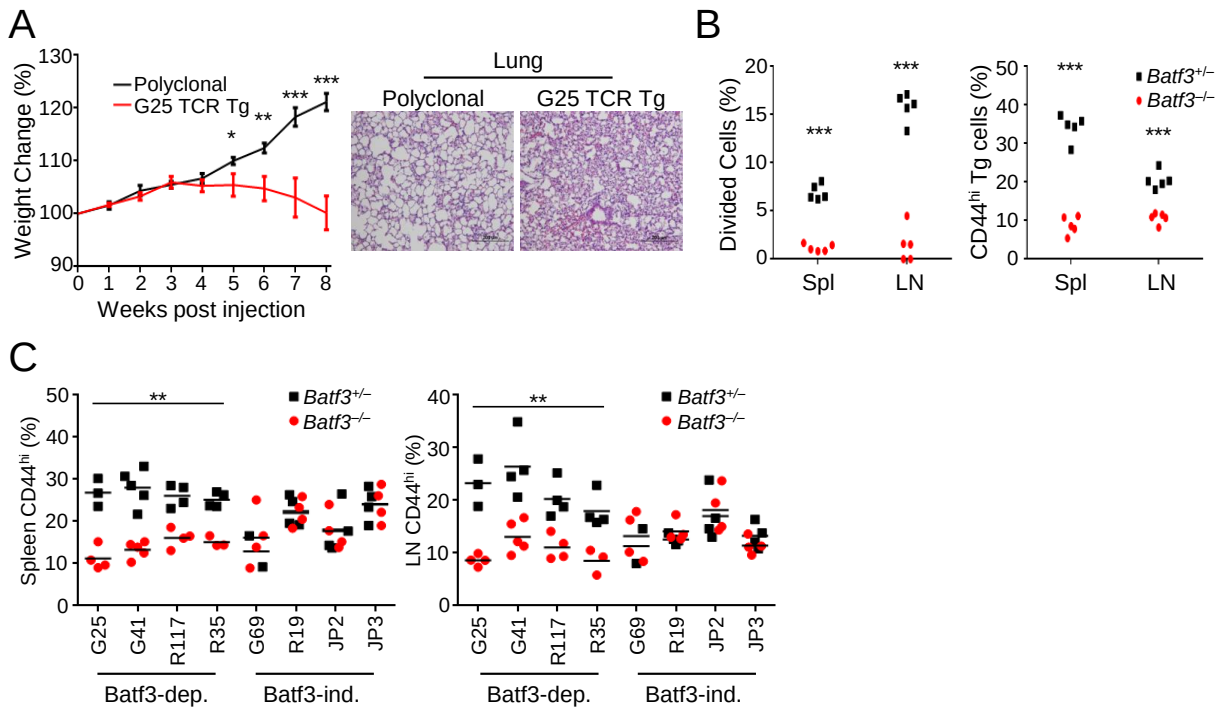

Figure 3. 11. Peripheral Batf3-dependent DCs are required for activation of thymic CD8a^{+} DC-dependent TCRs.

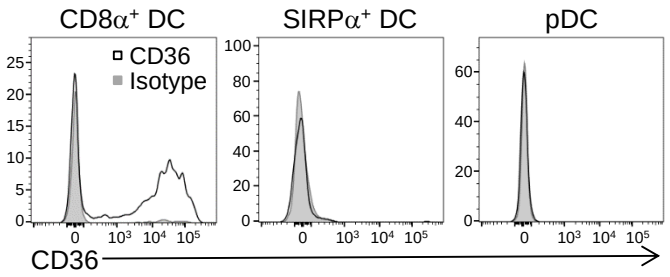

Figure 3. 12. CD36 expression is restricted to CD8a^{+} DCs in the thymus.

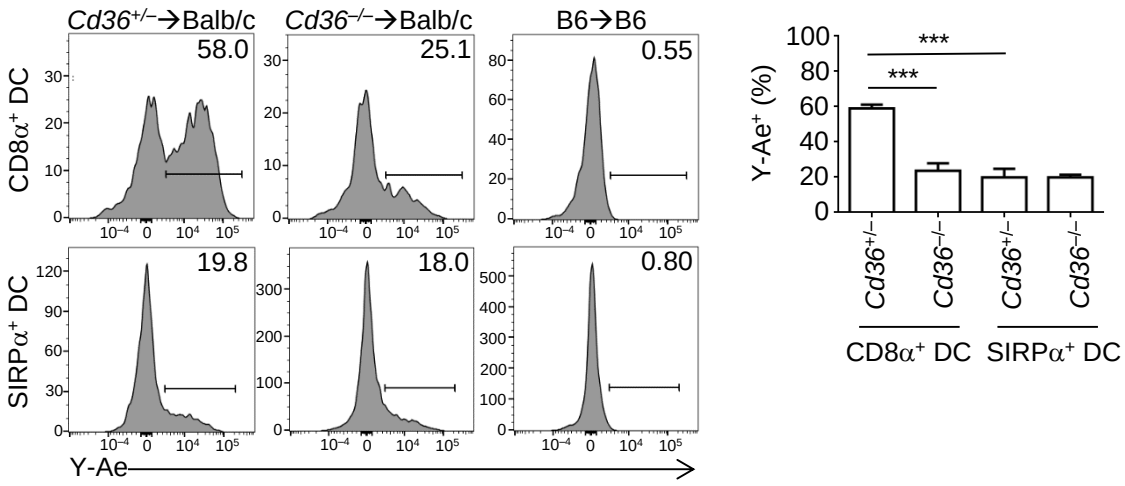

Figure 3. 13. CD36 is involved in transfer of cell-surface antigens from mTECs.

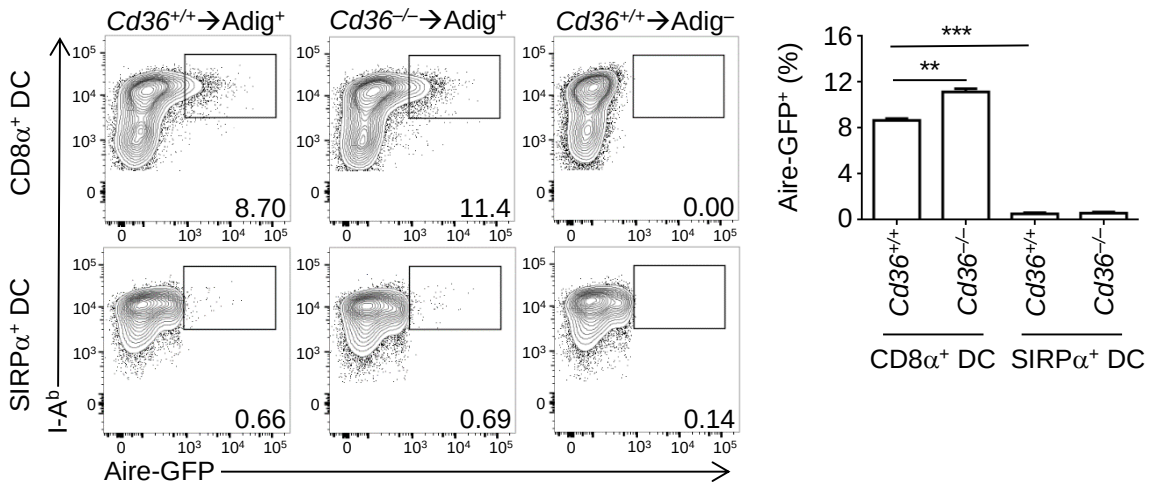

Figure 3. 14. CD8a^{+} DCs mediate transfer of cytoplasmic antigen independent of CD36.

	Cd36$^{+/-}$					*Cd36*$^{-/-}$				
				# of TCRs					# of TCRs	
Population	n mice (n expts)	Cells x10^3 Mean (SE)	# of reads	>.01% in 1 sample	>30% mice in 1 condition	n mice (n expts)	Cells x10^3 Mean (SE)	# of reads	>.01% in 1 sample	>30% mice in 1 condition
Foxp3$^-$	10 (2)	1488 (178)	680901	14982	1580	10 (2)	1460 (209)	656181	12587	1812
Foxp3$^+$	9 (2)	27.4 (13)	569609	6789	482	10 (2)	36.1 (15)	538141	6558	504

Figure 3. 15. TCR sequencing output for *Cd36*$^{+/-}$ and *Cd36*$^{-/-}$ mice.

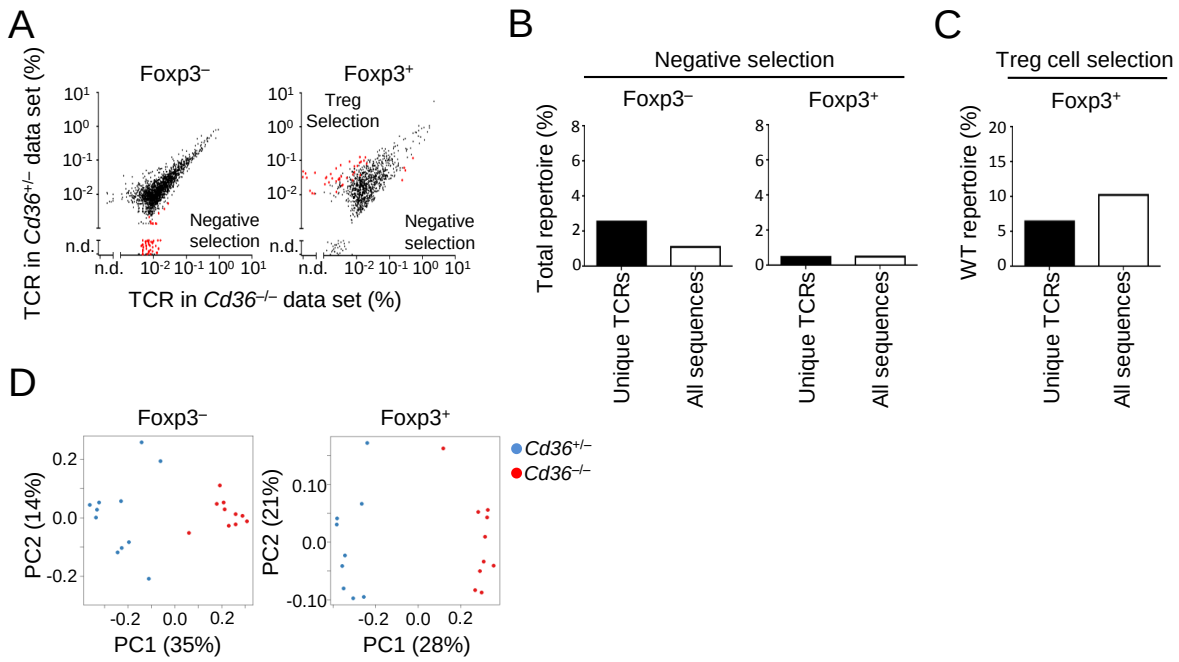

Figure 3. 16. Treg and Tconv cell TCR sequencing of *Cd36*$^{+/-}$ and *Cd36*$^{-/-}$ mice.

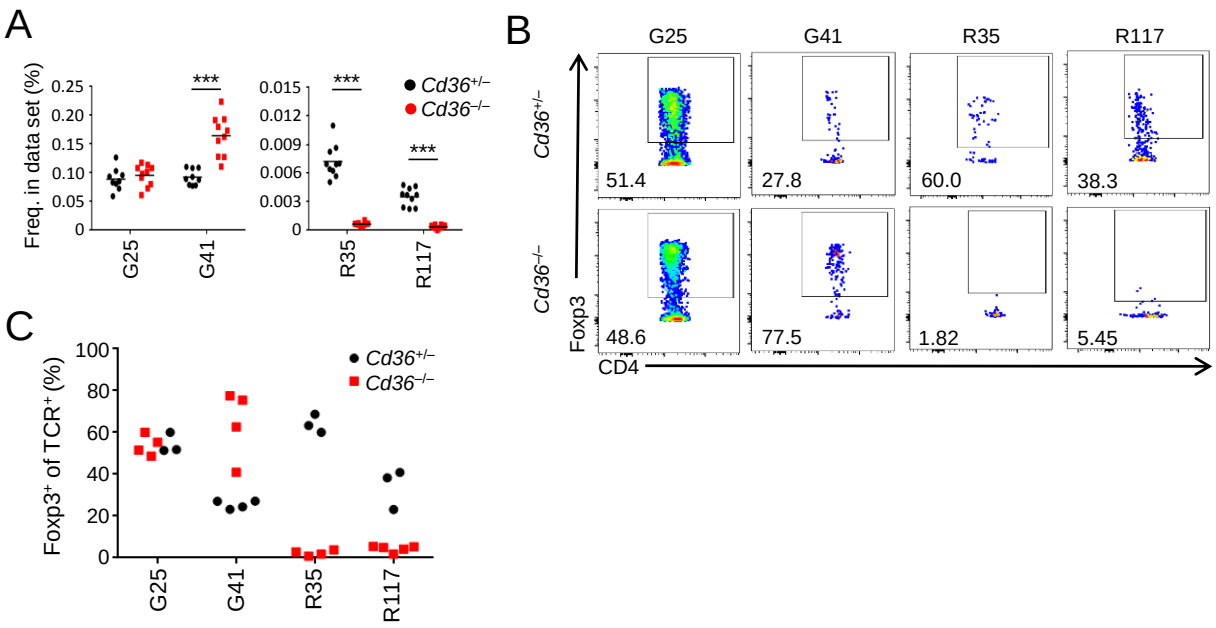

Figure 3. 17. *In vivo* validation of the behavior of Batf3/Aire-codependent Treg cell TCRs observed in *Cd36*$^{+/-}$ and *Cd36*$^{-/-}$ TCR sequencing.

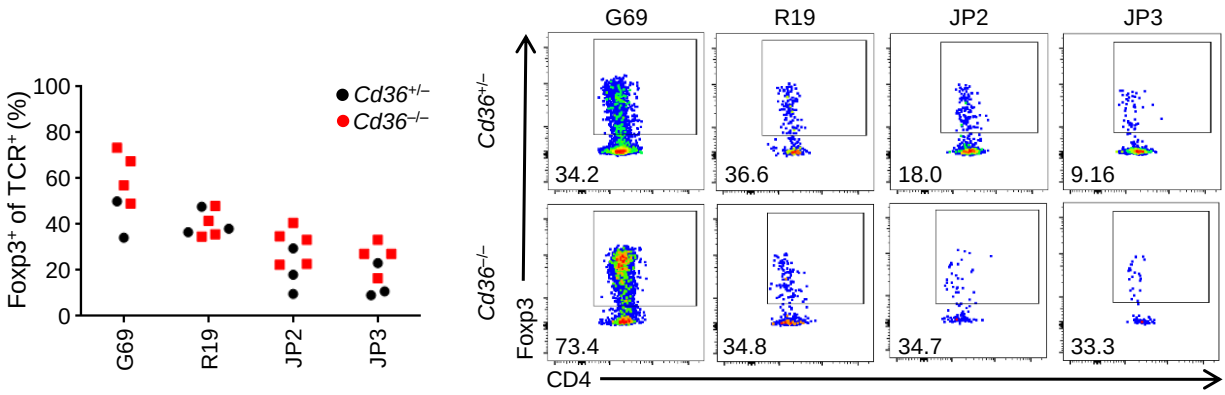

Figure 3. 18. *In vivo* validation of the behavior of Batf3/Aire-independent Treg cell TCRs observed in *Cd36*$^{+/-}$ and *Cd36*$^{-/-}$ TCR sequencing.

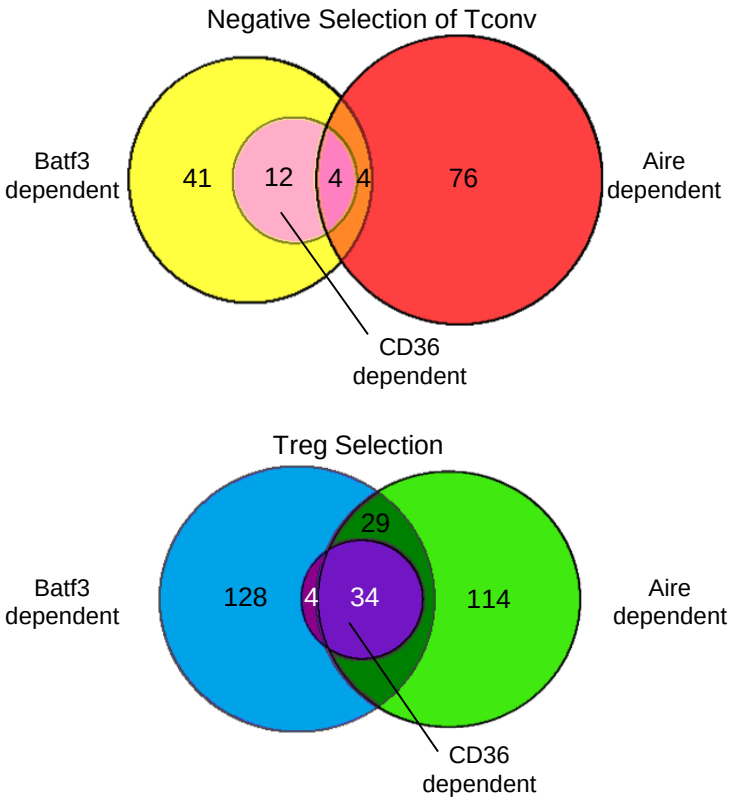

Figure 3. 19. Analysis of CD36/Batf3/Aire-codependence for deletion and Treg cell selection.

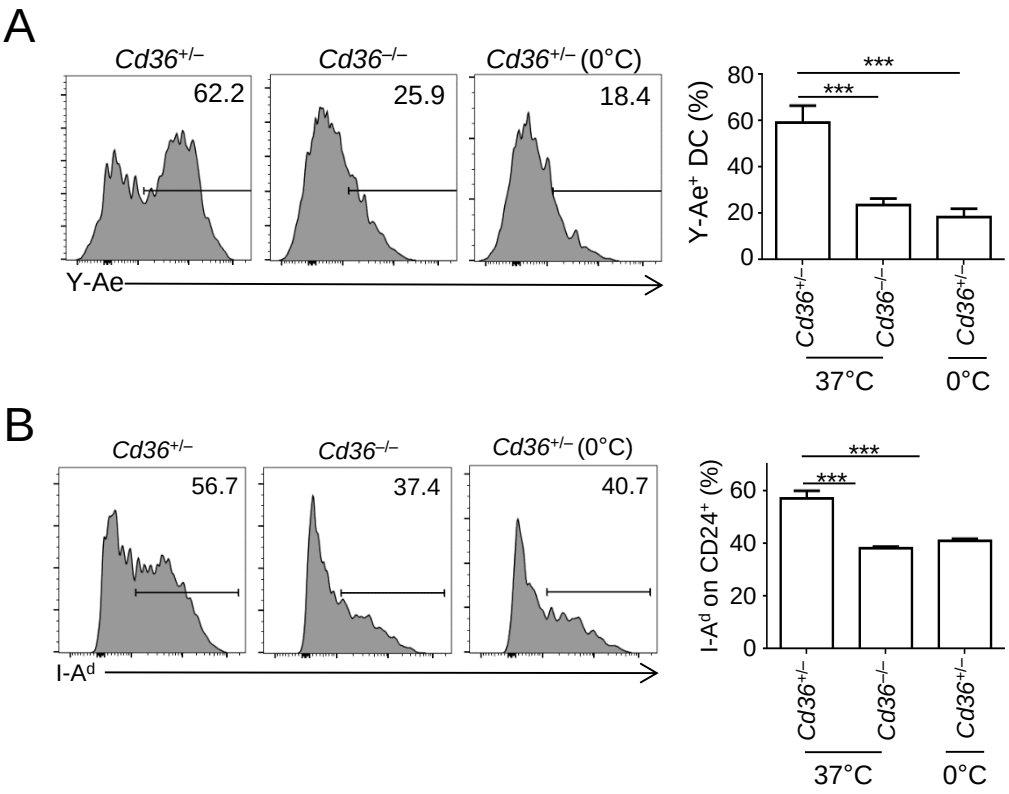

Figure 3. 20. CD36 mediates acquisition and presentation of intact peptide/MHC *in vitro*

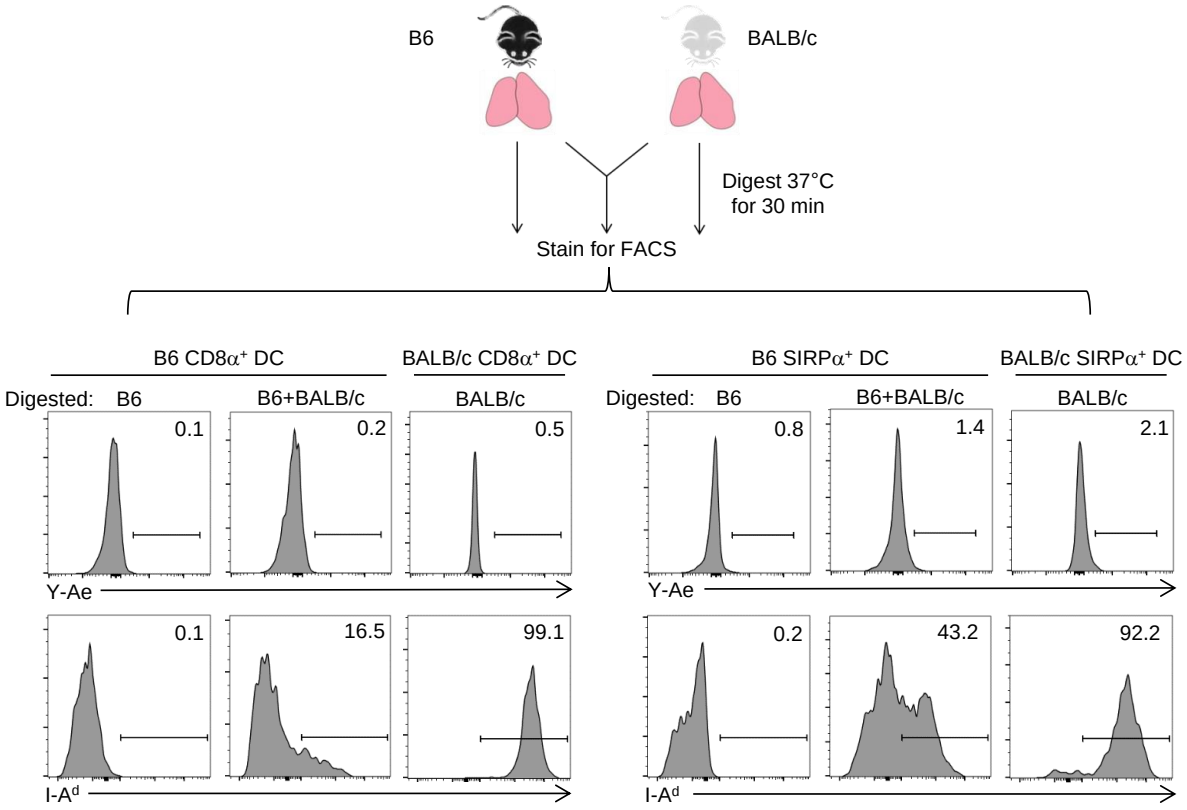

Figure 3. 21. Measurement of *in vivo* transferred intact peptide/MHC is obscured by thymic digestion.

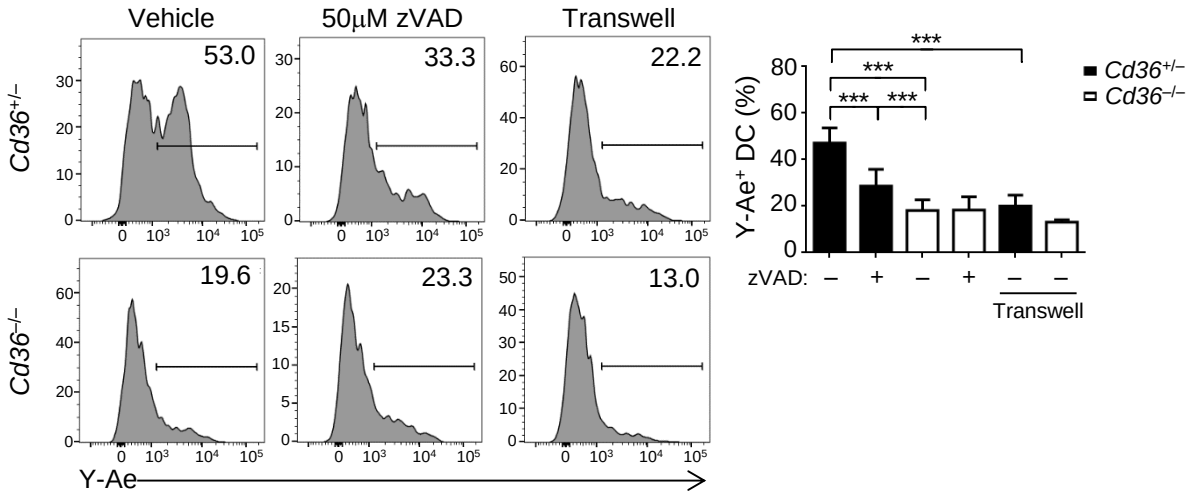

Figure 3. 22. CD36 acquires cell-surface antigen via scavenging of apoptotic bodies.

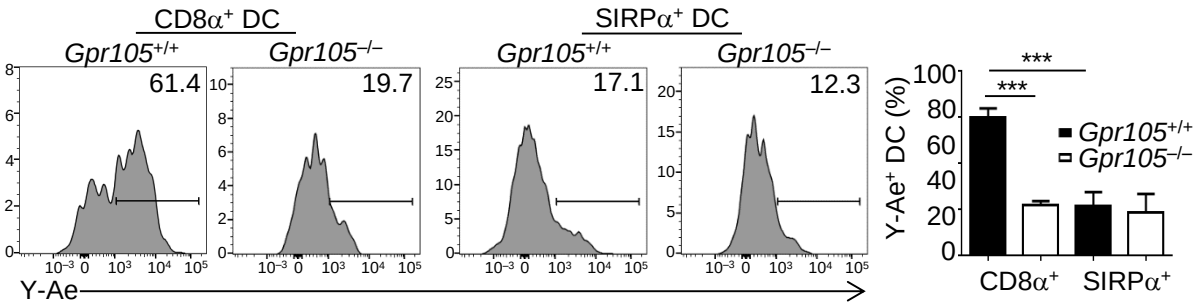

Figure 3. 23. The purinergic receptor GPR105 (P2Y14R) mediates transfer of cell-surface antigen from mTECs.

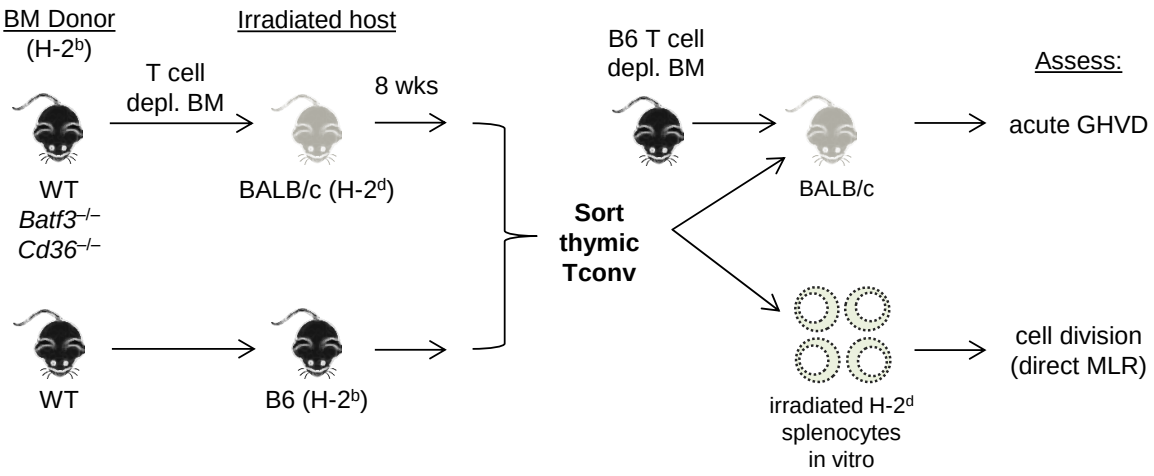

Figure 3. 24. Experimental design to assess tolerance during allogeneic bone marrow transplantation.

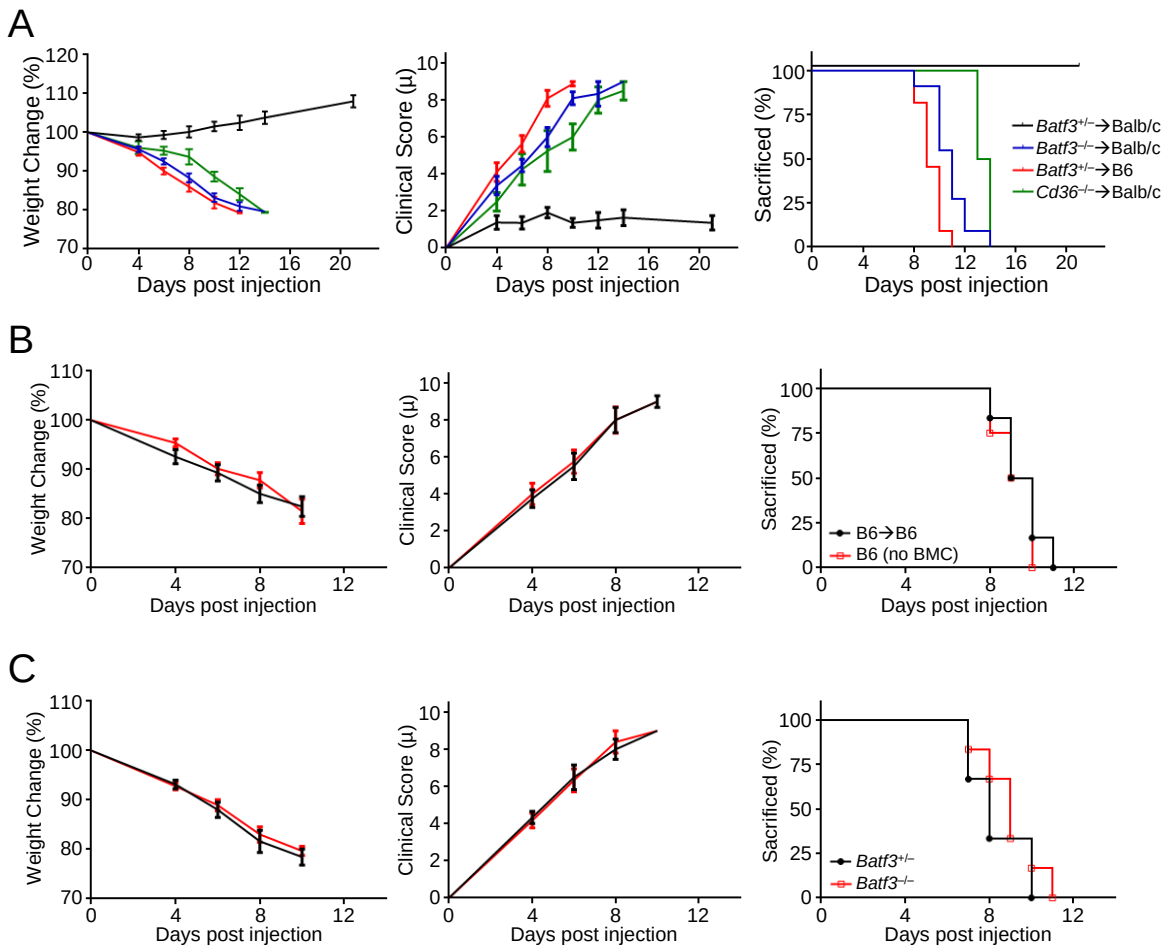

Figure 3. 25. Batf3/CD36-dependent antigen transfer facilitates allo-tolerance development and prevents catastrophic acute GVHD.

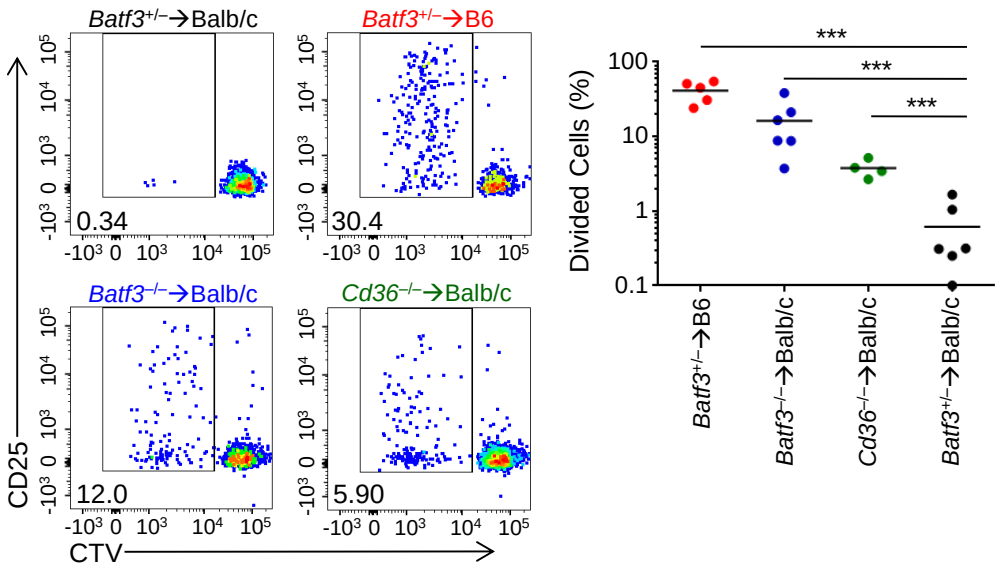

Figure 3. 26. CD36-dependent antigen transfer is necessary for direct allo-tolerance in the thymus.

Discussion

Although the process of antigen transfer of self-proteins from mTECs to BM APCs has been recognized for over 2 decades, a mechanism for this process has not been described. We make the following observations regarding cooperative antigen presentation of mTEC-derived antigens. First, Batf3-dependent CD8α^+ DCs play an important role in Aire-dependent thymic tolerance based on TCR repertoire analysis in a fixed TCRβ model. Second, antigen transfer from Aire-expressing mTECs to CD8α^+ DCs occurs via at least two distinct routes that segregate between cell-surface and cytoplasmic antigens. Third, cell-surface antigen transfer is mediated by CD36, a scavenger receptor preferentially expressed on the CD8α^+ subset of DCs. Finally, an intermediate step in CD36-mediated antigen transfer involves the display of cell-surface proteins, a.k.a. cross-dressing, which appears necessary for the generation of tolerance to host MHC during allo-bone marrow transplantation. Thus, our data demonstrate that antigen transfer can occur via multiple pathways, and suggest that CD36-mediated uptake of cell-surface proteins by CD8α^+ DCs plays an important role in tolerance to mTEC-derived antigens.

Previous studies have suggested that thymic CD8α^+ DCs are important in thymic tolerance. For example, CD8α^+ DCs have been reported to home to mTECs via the mTEC-derived chemokine XCL1 (Lei et al., 2011). Moreover, we recently showed using a panel of 8 TCRs that Batf3-dependent CD8α^+ DCs were associated with antigen transfer (Perry et al., 2014). Here, we have quantified the effect of Batf3-deficiency on the CD4SP TCR repertoire in a fixed TCRβ model. The analysis of a fully polyclonal repertoire introduces the experimental complexity of pairing α and β chains for

sequencing, as well as increased mouse to mouse variability due to the much greater repertoire diversity. With this restriction in mind, our results demonstrate that Batf3-dependent DCs affect both negative selection and Treg cell selection. Cross-correlation with effect of Aire on the TCR repertoire led to an estimate that CD8α^+ DCs contributes to only ~6-9% of Aire-dependent negative selection, versus ~ 34% for Aire-dependent Treg cell selection. This is reminiscent of our previous results with C2TAkd of MHCII on mTECs, which affected ~ 30% of Treg TCRs, but only 5% of negatively selected TCRs. We speculate that this may arise from differences in co-stimulatory molecules between APC subsets, or in the level of antigen presentation achieved after antigen transfer versus autologous presentation. While future experiments are required to test these hypotheses, our TCR repertoire analysis supports the notion that CD8α^+ DCs have substantial interactions with mTECs for cooperative antigen presentation and Treg cell selection.

The TCR repertoire data from Batf3-deficient mice suggests that there should be a loss of tolerance to certain Aire-dependent antigens. We confirmed that these defects in thymic selection result in enhanced immunopathology after transfer of thymocytes into lymphopenic hosts. These findings are similar to those observed in recipients of Tconv cells transferred from *Aire*-deficient mice, as well as in recipients of Tconv cells from Batf3/Aire-co-dependent Treg cell TCR (G25) transgenic mice. These data therefore support the TCR analysis suggesting that CD8α^+ DCs are involved in Aire-mediated tolerance.

However, overt autoimmunity has not been reported in Batf3-deficient mice. One possibility is that, similar to *Aire*-deficient mice on the C57BL/6 background (Hubert et

al., 2009), peripheral mechanisms restrain autoimmunity. Alternatively, we and others hypothesized that CD8α^+ DCs might be involved in both thymic tolerance as well as presentation of those antigens in the periphery (Klein et al., 2014; Perry et al., 2014). This hypothesis was supported by our observation that 4 Batf3-dependent TCRs showed diminished peripheral T cell activation in Batf3-deficient hosts. This is also consistent with recent work demonstrating that intrathymic injection of peripheral DCs from skin-draining LNs increased thymic Treg cell development of an Aire/BM APC-dependent Treg cell TCR (Lin et al., 2016). In addition, Batf3-deficiency on the NOD background protects mice from autoimmune diabetes (Ferris et al., 2014), suggesting an important role for this DC subset in peripheral autoantigen presentation. Taken together, our data imply that CD8α^+ DCs contribute to both thymic deletion and Treg cell selection of a subset of self-reactive TCRs, but may also be involved in antigen presentation to those same TCRs in the periphery.

The theory that CD8α^+ DCs might perform the same antigen presentation function in the thymus as well as the periphery raises the question whether antigen transfer in the thymus is a unique process. It may be beneficial for the immune system to use the same APCs in the thymus that present particular self-antigens in the periphery. First, it is well established that the antigen processing machinery in DCs is different than that of mTECs. This includes both the enzymes utilized to generate peptides from proteins (Nakagawa et al., 1998), as well as the phagocytic versus autophagy pathway by which antigens are routed to the MHCII presentation pathway in DCs versus mTECs, respectively (Aichinger et al., 2013; Joffre et al., 2012). Second, the receptors used by CD8α^+ DCs appear to be the same between the thymus and the

periphery. In fact, the decision to test CD36 and Gpr105 was based on gene-chip data from both peripheral and thymic CD8α^+/CD103$^+$ DCs, suggesting that presentation of apoptotic antigens may be a shared feature of thymic and peripheral CD8α^+ DCs. Third, cross-dressing of MHC molecules was originally described in the periphery (Wakim and Bevan, 2011). It is therefore tempting to speculate that this process is similar to what we have observed in the thymus. Taken together, the process of antigen transfer in the thymus may not represent a specialized interaction, but simply the use of peripheral antigen presentation mechanisms to standardize the generation of self-epitopes seen by immature and mature T cells.

The mechanism utilized by CD8α^+ DCs to acquire cell-surface antigens from mTECs appears to be the recognition of apoptotic bodies by CD36. CD36 is specifically expressed on thymic CD8α^+ DCs but not SIRPα^+ or pDCs, and is reported to bind PS present on apoptotic bodies. We found in TCR repertoire analysis that CD36 was involved in both negative selection and Treg cell differentiation with a strong bias toward co-dependence with Batf3 and Aire, implying that CD36 plays a role in antigen transfer to CD8α^+ DCs. In addition, absence of CD36 resulted in the loss of CD8α^+ DC acquisition and presentation of membrane-bound I-Eα antigen from mTECs *in vivo*. Finally, deficiency in the purinergic receptor Gpr105, which recognizes the “find-me” signal UDP released by apoptotic cells, decreased CD8α^+ DC presentation of cell-surface-bound antigen acquired from mTECs. Taken together, these data suggest a model in which mTECs mature, express Aire, and ultimately undergo apoptosis to generate bodies that are recognized by CD36 on CD8α^+ DCs.

Transfer and presentation of cell-surface proteins on MHCII could occur via at least two distinct mechanisms. First, I-Eα could be phagocytosed/endocytosed where it is degraded in the lysosome and loaded onto MHCII. Alternatively, cell-surface proteins could be directly transferred from one membrane to another in a process akin to trogocytosis. For MHCI presentation in the periphery, this process has been termed "cross-dressing." Internalization of transferred cell-surface proteins can then result in peptide presentation on MHCII. Although we cannot currently exclude a role for phagocytosis, our data suggest that CD36-mediated antigen transfer results in "cross-dressing" as evidenced by its role in direct allo-tolerance during bone marrow transplantation.

The observation that MHC is directly transferred to the CD8α^+ DC cell surface brings up the possibility that mTEC-loaded peptide:MHC complexes directly mediate negative selection or Treg cell differentiation (Koble and Kyewski, 2009). Alternatively, mTEC-derived cell surface antigens can be internalized, degraded, and loaded onto MHCII as detected by the peptide-in-groove antibody Y-Ae. This mechanism could explain the observation of antigen transfer using the RIP-mOVA transgene (Koble and Kyewski, 2009), which expresses a transmembrane protein conjugated to OVA peptide. Understanding which cell-surface proteins transferred from mTECs has unfortunately been limited by the possibility of cross-contamination during our thymic DC preparation protocol. Future studies are required to determine the relative importance of CD8α^+ presentation of intact peptide/MHC transferred from mTECs versus internalization and presentation of mTEC-associated cell-surface antigens.

In addition to CD36-dependent transfer of cell-surface proteins, we also observed transfer of cytoplasmic GFP from mTECs to CD8α^+ DCs via a CD36-independent mechanism, demonstrating the existence of an additional antigen-transfer pathway. It remains unresolved whether cytoplasmic antigen transfer involves a different mTEC-derived particle, as it remains possible that CD36 could be simply involved in the transfer of cell-surface proteins from apoptotic blebs which go on to be internalized via other mechanisms (Albert et al., 1998). Alternatively, uptake of different particles such as exosomes versus apoptotic blebs from mTECs could favor cytoplasmic versus cell-membrane proteins. Future studies will be required to clarify the mechanism by which cytoplasmic antigens are transferred.

In summary, these data suggest that antigen transfer from mTECs is mediated to a large part by CD8α^+ DCs and is demonstrably important to thymic T cell tolerance. We have also determined that CD36 facilitates direct transfer of MHC and presumably other cell-surface proteins onto the cell surface of CD8α^+ DCs. One intriguing hypothesis is that defects in this pathway may lead to loss of tolerance to cell-surface proteins, potentially contributing to antibody mediated diseases such as Graves autoimmune thyroiditis that target cell-surface receptors. In a similar vein, defects in the transfer of cell-surface antigens might contribute to the loss of allo-tolerance during bone marrow transplantation, resulting in chronic graft versus host disease.

CHAPTER 4

Concluding Remarks and Discussion

There have been a number of recent advances in our understanding of how self-reactive thymocytes are deleted or selected to become Treg cells. Recent data suggest that the medullary APCs subsets often function non-redundantly. pDCs and SIRPα^+ DCs appear more adept at acquiring and presenting peripheral and blood-borne antigen, whereas mTECs and B cells present different arrays of Aire-dependent peripheral tissue antigens. Recent data also highlight the cooperativity between the APC subsets. Batf3-dependent CD8α^+ DCs appear to preferentially acquire antigen from Aire$^+$ mTECs to facilitate the development of thymic Treg cells. In fact, cooperative antigen presentation of mTEC antigens transferred to BM APCs may be as important as cell-autonomous mTEC antigen presentation.

However, a number of issues remain. First, identification of naturally occurring Treg cell TCR ligands would be useful to address which APCs generate and present these ligands and to determine the TCR affinity required for Treg and negative selection. Second, quantification of the contribution of each APC subset, as well as the importance of transport of extra-thymic antigens by migratory APC populations, to Treg and negative selection is needed. Third, understanding the factors that determine the utilization of mTEC-autonomous versus cooperative antigen transfer pathways for tolerance would be important for understanding why and how antigen transfer occurs. Finally, it is important to examine whether these mechanisms are regulated during ontogeny such that certain periods of life favor tolerance versus immunity. Thus, future

studies will seek to define the interaction of the thymic antigenic repertoire with the APC subsets and the generation of thymic tolerance.

REFERENCES

Abramson, J., Giraud, M., Benoist, C., and Mathis, D. (2010). Aire's partners in the molecular control of immunological tolerance. Cell *140*, 123-135.

Aichinger, M., Wu, C., Nedjic, J., and Klein, L. (2013a). Macroautophagy substrates are loaded onto MHC class II of medullary thymic epithelial cells for central tolerance. J. Exp. Med. *210*, 287-300.

Aichinger, M., Wu, C., Nedjic, J., and Klein, L. (2013b). Macroautophagy substrates are loaded onto MHC class II of medullary thymic epithelial cells for central tolerance. The Journal of Experimental Medicine *210*, 287-300.

Akirav, E.M., Ruddle, N.H., and Herold, K.C. (2011). The role of AIRE in human autoimmune disease. Nat Rev Endocrinol *7*, 25-33.

Albert, M.L., Pearce, S.F.A., Francisco, L.M., Sauter, B., Roy, P., Silverstein, R.L., and Bhardwaj, N. (1998). Immature Dendritic Cells Phagocytose Apoptotic Cells via αvβ5 and CD36, and Cross-present Antigens to Cytotoxic T Lymphocytes. The Journal of Experimental Medicine *188*, 1359-1368.

Anderson, M.S., and Su, M.A. (2011). Aire and T cell development. Current Opinion in Immunology *23*, 198-206.

Anderson, M.S., Venanzi, E.S., Chen, Z., Berzins, S.P., Benoist, C., and Mathis, D. (2005). The Cellular Mechanism of Aire Control of T Cell Tolerance. Immunity *23*, 227-239.

Aschenbrenner, K., D'Cruz, L.M., Vollmann, E.H., Hinterberger, M., Emmerich, J., Swee, L.K., Rolink, A., and Klein, L. (2007). Selection of Foxp3+ regulatory T cells specific for self antigen expressed and presented by Aire+ medullary thymic epithelial cells. Nat Immunol *8*, 351-358.

Atibalentja, D.F., Byersdorfer, C.A., and Unanue, E.R. (2009). Thymus-blood protein interactions are highly effective in negative selection and regulatory T cell induction. J. Immunol. *183*, 7909-7918.

Atibalentja, D.F., Murphy, K.M., and Unanue, E.R. (2011). Functional Redundancy between Thymic CD8α+ and Sirpα+ Conventional Dendritic Cells in Presentation of Blood-Derived Lysozyme by MHC Class II Proteins. The Journal of Immunology *186*, 1421-1431.

Baba, T., Nakamoto, Y., and Mukaida, N. (2009a). Crucial contribution of thymic Sirp[alpha]+ conventional dendritic cells to central tolerance against blood-borne antigens in a CCR2-dependent manner. J. Immunol. *183*, 3053-3063.

Baba, T., Nakamoto, Y., and Mukaida, N. (2009b). Crucial Contribution of Thymic Sirpα+ Conventional Dendritic Cells to Central Tolerance against Blood-Borne Antigens in a CCR2-Dependent Manner. The Journal of Immunology *183*, 3053-3063.

Bachem, A., Hartung, E., Güttler, S., Mora, A., Zhou, X., Hegemann, A., Plantinga, M., Mazzini, E., Stoitzner, P., Gurka, S.*, et al.* (2012). Expression of XCR1 Characterizes the Batf3-Dependent Lineage of Dendritic Cells Capable of Antigen Cross-Presentation. Frontiers in Immunology *3*, 214.

Bania, J., Gatti, E., Lelouard, H., David, A., Cappello, F., Weber, E., Camosseto, V., and Pierre, P. (2003). Human cathepsin S, but not cathepsin L, degrades efficiently MHC class II-associated invariant chain in nonprofessional APCs. Proceedings of the National Academy of Sciences *100*, 6664-6669.

Bautista, J.L., Lio, C.-W.J., Lathrop, S.K., Forbush, K., Liang, Y., Luo, J., Rudensky, A.Y., and Hsieh, C.-S. (2009). Intraclonal competition limits the fate determination of regulatory T cells in the thymus. Nat Immunol *10*, 610-617.

Beers, C., Burich, A., Kleijmeer, M.J., Griffith, J.M., Wong, P., and Rudensky, A.Y. (2005). Cathepsin S Controls MHC Class II-Mediated Antigen Presentation by Epithelial Cells In Vivo. The Journal of Immunology *174*, 1205-1212.

Belz, G.T., Vremec, D., Febbraio, M., Corcoran, L., Shortman, K., Carbone, F.R., and Heath, W.R. (2002). CD36 Is Differentially Expressed by CD8+ Splenic Dendritic Cells But Is Not Required for Cross-Presentation In Vivo. The Journal of Immunology *168*, 6066-6070.

Bensinger, S.J., Bandeira, A., Jordan, M.S., Caton, A.J., and Laufer, T.M. (2001). Major Histocompatibility Complex Class II–Positive Cortical Epithelium Mediates the Selection of Cd4+25+ Immunoregulatory T Cells. The Journal of Experimental Medicine *194*, 427-438.

Bluestone, J.A., Bour-Jordan, H., Cheng, M., and Anderson, M. (2015). T cells in the control of organ-specific autoimmunity. The Journal of Clinical Investigation *125*, 2250-2260.

Bonasio, R., Scimone, M.L., Schaerli, P., Grabie, N., Lichtman, A.H., and von Andrian, U.H. (2006). Clonal deletion of thymocytes by circulating dendritic cells homing to the thymus. Nat Immunol *7*, 1092-1100.

Brennecke, P., Reyes, A., Pinto, S., Rattay, K., Nguyen, M., Kuchler, R., Huber, W., Kyewski, B., and Steinmetz, L.M. (2015). Single-cell transcriptome analysis reveals coordinated ectopic gene-expression patterns in medullary thymic epithelial cells. Nat Immunol *16*, 933-941.

Calderon, B., Carrero, J.A., and Unanue, E.R. (2014). The central role of antigen presentation in islets of Langerhans in autoimmune diabetes. Current Opinion in Immunology *26*, 32-40.

Chan, A.Y., and Anderson, M.S. (2015). Central tolerance to self revealed by the autoimmune regulator. Annals of the New York Academy of Sciences *1356*, 80-89.

Cooke, K., Kobzik, L., Martin, T., Brewer, J., Delmonte, J.J., Crawford, J., and Ferrara, J. (1996). An experimental model of idiopathic pneumonia syndrome after bone marrow transplantation: I. The roles of minor H antigens and endotoxin. Blood *88*, 3230-3239.

Cowan, J.E., Parnell, S.M., Nakamura, K., Caamano, J.H., Lane, P.J.L., Jenkinson, E.J., Jenkinson, W.E., and Anderson, G. (2013). The thymic medulla is required for Foxp3+ regulatory but not conventional CD4+ thymocyte development. The Journal of Experimental Medicine *210*, 675-681.

Daniely, D., Kern, J., Cebula, A., and Ignatowicz, L. (2010). Diversity of TCRs on Natural Foxp3+ T Cells in Mice Lacking Aire Expression. The Journal of Immunology *184*, 6865-6873.

Dengjel, J., Schoor, O., Fischer, R., Reich, M., Kraus, M., Müller, M., Kreymborg, K., Altenberend, F., Brandenburg, J., Kalbacher, H.*, et al.* (2005). Autophagy promotes MHC class II presentation of peptides from intracellular source proteins. Proceedings of the National Academy of Sciences *102*, 7922-7927.

Derbinski, J., and Kyewski, B. (2010). How thymic antigen presenting cells sample the body's self-antigens. Current Opinion in Immunology *22*, 592-600.

Eckler, M.J., and Chen, B. (2014). Fez family transcription factors: Controlling neurogenesis and cell fate in the developing mammalian nervous system. BioEssays *36*, 788-797.

English, L., Chemali, M., Duron, J., Rondeau, C., Laplante, A., Gingras, D., Alexander, D., Leib, D., Norbury, C., Lippe, R., and Desjardins, M. (2009). Autophagy enhances the presentation of endogenous viral antigens on MHC class I molecules during HSV-1 infection. Nat Immunol *10*, 480-487.

Febbraio, M., Abumrad, N.A., Hajjar, D.P., Sharma, K., Cheng, W., Pearce, S.F.A., and Silverstein, R.L. (1999). A Null Mutation in Murine CD36 Reveals an Important Role in Fatty Acid and Lipoprotein Metabolism. Journal of Biological Chemistry *274*, 19055-19062.

Ferris, Stephen T., Carrero, Javier A., Mohan, James F., Calderon, B., Murphy, Kenneth M., and Unanue, Emil R. (2014). A Minor Subset of Batf3-Dependent Antigen-Presenting Cells in Islets of Langerhans Is Essential for the Development of Autoimmune Diabetes. Immunity *41*, 657-669.

Fierer, N., Hamady, M., Lauber, C.L., and Knight, R. (2008). The influence of sex, handedness, and washing on the diversity of hand surface bacteria. Proceedings of the National Academy of Sciences.

Gallegos, A.M., and Bevan, M.J. (2004). Central Tolerance to Tissue-specific Antigens Mediated by Direct and Indirect Antigen Presentation. The Journal of Experimental Medicine *200*, 1039-1049.

Giudicelli, V., Duroux, P., Ginestoux, C., Folch, G., Jabado-Michaloud, J., Chaume, D., and Lefranc, M.-P. (2006). IMGT/LIGM-DB, the IMGT® comprehensive database of immunoglobulin and T cell receptor nucleotide sequences. Nucleic Acids Research *34*, D781-D784.

Gray, D., Abramson, J., Benoist, C., and Mathis, D. (2007). Proliferative arrest and rapid turnover of thymic epithelial cells expressing Aire. The Journal of Experimental Medicine *204*, 2521-2528.

Hildner, K., Edelson, B.T., Purtha, W.E., Diamond, M., Matsushita, H., Kohyama, M., Calderon, B., Schraml, B.U., Unanue, E.R., Diamond, M.S.*, et al.* (2008). Batf3 Deficiency Reveals a Critical Role for CD8α+ Dendritic Cells in Cytotoxic T Cell Immunity. Science *322*, 1097-1100.

Hinterberger, M., Aichinger, M., da Costa, O.P., Voehringer, D., Hoffmann, R., and Klein, L. (2010). Autonomous role of medullary thymic epithelial cells in central CD4+ T cell tolerance. Nat Immunol *11*, 512-519.

Hinterberger, M., Wirnsberger, G., and Klein, L. (2011). B7/CD28 in central tolerance: costimulation promotes maturation of regulatory T cell precursors and prevents their clonal deletion. Frontiers in immunology *2*.

Hsieh, C.-S., Lee, H.-M., and Lio, C.-W.J. (2012a). Selection of regulatory T cells in the thymus. Nat Rev Immunol *12*, 157-167.

Hsieh, C.-S., Liang, Y., Tyznik, A.J., Self, S.G., Liggitt, D., and Rudensky, A.Y. (2004). Recognition of the Peripheral Self by Naturally Arising CD25+ CD4+ T Cell Receptors. Immunity *21*, 267-277.

Hsieh, C.S., Lee, H.M., and Lio, C.W. (2012b). Selection of regulatory T cells in the thymus. Nature Rev. Immunol. *12*, 157-167.

Hubert, F.-X., Kinkel, S.A., Crewther, P.E., Cannon, P.Z.F., Webster, K.E., Link, M., Uibo, R., O'Bryan, M.K., Meager, A., Forehan, S.P.*, et al.* (2009). Aire-Deficient C57BL/6 Mice Mimicking the Common Human 13-Base Pair Deletion Mutation Present with Only a Mild Autoimmune Phenotype. The Journal of Immunology *182*, 3902-3918.

Hubert, F.-X., Kinkel, S.A., Davey, G.M., Phipson, B., Mueller, S.N., Liston, A., Proietto, A.I., Cannon, P.Z.F., Forehan, S., Smyth, G.K.*, et al.* (2011). Aire regulates the transfer of antigen from mTECs to dendritic cells for induction of thymic tolerance. Blood *118*, 2462-2472.

Hubert, F.X. (2011). Aire regulates the transfer of antigen from mTECs to dendritic cells for induction of thymic tolerance. Blood *118*, 2462-2472.

Humblet, C., Rudensky, A.Y., and Kyewski, B. (1994). Presentation and intercellular transfer of self antigen within the thymic microenvironment: expression of the Eα peptide-I-Ab complex by isolated thymic stromal cells. International Immunology *6*, 1949-1958.

Irla, M., Hugues, S., Gill, J., Nitta, T., Hikosaka, Y., Williams, I.R., Hubert, F.-X., Scott, H.S., Takahama, Y., Holländer, G.A., and Reith, W. (2008). Autoantigen-Specific Interactions with CD4+ Thymocytes Control Mature Medullary Thymic Epithelial Cell Cellularity. Immunity *29*, 451-463.

Joffre, O.P., Segura, E., Savina, A., and Amigorena, S. (2012). Cross-presentation by dendritic cells. Nat Rev Immunol *12*, 557-569.

Jordan, M.S., Boesteanu, A., Reed, A.J., Petrone, A.L., Holenbeck, A.E., Lerman, M.A., Naji, A., and Caton, A.J. (2001). Thymic selection of CD4+CD25+ regulatory T cells induced by an agonist self-peptide. Nat Immunol *2*, 301-306.

Josefowicz, S.Z., Lu, L.-F., and Rudensky, A.Y. (2012). Regulatory T Cells: Mechanisms of Differentiation and Function. Annual Review of Immunology *30*, 531-564.

Klein, L. (2009). Dead man walking: how thymocytes scan the medulla. Nature Immunol. *10*, 809-811.

Klein, L., and Jovanovic, K. (2011). Regulatory T cell lineage commitment in the thymus. Seminars in Immunology *23*, 401-409.

Klein, L., Kyewski, B., Allen, P.M., and Hogquist, K.A. (2014). Positive and negative selection of the T cell repertoire: what thymocytes see (and don't see). Nat Rev Immunol *advance online publication*.

Klein, L., Roettinger, B., and Kyewski, B. (2001). Sampling of complementing self-antigen pools by thymic stromal cells maximizes the scope of central T cell tolerance. European Journal of Immunology *31*, 2476-2486.

Koble, C., and Kyewski, B. (2009a). The thymic medulla: a unique microenvironment for intercellular self-antigen transfer. The Journal of Experimental Medicine *206*, 1505-1513.

Koble, C., and Kyewski, B. (2009b). The thymic medulla: a unique microenvironment for intercellular self-antigen transfer. J. Exp. Med. *206*, 1505-1513.

Lee, H.-M., Bautista, Jhoanne L., Scott-Browne, J., Mohan, James F., and Hsieh, C.-S. (2012). A Broad Range of Self-Reactivity Drives Thymic Regulatory T Cell Selection to Limit Responses to Self. Immunity *37*, 475-486.

Lee, H.K., Mattei, L.M., Steinberg, B.E., Alberts, P., Lee, Y.H., Chervonsky, A., Mizushima, N., Grinstein, S., and Iwasaki, A. (2010). In Vivo Requirement for Atg5 in Antigen Presentation by Dendritic Cells. Immunity *32*, 227-239.

Lei, Y., Ripen, A.M., Ishimaru, N., Ohigashi, I., Nagasawa, T., Jeker, L.T., Bösl, M.R., Holländer, G.A., Hayashi, Y., de Waal Malefyt, R.*, et al.* (2011). Aire-dependent production of XCL1 mediates medullary accumulation of thymic dendritic cells and contributes to regulatory T cell development. The Journal of Experimental Medicine *208*, 383-394.

Li, J., Park, J., Foss, D., and Goldschneider, I. (2009). Thymus-homing peripheral dendritic cells constitute two of the three major subsets of dendritic cells in the steady-state thymus. J. Exp. Med. *206*, 607-622.

Li, X., Ye, Y., Zhou, X., Huang, C., and Wu, M. (2015). Atg7 Enhances Host Defense against Infection via Downregulation of Superoxide but Upregulation of Nitric Oxide. The Journal of Immunology *194*, 1112-1121.

Li, X., and Zheng, Y. (2015). Regulatory T cell identity: formation and maintenance. Trends in Immunology *36*, 344-353.

Lin, J., Yang, L., Silva, H.M., Trzeciak, A., Choi, Y., Schwab, S.R., Dustin, M.L., and Lafaille, J.J. (2016). Increased generation of Foxp3+ regulatory T cells by manipulating antigen presentation in the thymus. Nat Commun *7*.

Lio, C.-W.J., Dodson, L.F., Deppong, C.M., Hsieh, C.-S., and Green, J.M. (2010). CD28 Facilitates the Generation of Foxp3− Cytokine Responsive Regulatory T Cell Precursors. The Journal of Immunology *184*, 6007-6013.

Liston, A., Lesage, S., Wilson, J., Peltonen, L., and Goodnow, C.C. (2003). Aire regulates negative selection of organ-specific T cells. Nat Immunol *4*, 350-354.

Liston, A., Nutsch, K.M., Farr, A.G., Lund, J.M., Rasmussen, J.P., Koni, P.A., and Rudensky, A.Y. (2008). Differentiation of regulatory Foxp3+ T cells in the thymic cortex. Proceedings of the National Academy of Sciences *105*, 11903-11908.

Liu, E., Van Grol, J., and Subauste, C.S. (2015). Atg5 but not Atg7 in dendritic cells enhances IL-2 and IFN-γ production by Toxoplasma gondii-reactive CD4+ T cells. Microbes and Infection *17*, 275-284.

Malchow, S., Leventhal, D.S., Nishi, S., Fischer, B.I., Shen, L., Paner, G.P., Amit, A.S., Kang, C., Geddes, J.E., Allison, J.P.*, et al.* (2013). Aire-Dependent Thymic Development of Tumor-Associated Regulatory T Cells. Science *339*, 1219-1224.

Mathis, D., and Benoist, C. (2009a). Aire. Annual Review of Immunology *27*, 287-312.

Mathis, D., and Benoist, C. (2009b). Aire. Annu. Rev. Immunol. *27*, 287-312.

McCaughtry, T.M., Baldwin, T.A., Wilken, M.S., and Hogquist, K.A. (2008). Clonal deletion of thymocytes can occur in the cortex with no involvement of the medulla. The Journal of Experimental Medicine *205*, 2575-2584.

Meredith, M., Zemmour, D., Mathis, D., and Benoist, C. (2015). Aire controls gene expression in the thymic epithelium with ordered stochasticity. Nat Immunol *16*, 942-949.

Metzger, T.C., and Anderson, M.S. (2011). Control of central and peripheral tolerance by Aire. Immunological Reviews *241*, 89-103.

Millet, V., Naquet, P., and Guinamard, R.R. (2008). Intercellular MHC transfer between thymic epithelial and dendritic cells. Eur. J. Immunol. *38*, 1257-1263.

Moran, A.E., Holzapfel, K.L., Xing, Y., Cunningham, N.R., Maltzman, J.S., Punt, J., and Hogquist, K.A. (2011). T cell receptor signal strength in Treg and iNKT cell development demonstrated by a novel fluorescent reporter mouse. The Journal of Experimental Medicine *208*, 1279-1289.

Nakagawa, T., Roth, W., Wong, P., Nelson, A., Farr, A., Deussing, J., Villadangos, J.A., Ploegh, H., Peters, C., and Rudensky, A.Y. (1998). Cathepsin L: Critical Role in Ii Degradation and CD4 T Cell Selection in the Thymus. Science *280*, 450-453.

Nedjic, J., Aichinger, M., Emmerich, J., Mizushima, N., and Klein, L. (2008a). Autophagy in thymic epithelium shapes the T-cell repertoire and is essential for tolerance. Nature *455*, 396-400.

Nedjic, J., Aichinger, M., Emmerich, J., Mizushima, N., and Klein, L. (2008b). Autophagy in thymic epithelium shapes the T-cell repertoire and is essential for tolerance. Nature *455*, 396-400.

Oh, J., and Shin, J.-S. (2015). The Role of Dendritic Cells in Central Tolerance. Immune Netw *15*, 111-120.

Oh, J., Wu, N., Baravalle, G., Cohn, B., Ma, J., Lo, B., Mellman, I., Ishido, S., Anderson, M., and Shin, J.-S. (2013). MARCH1-mediated MHCII ubiquitination promotes dendritic cell selection of natural regulatory T cells. The Journal of Experimental Medicine *210*, 1069-1077.

Ohnmacht, C., Pullner, A., King, S.B.S., Drexler, I., Meier, S., Brocker, T., and Voehringer, D. (2009). Constitutive ablation of dendritic cells breaks self-tolerance of CD4 T cells and results in spontaneous fatal autoimmunity. The Journal of Experimental Medicine *206*, 549-559.

Oukka, M., Cohen-Tannoudji, M., Tanaka, Y., Babinet, C., and Kosmatopoulos, K. (1996). Medullary thymic epithelial cells induce tolerance to intracellular proteins. J. Immunol. *156*, 968-975.

Pacholczyk, R., Kern, J., Singh, N., Iwashima, M., Kraj, P., and Ignatowicz, L. (2007). Nonself-Antigens Are the Cognate Specificities of Foxp3+ Regulatory T Cells. Immunity *27*, 493-504.

Palmer, E. (2003). Negative selection [mdash] clearing out the bad apples from the T-cell repertoire. Nat Rev Immunol *3*, 383-391.

Paludan, C., Schmid, D., Landthaler, M., Vockerodt, M., Kube, D., Tuschl, T., and Münz, C. (2005). Endogenous MHC Class II Processing of a Viral Nuclear Antigen After Autophagy. Science *307*, 593-596.

Perry, Justin S.A., Lio, C.-Wang J., Kau, Andrew L., Nutsch, K., Yang, Z., Gordon, Jeffrey I., Murphy, Kenneth M., and Hsieh, C.-S. (2014). Distinct Contributions of Aire

and Antigen-Presenting-Cell Subsets to the Generation of Self-Tolerance in the Thymus. Immunity *41*, 414-426.

Polychronakos, C., and Li, Q. (2011). Understanding type 1 diabetes through genetics: advances and prospects. Nat Rev Genet *12*, 781-792.

Proietto, A.I., Lahoud, M.H., and Wu, L. (2008a). Distinct functional capacities of mouse thymic and splenic dendritic cell populations. Immunol Cell Biol *86*, 700-708.

Proietto, A.I., van Dommelen, S., Zhou, P., Rizzitelli, A., D'Amico, A., Steptoe, R.J., Naik, S.H., Lahoud, M.H., Liu, Y., Zheng, P.*, et al.* (2008b). Dendritic cells in the thymus contribute to T-regulatory cell induction. Proceedings of the National Academy of Sciences *105*, 19869-19874.

Richards, D.M., Kyewski, B., and Feuerer, M. (2016). Re-examining the Nature and Function of Self-Reactive T cells. Trends in Immunology *37*, 114-125.

Román, E., Shino, H., Qin, F.X.-F., and Liu, Y.J. (2010). Cutting Edge: Hematopoietic-Derived APCs Select Regulatory T Cells in Thymus. The Journal of Immunology *185*, 3819-3823.

Rudensky, A.Y. (2011). Regulatory T cells and Foxp3. Immunological Reviews *241*, 260-268.

Rudensky, A.Y., Rath, S., Preston-Hurlburt, P., Murphy, D.B., and Janeway, C.A. (1991). On the complexity of self. Nature *353*, 660-662.

Sakaguchi, S., and Powrie, F. (2007). Emerging Challenges in Regulatory T Cell Function and Biology. Science *317*, 627-629.

Satpathy, A.T., Wu, X., Albring, J.C., and Murphy, K.M. (2012). Re(de)fining the dendritic cell lineage. Nat Immunol *13*, 1145-1154.

Sawicka, M.S., Gretta; Reynolds, Joseph; Abourashchi, Niloufar; Lythe, Grant; Molina-Paris, Carmen; Hogquist, Kristin (2014). From pre-DP, post-DP, SP4 and SP8 thymocyte cell counts to a dynamical model of cortical and medullary selection. Frontiers in Immunology *5*.

Schmid, D., Pypaert, M., and Münz, C. (2007). Antigen-Loading Compartments for Major Histocompatibility Complex Class II Molecules Continuously Receive Input from Autophagosomes. Immunity *26*, 79-92.

Schulz, O., Pennington, D.J., Hodivala-Dilke, K., Febbraio, M., and Reis e Sousa, C. (2002). CD36 or αvβ3 and αvβ5 Integrins Are Not Essential for MHC Class I Cross-Presentation of Cell-Associated Antigen by CD8α+ Murine Dendritic Cells. The Journal of Immunology *168*, 6057-6065.

Schuster, C., Gerold, Kay D., Schober, K., Probst, L., Boerner, K., Kim, M.-J., Ruckdeschel, A., Serwold, T., and Kissler, S. (2015). The Autoimmunity-Associated

Gene CLEC16A Modulates Thymic Epithelial Cell Autophagy and Alters T Cell Selection. Immunity *42*, 942-952.

Skogberg, G., Lundberg, V., Berglund, M., Gudmundsdottir, J., Telemo, E., Lindgren, S., and Ekwall, O. (2015). Human thymic epithelial primary cells produce exosomes carrying tissue-restricted antigens. Immunol Cell Biol *93*, 727-734.

Soleimanpour, S.A., Ferrari, A.M., Raum, J.C., Groff, D.N., Yang, J., Kaufman, B.A., and Stoffers, D.A. (2015). Diabetes susceptibility genes Pdx1 and Clec16a function in a pathway regulating mitophagy in β-cells. Diabetes.

Soleimanpour, Scott A., Gupta, A., Bakay, M., Ferrari, Alana M., Groff, David N., Fadista, J., Spruce, Lynn A., Kushner, Jake A., Groop, L., Seeholzer, Steven H.*, et al.* (2014). The Diabetes Susceptibility Gene Clec16a Regulates Mitophagy. Cell *157*, 1577-1590.

Stoeckle, C., Quecke, P., Rückrich, T., Burster, T., Reich, M., Weber, E., Kalbacher, H., Driessen, C., Melms, A., and Tolosa, E. (2012). Cathepsin S dominates autoantigen processing in human thymic dendritic cells. Journal of Autoimmunity *38*, 332-343.

Stritesky, G.L., Jameson, S.C., and Hogquist, K.A. (2012). Selection of Self-Reactive T Cells in the Thymus. Annual Review of Immunology *30*, 95-114.

Stritesky, G.L., Xing, Y., Erickson, J.R., Kalekar, L.A., Wang, X., Mueller, D.L., Jameson, S.C., and Hogquist, K.A. (2013). Murine thymic selection quantified using a unique method to capture deleted T cells. Proceedings of the National Academy of Sciences *110*, 4679-4684.

Sukseree, S., Mildner, M., Rossiter, H., Pammer, J., Zhang, C.-F., Watanapokasin, R., Tschachler, E., and Eckhart, L. (2012). Autophagy in the Thymic Epithelium Is Dispensable for the Development of Self-Tolerance in a Novel Mouse Model. PLoS ONE *7*, e38933.

Takaba, H., Morishita, Y., Tomofuji, Y., Danks, L., Nitta, T., Komatsu, N., Kodama, T., and Takayanagi, H. (2015). Fezf2 Orchestrates a Thymic Program of Self-Antigen Expression for Immune Tolerance. Cell *163*, 975-987.

Taniguchi, R.T., and Anderson, M.S. (2011). The role of Aire in clonal selection. Immunol Cell Biol *89*, 40-44.

Taniguchi, R.T., DeVoss, J.J., Moon, J.J., Sidney, J., Sette, A., Jenkins, M.K., and Anderson, M.S. (2012). Detection of an autoreactive T-cell population within the polyclonal repertoire that undergoes distinct autoimmune regulator (Aire)-mediated selection. Proceedings of the National Academy of Sciences *109*, 7847-7852.

van Meerwijk, J.P.M., Marguerat, S., Lees, R.K., Germain, R.N., Fowlkes, B.J., and MacDonald, H.R. (1997). Quantitative Impact of Thymic Clonal Deletion on the T Cell Repertoire. The Journal of Experimental Medicine *185*, 377-384.

Vrisekoop, N., Monteiro, João P., Mandl, Judith N., and Germain, Ronald N. (2014). Revisiting Thymic Positive Selection and the Mature T Cell Repertoire for Antigen. Immunity *41*, 181-190.

Wakim, L.M., and Bevan, M.J. (2011). Cross-dressed dendritic cells drive memory CD8+ T-cell activation after viral infection. Nature *471*, 629-632.

Weissler, K.A., and Caton, A.J. (2014). The role of T-cell receptor recognition of peptide:MHC complexes in the formation and activity of Foxp3+ regulatory T cells. Immunological Reviews *259*, 11-22.

Weissler, K.A.C., Andrew, J. (2014). The role of T cell receptor recognition of peptideMHC complexes in the formation and activity of Foxp3+ regulatory T cells. Immunological Reviews *259*, 11-22.

Wendland, M., Czeloth, N., Mach, N., Malissen, B., Kremmer, E., Pabst, O., and Förster, R. (2007). CCR9 is a homing receptor for plasmacytoid dendritic cells to the small intestine. Proceedings of the National Academy of Sciences *104*, 6347-6352.

Wing, K., and Sakaguchi, S. (2010). Regulatory T cells exert checks and balances on self tolerance and autoimmunity. Nat Immunol *11*, 7-13.

Wong, J., Obst, R., Correia-Neves, M., Losyev, G., Mathis, D., and Benoist, C. (2007). Adaptation of TCR Repertoires to Self-Peptides in Regulatory and Nonregulatory CD4+ T Cells. The Journal of Immunology *178*, 7032-7041.

Wu, L., and Shortman, K. (2005). Heterogeneity of thymic dendritic cells. Semin. Immunol. *17*, 304-312.

Zhao, Z., Fux, B., Goodwin, M., Dunay, I.R., Strong, D., Miller, B.C., Cadwell, K., Delgado, M.A., Ponpuak, M., Green, K.G.*, et al.* (2008). Autophagosome-Independent Essential Function for the Autophagy Protein Atg5 in Cellular Immunity to Intracellular Pathogens. Cell Host & Microbe *4*, 458-469.